UNIVERSIDADE FEDERAL DO RIO GRANDE DO SUL
INSTITUTO DE CIÊNCIAS BÁSICAS DA SAÚDE
PROGRAMA DE PÓS-GRADUAÇÃO EM CIÊNCIAS BIOLÓGICAS: BIOQUÍMICA

MICROENCAPSULAÇÃO DE CÉLULAS RECOMBINANTES SUPEREXPRESSANDO α-L-IDURONIDASE PARA O TRATAMENTO DA MUCOPOLISSACARIDOSE TIPO I

Barbara Zambiasi Martinelli

Orientador: Prof. Dr. Roberto Giugliani
Co-orientadora: Profa. Dra. Ursula Matte

Porto Alegre
2014

UNIVERSIDADE FEDERAL DO RIO GRANDE DO SUL
INSTITUTO DE CIÊNCIAS BÁSICAS DA SAÚDE
PROGRAMA DE PÓS-GRADUAÇÃO EM CIÊNCIAS BIOLÓGICAS: BIOQUÍMICA

MICROENCAPSULAÇÃO DE CÉLULAS RECOMBINANTES SUPEREXPRESSANDO α-L-IDURONIDASE PARA O TRATAMENTO DA MUCOPOLISSACARIDOSE TIPO I

Barbara Zambiasi Martinelli

Dissertação apresentada ao Programa de Pós-Graduação em Ciências Biológicas: Bioquímica da Universidade Federal do Rio Grande do Sul como requisito parcial à obtenção do grau de Mestre em Bioquímica.

Porto Alegre
2014

CIP - Catalogação na Publicação

Zambiasi Martinelli, Barbara
Microencapsulação de células recombinantes superexpressando alpha-L-iduronidase para o tratamento da Mucopolissacaridose tipo I / Barbara Zambiasi Martinelli. -- 2014.
116 f.

Orientador: Roberto Giugliani.
Coorientadora: Ursula Matte.

Dissertação (Mestrado) -- Universidade Federal do Rio Grande do Sul, Instituto de Ciências Básicas da Saúde, Programa de Pós-Graduação em Ciências Biológicas: Bioquímica, Porto Alegre, BR-RS, 2014.

1. Mucopolissacaridose tipo I. 2. Microcápsulas. 3. Biomateriais. 4. Células recombinantes. 5. Terapia gênica e celular. I. Giugliani, Roberto, orient. II. Matte, Ursula, coorient. III. Título.

Elaborada pelo Sistema de Geração Automática de Ficha Catalográfica da UFRGS com os dados fornecidos pelo(a) autor(a).

AGRADECIMENTOS

Gostaria de deixar meu agradecimento àqueles que direta ou indiretamente contribuíram para a conclusão deste trabalho.

Ao Professor Roberto Giugliani e à Professora Ursula Matte, pela orientação durante esta etapa da minha formação e pela oportunidade de crescimento profissional.

Ao Professor Guilherme Baldo, por tudo o que me ensinou e pela disponibilidade em ajudar.

Aos colegas do Centro de Terapia Gênica, pelo companheirismo e troca de experiências durante anos.

Aos amigos de perto e de longe, pelo apoio.

À Mariel Barbachan, por estar ao meu lado em todos os momentos.

À minha família, pelo incentivo, amor, confiança e compreensão que sempre recebi.

Por fim, agradeço ao CNPq pela bolsa de mestrado e ao HCPA pelo financiamento desta pesquisa.

ÍNDICE

PARTE I 1

RESUMO 2

ABSTRACT 3

LISTA DE ABREVIATURAS 4

INTRODUÇÃO 5

1. MUCOPOLISSACARIDOSES 5

1.1 Mucopolissacaridose tipo I 6

1.1.1 Aspectos clínicos 6

1.1.2 Aspectos moleculares e bioquímicos 8

1.1.3 Diagnóstico 9

1.1.4 Tratamentos 10

Transplante de células tronco hematopoiéticas 10

Terapia de reposição enzimática 12

1.1.5 Novas abordagens terapêuticas 13

1.1.6. Modelos animais 14

2. MICROENCAPSULAÇÃO CELULAR 14

2.1. Biomateriais 16

Alginato 16

Cross-linkers 19

2.2. Aplicação Terapêutica 20

OBJETIVOS 23

1. *OBJETIVO GERAL* 23

2. *OBJETIVOS ESPECÍFICOS* 23

PARTE II 24

CAPÍTULO I 25

Subcutaneous implantation of recombinant microencapsulated cells overexpressing α-L-iduronidase increases enzyme levels in Mucopolysaccharidosis type I mice 25

CAPÍTULO II 48

Omentum is a safe site for microcapsule implant in rodents: study on the Mucopolysaccharidosis type I model 48

PARTE III 64

DISCUSSÃO 65

CONCLUSÕES 74

REFERÊNCIAS 75

ANEXOS 82

PRODUÇÃO CIENTÍFICA RELACIONADA 82

ANEXO I 83

ANEXO II 96

ANEXO III 104

PARTE I

RESUMO

A Mucopolissacaridose tipo I (MPS I) é causada pela deficiência da α-L-iduronidase (IDUA), uma hidrolase lisosomal responsável pela degradação dos glicosaminoglicanos (GAG) heparan e dermatan sulfato. Diversos processos bioquímicos e fisiológicos são afetados pelo acúmulo desses substratos nas células, levando a uma condição patológica multisistêmica. Apesar dos benefícios clínicos obtidos com os tratamentos atualmente disponíveis, várias limitações têm sido relatadas, sendo necessária a busca de novas estratégias terapêuticas. Uma abordagem promissora de terapia gênica/celular para o tratamento da MPS I é a microencapsulação de células geneticamente modificadas. Neste trabalho, produzimos microcápsulas com células recombinantes superexpressando IDUA, as quais foram implantadas em camundongos MPS I a fim de avaliar sua eficiência como uma terapia. No primeiro estudo, as cápsulas foram implantadas no tecido subcutâneo para um tratamento de 120 dias. A atividade de IDUA no soro teve um leve aumento nos primeiros 45 dias. Depois de 120 dias, a atividade de IDUA foi detectada no fígado, rim e coração. A dosagem bioquímica do acúmulo de GAG nos tecidos mostrou níveis reduzidos no rim. A análise histológica confirmou esses resultados e, de modo interessante, mostrou uma reorganização no parênquima hepático com menos células vacuolizadas. Além disso, as microcápsulas foram recuperadas para análise histológica e foi observada a presença de células inflamatórias e uma camada fibrótica em torno das cápsulas. O segundo estudo foi um tratamento de 60 dias com as microcápsulas implantadas no epíplon. Os níveis de IDUA no soro foram transitórios durante o tratamento e 60 dias depois da implantação a atividade enzimática foi detectada apenas no coração. A avaliação do acúmulo de GAG não apresentou diferenças entre os camundongos MPS I tratados e não tratados. Em ambos os estudos, alguns animais foram utilizados para um experimento em curto prazo e um aumento nos níveis de IDUA foi observado nos tecidos 24 horas após a implantação das cápsulas. Concluindo, as células microencapsuladas foram capazes de corrigir alguns aspectos da doença. No entanto, fatores como uma resposta imune contra a enzima e ao biomaterial, ou a dose de células nas cápsulas, podem ter prejudicado a eficiência do tratamento, sugerindo que modificações na técnica são necessárias para obter um melhor desempenho.

ABSTRACT

Mucopolysaccharidosis type I (MPS I) is caused by a deficiency of α-L-iduronidase (IDUA), a lysosomal hydrolase responsible for the degradation of the glycosaminoglycans (GAG) heparan and dermatan sulfate. The consequent accumulation of these substrates throughout the cells affects several biochemical and physiological processes, leading to multisystemic pathological condition. Although the clinical benefits of the treatments currently available, several limitations have been noted and the search for alternative therapeutic strategies are necessary. A promising gene/cell therapy approach for treating MPS I is the microencapsulation of genetically modified cells. In this work, we produced microcapsules containing recombinant cells overexpressing IDUA, which were implanted in MPS I mice in order to evaluate their efficiency as a treatment. In the first study, capsules were implanted in the subcutaneous tissue for a 120-days treatment. Serum IDUA activity was slightly increased in the first 45 days. After 120 days, IDUA activity was detected in the liver, kidney and heart. The biochemical measurement of GAG accumulation in the tissues revealed decreased levels in the kidney. The histological analysis confirmed these results and, interestingly, showed a re-organization of the hepatic parenchyma with less cell vacuolization. In addition, microcapsules were retrieved for histological analysis and it was observed the presence of inflammatory cells and a fibrotic layer around the capsules. The second study was a 60-day treatment with the microcapsules implanted in the omentum. Serum IDUA levels were transient over treatment and 60 days post-implantation the enzyme activity was detected only in the heart. The evaluation of GAG storage did not reveal differences between treated and untreated MPS I mice. In both studies, some animals were used for a short-term experiment and increased IDUA levels were observed in the tissues 24 h after capsules implantation. In conclusion, microencapsulated cells were able to correct some aspects of the disease. However, factors such as immune response against the enzyme and the biomaterial or the dose of cells in the capsules could be impairing the efficiency of the treatment, suggesting that modifications on the technique are necessary to achieve a better performance.

LISTA DE ABREVIATURAS

APA – Alginato-PLL-Alginato

BHK - *Baby Hamster Kidney*

DL - Doenças Lisossômicas

DS – Dermatan Sulfato

FDA – do inglês *Food and Drug Administration*

GAG – Glicosaminoglicanos

HS – Heparan Sulfato

IDUA - Alfa-L-iduronidase

M6P - Manose-6-fosfato

M6PR - Receptor de manose-6-fosfato

MDCK - *Madin-Darby Canine Kidney*

MPS – Mucopolissacaridose

MPS I – Mucopolissacaridose tipo I

OMIM – do inglês *Online Mendelian Inheritance in Man*

PLL - Poli-L-lisina

rBHK - *Baby Hamster Kidney* recombinante

SNC – Sistema Nervoso Central

TCTH - Transplante de células-tronco hematopoiéticas

TRE - Terapia de reposição enzimática

INTRODUÇÃO

1. MUCOPOLISSACARIDOSES

As doenças lisossômicas (DL) constituem um grupo heterogêneo de doenças metabólicas hereditárias resultantes da deficiência em uma ou mais das 80 enzimas ou transportadores presentes normalmente no compartimento lisossomal (Platt *et al*, 2012). Especificamente, as mucopolissacaridoses (MPS) são DL caracterizadas por mutações em genes que codificam enzimas envolvidas nas vias de degradação dos glicosaminoglicanos (GAG).

Os GAG são polissacarídeos lineares não ramificados compostos por unidades dissacarídicas. De acordo com a função dos seus resíduos glicídicos, do tipo de ligação e do número e posição dos grupamentos sulfato, são diferenciados em 4 tipos: dermatan sulfato (DS), heparan sulfato (HS), keratan sulfato (KS) e condroitin sulfato (CS) (Harper 1998). Na superfície celular e na matriz extracelular, apresentam-se ligados a um núcleo protéico formando os proteoglicanos (Gandhi & Mancera, 2008). Estes compostos controlam a organização estrutural da matriz extracelular, modulam a atividade de fatores de crescimento e processos de migração celular, proliferação, morfogênese e apoptose, além de terem um papel essencial na sinalização celular (Bishop *et al*, 2007). Em seu catabolismo, após a clivagem proteolítica dos proteoglicanos, os GAG são sequencialmente degradados por diversas enzimas lisossômicas formando monossacarídeos e sulfatos inorgânicos (Gandhi & Mancera, 2008). A redução ou a perda da atividade dessas enzimas causa o acúmulo progressivo de macromoléculas não degradas e, consequentemente, a perturbação das funções lisossômicas e celulares (Cheng, 2014).

As MPS são doenças raras, mas que em conjunto representam uma proporção significativa das doenças metabólicas hereditárias graves, com uma incidência mundial estimada de 1:22.000 nascidos vivos (Giugliani, 2012). Há 11 tipos de MPS já identificadas e descritas, sendo classificadas numericamente de MPS I a MPS IX de acordo com a enzima deficiente e o tipo de GAG acumulado – os tipos V e VIII não existem e os tipos III e IV são subclassificados, respectivamente, em A, B, C e D e em A e B**.** Assim como a maioria das DL, as MPS são herdadas de modo autossômico recessivo, com exceção da MPS tipo II, na qual a herança é ligada ao X (Muenzer, 2011).

1.1 Mucopolissacaridose tipo I

Primeiramente descrita em 1919 pela pediatra alemã Gertrud Hurler, a Mucopolissacaridose tipo I (MPS I) é uma DL causada por mutações no gene que codifica a enzima alfa-L-iduronidase (IDUA; EC 3.2.1.76) (Matte *et al*, 2003), resultando no acúmulo de seus substratos, os GAG heparan e dermatan sulfato. A MPS I é uma doença multisistêmica, progressiva e com manifestações clínicas heterogêneas, cuja incidência estimada é de 1:100.000 nascidos vivos (Beck *et al*, 2014).

1.1.1 Aspectos clínicos

Devido ao fato de os lisossomos estarem presentes em todas as células eucarióticas (com exceção dos eritrócitos) e de que seus substratos têm papéis fundamentais em diversas funções celulares, os efeitos da deficiência de uma única enzima lisossômica são abrangentes e variados. A heterogeneidade de fenótipos da MPS I é dividida em 3 diferentes categorias baseadas nas principais manifestações clínicas: a síndrome de Hurler (OMIM # 607014), a síndrome de Hurler-Scheie (OMIM # 607015) e síndrome de Scheie (OMIM # 607016). As síndromes são diferenciadas principalmente pela variação na idade

de início dos sintomas e pela velocidade na progressão da doença, sendo que todos os fenótipos são caracterizados pelo envolvimento multisistêmico e pela disfunção progressiva dos órgãos (Giugliani *et al*, 2010).

A síndrome de Hurler é a forma mais grave da doença, onde há um significativo atraso no desenvolvimento e comprometimento neurológico. Os pacientes são diagnosticados em torno dos 9 meses de idade devido a sintomas como infecções recorrentes no trato respiratório superior, hérnias umbilical e inguinal, deformidades esqueléticas e hepatoesplenomegalia (D'Aco *et al*, 2012). Progressivamente, ocorre opacificação da córnea, perda de audição, anormalidades esqueléticas, rigidez articular, problemas cardíacos e atraso no desenvolvimento. Quando não tratados, os pacientes geralmente morrem antes dos 10 anos de idade, devido principalmente ao progressivo dano neurológico e insuficiência cardiorrespiratória (Muenzer, 2011).

O fenótipo da síndrome de Scheie é caracterizado por manifestações clínicas atenuadas, apresentadas tardiamente e com progressão mais lenta do que na forma grave. O início dos sintomas ocorre em torno dos 5 anos de idade e consiste principalmente em problemas esqueléticos, anormalidades nas válvulas cardíacas, síndrome do túnel do carpo, infecções respiratórias, apnéia obstrutiva, contraturas articulares, opacificação da córnea e problemas no crescimento. Apesar disso, os pacientes geralmente possuem um funcionamento cognitivo normal e sobrevivem até a idade adulta (Thomas *et al*, 2010).

Na síndrome de Hurler-Scheie, o fenótipo clínico é intermediário entre as formas anteriormente descritas. O início dos sintomas ocorre entre 3 e 8 anos de idade, onde é observada opacificação da córnea, perda da audição e enrijecimento articular. Geralmente não há prejuízo neurológico, apesar de alguns pacientes apresentarem dificuldades no aprendizado. É comum a sobrevivência até a idade adulta, mas a expectativa de vida é

reduzida para cerca de 20 ou 30 anos de idade e a morte ocorre por complicações respiratórias e cardiovasculares (Giugliani *et al*, 2010; Muenzer, 2011).

1.1.2 Aspectos moleculares e bioquímicos

O gene humano da IDUA está situado no cromossomo 4p16.3, contém 14 exons e 19 kb (Scott *et al*, 1991). Há mais de 150 mutações, entre mutações de ponto e pequenas deleções e inserções, e as correlações genótipo-fenótipo ainda são limitadas. Acredita-se que as mutações que impedem totalmente a produção da enzima funcional levem a um fenótipo grave, enquanto mutações que permitem alguma atividade residual da enzima levem a um fenótipo atenuado (Terlato & Cox, 2003). Além disso, foram descritos diversos polimorfismos propensos a modificar o fenótipo da MPS I quando presentes em conjunto com as mutações causadoras da doença.

A IDUA é uma glicosidase de 69 kDa responsável pela hidrólise de resíduos ácidos alfa-L-idurônicos dos GAG HS e DS. O HS é composto principalmente por ácido glicurônico e N-acetilglicosaminas, está presente em proteoglicanos associados à membrana plasmática de diversos tipos celulares e possui um papel de grande importância na sinalização celular. O dermatan sulfato é composto principalmente por ácido L-idurônico e N-acetilgalactosamina sulfatada e está presente em vasos sanguíneos, tendões e válvulas cardíacas (Bishop *et al*, 2007; Gandhi & Mancera, 2008). Uma vez que há uma deficiência na atividade da IDUA, o *turnover* desses GAG é comprometido.

Historicamente, acreditava-se que o acúmulo de GAG não degradados nos lisossomos de pacientes com deficiência de IDUA levava diretamente aos sintomas associados à doença. De fato, as substâncias que se acumulam como consequência direta do defeito genético são os produtos de armazenamento primário e representam o evento patogênico inicial. No entanto, diversos estudos sobre a fisiopatologia da MPS I, bem

como de outras DL, mostraram que este processo é muito mais complexo e parece envolver diversos processos bioquímicos e fisiológicos onde há o acúmulo secundário de outras substâncias, influenciando assim as vias de sinalização intracelular e alterando a atividade de outras enzimas lisossômicas (Heard *et al*, 2010; Platt *et al*, 2012).

Alguns mecanismos patológicos da MPS I estão relacionados ao acúmulo de gangliosídeos e colesterol em neurônios (McGlynn *et al*, 2004), ativação de células gliais (Ohmi *et al*, 2003), alterações na homeostase do cálcio e na permeabilidade da membrana do lisossomo, levando a um aumento do pH e comprometimento da atividade de outras enzimas lisossômicas (Pereira *et al*, 2010). Além disso, a sulfatação do HS acumulado nas MPS é anormal (Holley *et al*, 2011), o que tem um impacto ainda maior em vias de sinalização, uma vez que fatores de crescimento dependem do HS para se ligarem e desempenharem sua função.

1.1.3 Diagnóstico

A MPS I, assim como outras DL, não é evidente no momento do nascimento e o diagnóstico pré-natal é realizado apenas em casos onde há algum familiar afetado. Por possuir uma natureza progressiva, o diagnóstico precoce é essencial para a eficácia dos tratamentos disponíveis. Entretanto, isso pode ser difícil devido à heterogeneidade dos sintomas e às semelhanças clínicas entre muitas doenças lisossômicas. Consequentemente, a demora entre o início dos sintomas e o diagnóstico é comum.

Quando há suspeita clínica, uma bateria de testes pode ser necessária para se chegar a um diagnóstico definitivo. Em pacientes não tratados, uma grande quantidade de GAG não degradados é excretada na urina, sendo este um marcador para a triagem inicial (Tomatsu *et al*, 2010). Além disso, também são realizadas dosagens da atividade da enzima no plasma, leucócitos ou fibroblastos. Para a complementação do diagnóstico é

feita a análise do gene da IDUA. Tanto os níveis aumentados de GAG na urina como a deficiência na atividade enzimática são observados nas três apresentações clínicas da MPS I, o que não possibilita predizer a gravidade. O diagnóstico molecular, além de identificar as mutações causadoras da doença, possibilita estabelecer uma correlação genótipo-fenótipo em alguns casos (Giugliani, 2012; Matte *et al*, 2003; Sugawara *et al*, 2008).

1.1.4 Tratamentos

Há duas opções de tratamento disponíveis para a MPS I, o transplante de células tronco hematopoiéticas (TCTH) e a terapia de reposição enzimática (TRE). Baseando-se no fato de que a enzima alfa-L-iduronidase pode ser secretada e captada pelos receptores de manose-6-fosfato (M6PR) das células dos pacientes, o objetivo de ambos é fornecer a enzima ativa, seja através da síntese e subsequente liberação da enzima pelas células transplantadas ou pela sua infusão intravenosa, resultando no aumento do catabolismo dos GAG acumulados. Além do TCTH e da TRE, outras abordagens para a MPS I estão sendo testadas em fase experimental ou em ensaios clínicos preliminares.

Transplante de células tronco hematopoiéticas

O TCTH foi primeiramente utilizado para o tratamento de um paciente com MPS I em 1980 e desde então mais de 500 pacientes foram tratados com esta abordagem terapêutica (Boelens *et al*, 2010). No TCTH, os pacientes recebem células tronco da medula óssea ou do cordão umbilical de doadores saudáveis. As células transplantadas produzem e liberam a enzima, a qual é internalizada pelas células deficientes e atingem diferentes órgãos e sistemas do corpo. Devido aos riscos associados, como a possibilidade de doença do enxerto contra o hospedeiro, esse tratamento é indicado em situações específicas que incluem pacientes com a forma grave da MPS I (síndrome de Hurler) e

com idade de até 2,5 anos, ressaltando a importância do diagnóstico precoce. Se o transplante for feito tardiamente, não será capaz de prevenir o acentuado dano neurológico e, portanto, outras terapias são preferíveis devido ao alto risco de morbidade e mortalidade associado ao procedimento (Beck *et al*, 2014; Boelens *et al*, 2010; Giugliani, 2012).

Quando bem sucedido, o TCTH é capaz de prolongar a expectativa de vida e melhorar diversos parâmetros clínicos. Os principais resultados positivos são observados em curto prazo e se referem às alterações viscerais, com redução da hepatoesplenomegalia e opacidade da córnea. O tratamento também leva à diminuição das complicações cardíacas, com regressão da hipertrofia ventricular, melhora na audição e melhora nos sintomas de obstrução das vias aéreas. Embora o dano cerebral pré-existente ao TCTH seja irreversível, o transplante pode prevenir a progressão do comprometimento neurológico e melhorar as funções cognitivas (Beck *et al*, 2014; Noh & Lee, 2014).

Apesar dos resultados positivos, as manifestações musculoesqueléticas parecem responder mal e muitos pacientes continuam com uma doença esquelética progressiva, muitas vezes necessitando de múltiplas intervenções ortopédicas nos anos seguintes ao TCTH (Prasad & Kurtzberg, 2010). Outras limitações incluem a dificuldade de encontrar doadores HLA compatíveis e a necessidade da administração de altas doses de quimioterapia, o que está associado com riscos de mortalidade precoce e posterior morbidade, incluindo efeitos adversos em relação ao crescimento, fertilidade e dentição (Prasad & Kurtzberg, 2010). Esses fatores, aliados a necessidade de tratamento precoce, fazem com que menos de 1% dos pacientes da América Latina sejam transplantados, em comparação a 27% dos pacientes do resto do mundo (Muñoz-Rojas *et al*, 2011).

Terapia de reposição enzimática

Aprovada pelo FDA em 2003, a TRE para o tratamento da MPS I utiliza uma versão recombinante e purificada da enzima alfa-L-iduronidase, a Laronidase (Aldurazyme®, Biomarin/Genzyme, EUA). Essa terapia consiste na administração intravenosa da enzima, semanalmente (dose de 0,6 mg/kg de peso corporal) ou quinzenalmente (1,2 mg/kg de peso) (Giugliani *et al*, 2009), sendo a primeira opção de tratamento.

A avaliação de parâmetros clínicos em pacientes que recebem a TRE demonstra sua eficácia na melhora da função pulmonar, redução no volume do fígado e baço e diminuição na excreção de GAG na urina (Clarke *et al*, 2009; Muenzer, 2014). Entretanto, os resultados são divergentes em relação à correção dos problemas articulares e cardíacos, havendo relatos de melhoras em alguns casos e de pouco ou nenhuma eficácia em outros (Clarke *et al*, 2009; Sifuentes *et al*, 2007). Devido à complexidade e à natureza multisistêmica da MPS I, um acompanhamento multidisciplinar dos pacientes é importante e, além do tratamento específico para a doença, o tratamento de complicações sistêmicas (correção cirúrgica de hérnias e uso de aparelhos auditivos, por exemplo) deve ser considerado (Valayannopoulos & Wijburg, 2011).

Em relação às limitações da TRE, pode-se destacar o fato de que essa terapia não é capaz de prevenir o declínio cognitivo e melhorar os sintomas neurológicos da doença, uma vez que a enzima não é capaz de atravessar a barreira hematoencefálica. Além disso, em cerca de 90% dos pacientes ocorre a formação de anticorpos contra enzima (Valayannopoulos & Wijburg, 2011), o que pode interferir na eficácia da terapia. Reações adversas à TRE também são observadas em alguns pacientes, como cefaleia, dor abdominal, dispneia, hipertensão/hipotensão, reações de hipersensibilidade e exantema (Giugliani *et al*, 2010). Outro fator a ser destacado é o alto custo da TRE, tornando-a

muito dispendiosa para o sistema público de saúde, sendo que os valores gastos anualmente variam de R$150.000,00 a 300.000,00 por paciente.

1.1.5 Novas abordagens terapêuticas

A heterogeneidade clínica da MPS I e as limitações apresentadas pelas terapias convencionais representam um desafio para o tratamento dos pacientes. Portanto, torna-se necessária a investigação de novas alternativas terapêuticas a fim de melhorar a eficiência do tratamento e a qualidade de vida dos pacientes. Atualmente, diversos estudos estão sendo realizados, focando em diferentes aspectos da doença e desenvolvendo abordagens específicas, entre elas estão a terapia de redução da síntese do substrato, a tradução alternativa e a terapia gênica.

A terapia de redução da síntese do substrato tem como objetivo diminuir a quantidade de GAG acumulado através da inibição das enzimas responsáveis por sua síntese, compensando a deficiência na atividade de IDUA (Delgadillo *et al*, 2011). A tradução alternativa ou *readthrough* traducional consiste na supressão de códons de terminação prematura através da incorporação de um aminoácido aleatório no lugar de mutações sem sentido, permitindo a produção da proteína (Brooks *et al*, 2006; Mayer *et al*, 2013). Estratégias de terapia gênica também estão sendo desenvolvidas para a MPS I, onde ocorre o aumento ou correção da expressão dos genes de interesse através da utilização de vetores virais ou não virais (Baldo *et al*, 2014; Ponder & Haskins, 2007), sendo que uma forma de terapia gênica não viral é o uso de células geneticamente modificadas e microencapsuladas (Matte *et al*, 2011).

1.1.6. Modelos animais

A disponibilidade de modelos animais para DL possibilitou o entendimento de diversos aspectos da fisiopatologia dessas doenças, uma vez que a heterogeneidade clínica e questões éticas dificultam estudos controlados em seres humanos. Essa ainda é uma ferramenta de grande importância para a investigação dos mecanismos patogênicos e para estudos terapêuticos.

Para a MPS I, existem modelos em camundongos (Clarke *et al*, 1997; Ohmi *et al*, 2003; Wang *et al*, 2010) e em animais maiores como gatos e cachorros (Haskins, 2007). Em relação aos modelos murinos, há três já descritos. O primeiro deles foi criado através de uma interrupção no éxon 6 do gene da *Idua* (Clarke *et al*, 1997), resultando em animais que mimetizam a síndrome de Hurler, nos quais a atividade enzimática é indetectável e há níveis elevados de GAG nos tecidos e na urina. O segundo modelo também é *knock out* para o gene da *Idua* com a interrupção no éxon 6, com um gene de resistência à neomicina inserido no sentido inverso. A criação foi feita pelo grupo da Dra. Elizabeth Neufeld (Ohmi *et al*, 2003), sendo este o modelo utilizado em nosso grupo de pesquisa. O terceiro modelo murino é *knock in* (Wang *et al*, 2010), no qual foi inserida a mutação mais comum do gene da IDUA encontrado em pacientes (p.W402X) e que está associada ao fenótipo mais grave da doença.

2. MICROENCAPSULAÇÃO CELULAR

A microencapsulação celular consiste basicamente na imobilização de células em matrizes poliméricas para a entrega de compostos biologicamente ativos. Estudos pioneiros feitos por Chang em 1964 (Chang, 1964) já tinham como base uma possível aplicação terapêutica e, desde então, é considerada uma abordagem biotecnológica

promissora. Utilizando essa tecnologia, células geneticamente modificadas podem ser encapsuladas em membranas semipermeáveis, onde funcionam como "fábricas", produzindo e liberando fatores terapêuticos continuamente, de forma controlada e localizada. A semipermeabilidade da membrana permite a difusão bi-direcional de nutrientes, oxigênio e produtos biologicamente ativos entre as células isoladas e o ambiente externo. Além disso, a microcápsula é uma proteção contra o sistema imune do hospedeiro, impedindo a entrada de moléculas com elevado peso molecular (> 150 kDa), imunoglobulinas e outros componentes que podem entrar em contato com as células recombinantes e destruí-las (figura 1) (de Vos *et al*, 2009; Orive *et al*, 2014).

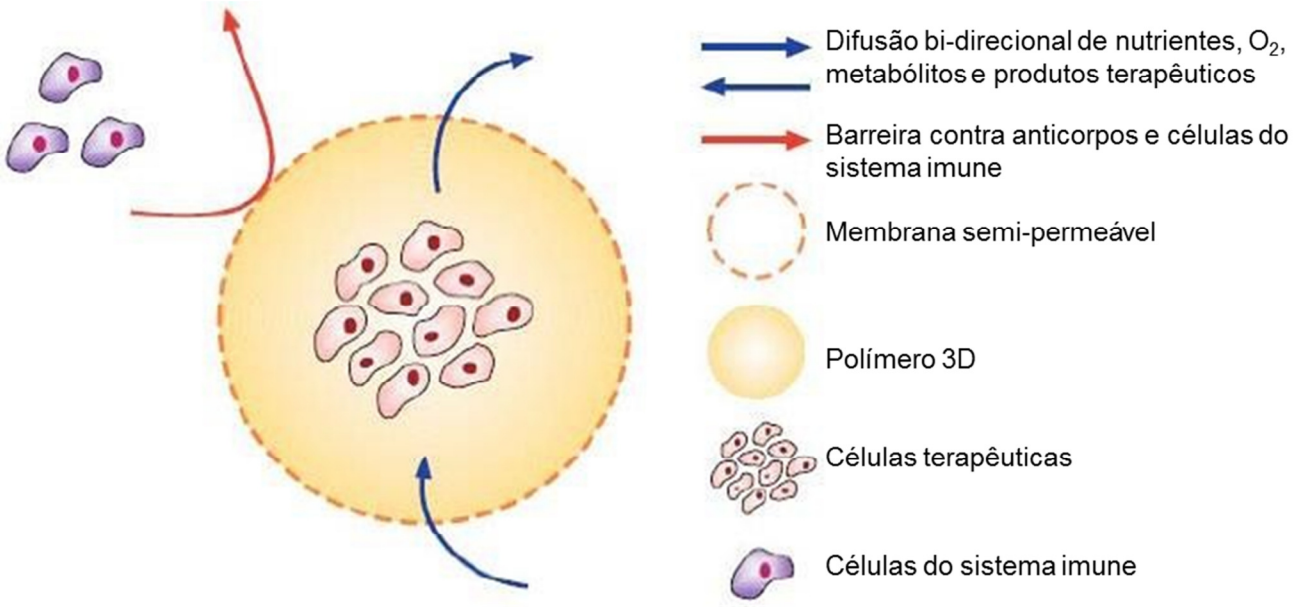

Figura 1. Representação de uma microcápsula e suas características (adaptado de Orive, 2010).

Uma relação adequada entre a estabilidade, biocompatibilidade, durabilidade e propriedades de difusão garante a funcionalidade das células em longo prazo, permitindo assim a utilização no tratamento de doenças crônicas (Orive *et al*, 2014).

Teoricamente, pode-se atribuir à encapsulação de células dois possíveis benefícios principais: 1) o transplante sem a necessidade de drogas imunossupressoras, devido a

imunoproteção exercida pela cápsula e 2) a utilização de células a partir de uma variedade de fontes, tais como células primárias ou células geneticamente modificadas, que podem ser induzidas a expressar qualquer proteína de interesse, sem a modificação do genoma do hospedeiro (Lim *et al*, 2010; Orive *et al*, 2014; Santos *et al*, 2013).

2.1. Biomateriais

A escolha do biomaterial representa o primeiro ponto crítico no processo de encapsulação, pois as propriedades do polímero estão diretamente relacionadas com o sucesso na aplicação das microcápsulas. Os hidrogéis são amplamente utilizados, uma vez que possuem muitas características desejáveis, como biocompatibilidade e permeabilidade, além de criarem um microambiente altamente hidratado e capaz de fornecer condições bioquímicas e físicas para o metabolismo celular (Hernández *et al*, 2010; Rokstad *et al*, 2014).

Há uma grande variedade de biomateriais disponíveis sendo estudados, incluindo alginato, agarose, ácido hialurônico, quitosana, colágeno e fibrina. Entre eles, o alginato apresenta o melhor nível de desempenho e é o mais frequentemente utilizado na área da microencapsulação celular (Santos *et al*, 2013).

Alginato

Alginatos são polissacarídeos aniônicos não ramificados extraídos principalmente de algas marrons. O alginato é o biomaterial mais amplamente utilizado para a imobilização de células devido a sua abundância, fácil manipulação, capacidade de geleificação e aparente biocompatibilidade (Hernández *et al*, 2010; Rokstad *et al*, 2014). É um dos poucos materiais que pode ser processado em condições fisiológicas, o que permite a produção de cápsulas à temperatura ambiente e utilizando soluções isotônicas.

Além disso, alginatos com novas propriedades podem ser facilmente produzidos por modificações simples (Lee & Mooney, 2012).

Quimicamente, são constituídos por copolímeros em blocos lineares contendo resíduos de ácidos 1,4-β-D-manurônico (M) e α-L-gulurônico (G). Esses monômeros estão ligados em blocos de homopolímeros (GG e MM) e heteropolímeros (GM ou MG) formando cadeias, as quais se associam através de ligações cruzadas com cátions bivalentes (como o Ca^{2+}) para a formação de estruturas tridimensionais (Bidarra *et al*, 2014; de Vos *et al*, 2014).

O processo mais utilizado para a fabricação de microcápsulas consiste na extrusão de uma suspensão de alginato contendo as células terapêuticas com uma solução de reticulação contendo agentes iônicos (*cross-linkers*) que permitem a formação de ligações cruzadas. Nas ligações cruzadas, o íon interage com os resíduos G da cadeia polimérica e induz a formação de zonas de junção, de modo que as cadeias adjacentes se associam e formam o hidrogel. Esse modelo de ligação é conhecido como "egg-box" e está representado na figura 2 (Donati & Paoletti, 2009).

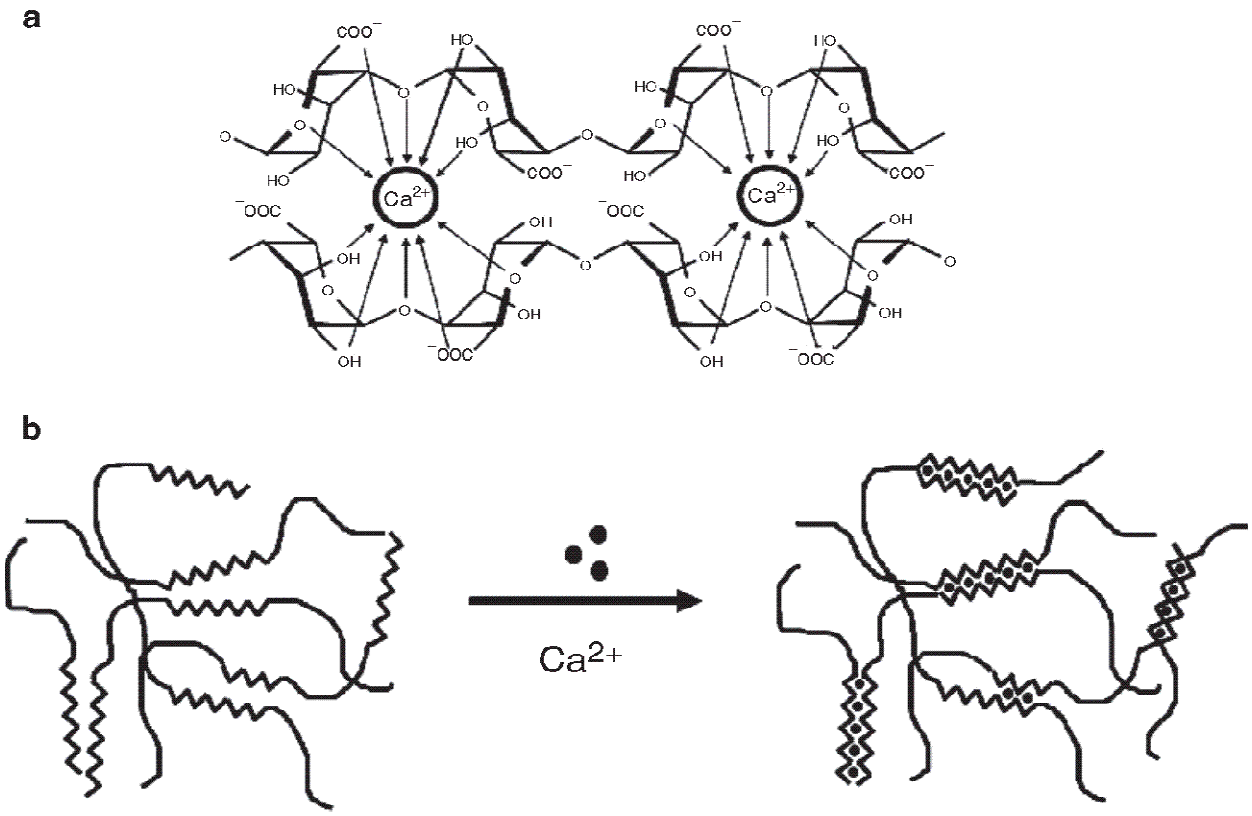

Figura 2: Representação do modelo "egg-box" **a)** Ligações cruzadas entre o alginato e o Ca^{2+} **b)** interação entre as cadeias de alginato formando o hidrogel (Donati & Paoletti, 2009).

A afinidade do alginato é diferente para cada tipo de íon e, portanto, a estabilidade, permeabilidade e resistência serão diferentes dependendo do cátion utilizado (Mørch *et al*, 2006). Alginatos com alto conteúdo de G são preferíveis em casos onde uma estrutura mais rígida é necessária e os alginatos com um maior teor de M são aplicados para a obtenção de géis mais flexíveis. Essa versatilidade do alginato se deve a maior afinidade dos resíduos de ácido gulurônico pelos íons bivalentes (de Vos *et al*, 2014).

O comprimento dos blocos, a proporção e a distribuição sequencial de G e M diferem de acordo com a fonte de extração do alginato (Augst *et al*, 2006), determinando importantes propriedades físico-químicas para sua aplicação, as quais controlam significativamente a estabilidade dos géis, a taxa de libertação de compostos terapêuticos e a morfologia e função das células encapsuladas (Lee & Mooney, 2012).

Cross-linkers

Soluções de reticulação contendo agentes iônicos são utilizadas para a formação de hidrogéis a partir de uma solução de alginato, de modo que quando estão em contato, ocorre a troca de íons sódio das unidades de ácido gulurônico do alginato por cátions bivalentes, como Ca^{2+}, Sr^{2+} ou Ba^{2+}, formando as microcápsulas de alginato. Outros cátions bivalentes como Pb^{2+}, Cu^{2+}, Cd^{2+}, Co^{2+}, Ni^{2+}, Zn^{2+} e Mn^{2+} também possibilitam a formação de ligações cruzadas, mas a sua aplicação é evitada pelo fato de serem tóxicos para as células (Mørch *et al*, 2006).

Geralmente, Ca^{2+} é o cátion de preferência devido às suas qualidades fisiológicas e biocompatibilidade que proporcionam uma boa viabilidade para as células imobilizadas (Lee & Mooney, 2012; Santos *et al*, 2013), sendo utilizado como solução de cloreto de cálcio ($CaCl_2$). No entanto, em soluções fisiológicas ou quando implantadas, as cápsulas de alginato de cálcio têm uma tendência a aumentar sua permeabilidade devido à constante troca de cargas entre o Ca^{2+} e outros íons como Na^{+}, Mg^{2+}, o que pode levar a uma desestabilização da matriz polimérica (Mørch *et al*, 2006). A fim de solucionar este problema, as cápsulas são geralmente recobertas com uma camada adicional de policátions após sua formação, permitindo uma maior resistência mecânica e ajustando sua permeabilidade. Os policátions penetram na matriz e, dessa forma, a superfície da cápsula é composta por uma única camada mista formada pela complexação alginato-polication (de Vos *et al*, 2014). No entanto, a carga positiva do policátion é imunogênica, sendo necessário o recobrimento com uma camada adicional de alginato para a neutralização dessas cargas (Santos *et al*, 2013).

Diferentes policátions podem ser aplicados na cobertura de microcápsulas de alginato, como poli-L-lisina (PLL), poli-L-ornitina (PLO), quitonasa, oligoquitosan e biomateriais fotopolimerizadores (Santos *et al*, 2013). A complexação polieletrolítica do

alginato com a PLL forma cápsulas conhecidas como microcápsulas APA (alginato-PLL-alginato), as quais possuem uma ampla variedade de aplicações e têm sido as mais utilizadas (Hernández *et al*, 2010).

2.2. Aplicação Terapêutica

A aplicação terapêutica de células microencapsuladas foi demonstrada pela primeira vez em 1980, quando Lim e Sun transplantaram ilhotas pancreáticas em ratos diabéticos, os quais mantiveram a normoglicemia por 2-3 semanas devido à liberação de insulina pelas cápsulas (Lim & Sun, 1980). Desde então, esse é o sistema de microencapsulação mais estudado e, além de estudos em modelos animais, essa abordagem já está sendo utilizada em estudos clínicos (Calafiore & Basta, 2014; Pareta *et al*, 2014). Para doenças neurológicas, estudos mostram o implante de microcápsulas diretamente no SNC, como microcápsulas com células cromafim liberando catecolaminas e opióides utilizadas para o tratamento da dor crônica (Kim *et al*, 2004). Estudos pré-clínicos obtiveram resultados promissores no uso de células geneticamente modificadas secretando fatores tróficos para o tratamento da doença de Parkinson, Huntington e Alzheimer, de modo que já há ensaios clínicos bem sucedidos (Garcia *et al*, 2010; Klinge *et al*, 2011). Além disso, há estudos utilizando células microencapsuladas para o tratamento de doenças cardíacas (Paul *et al*, 2009), câncer (Goren *et al*, 2010; Zhang *et al*, 2007) e anemia crônica (Murua *et al*, 2011), entre outras.

Doenças lisossômicas são excelentes candidatas ao tratamento com células microencapsuladas, pois as enzimas lisossômicas são secretadas e recaptadas via receptores de manose-6-fosfato (M6PR) presentes na superfície celular e seus genes possuem mecanismos simples de regulação de expressão. Para esse propósito, uma linhagem celular é transfectada *ex vivo* com um plasmídeo contendo o gene de interesse,

de modo que as células serão capazes de superexpressar a enzima deficiente na doença. As enzimas lisossômicas produzidas e secretadas são internalizadas pelas células deficientes e direcionadas aos lisossomos através da via M6PR (figura 3) (Matte *et al*, 2011).

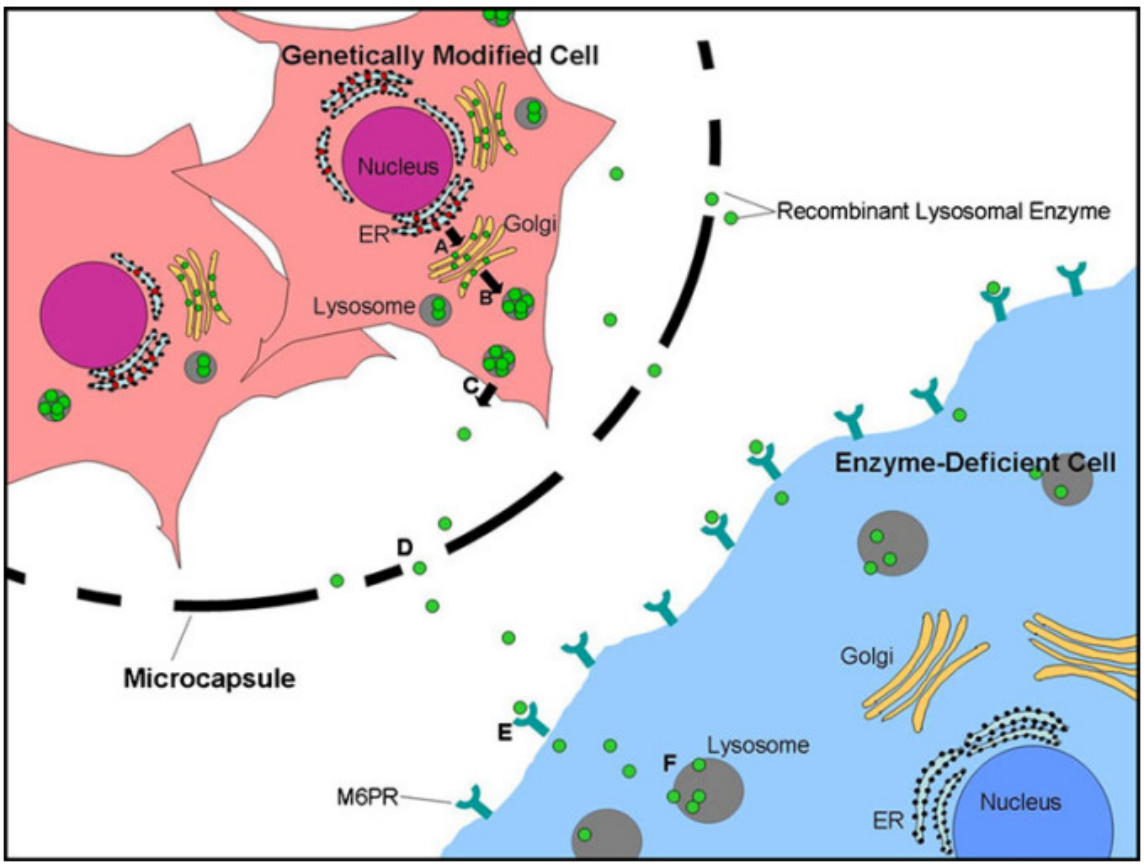

Figura 3. Tráfego de enzimas lisossômicas após encapsulação celular. As enzimas lisossômicas nascentes são glicosiladas no retículo endoplasmático da célula geneticamente modificada. (A) As enzimas são fosforiladas no resíduo de manose 6-fosfato no complexo de Golgi. (B) A maioria das enzimas é transportada para o lisossomo maduro. (C) Algumas, no entanto, são secretadas para o ambiente extracelular, e (D) para fora das cápsulas. (E) Enzimas fosforiladas se ligam aos receptores de manose 6-fosfato (M6PR) das células deficientes (F) onde são endocitadas e voltam para os lisossomos (Matte *et al*, 2011).

Diferentes linhagens celulares já foram geneticamente modificadas para expressar IDUA, encapsuladas e testadas *in vitro* e *in vivo* nos modelos animais de MPS I. Células *Madin-Darby Canine Kidney* (MDCK) recombinantes imobilizadas em microcápsulas APA foram implantadas no cérebro de cachorros MPS I (Barsoum *et al*, 2003), levando a um aumento discreto na atividade enzimática, porém não houve melhoras em relação ao

acúmulo de GAG e em aspectos clínicos. Em outro estudo, resultados interessantes foram obtidos com a utilização de microcápsulas APA contendo mioblastos recombinantes (C2C12), as quais foram implantadas intraperitonealmente no modelo murino de MPS I (Piller Puicher *et al*, 2012). O tratamento aumentou consideravelmente a atividade enzimática e foi capaz de reduzir o acúmulo de GAG nos tecidos. Entretanto, a completa normalização nos níveis de GAG foi observada em apenas 2 dos 12 animais tratados.

Nosso grupo de pesquisa desenvolveu uma linhagem de células *Baby Hamster Kidney* (BHK) geneticamente modificada de forma que superexpressam IDUA. Baldo e colaboradores produziram microcápsulas de alginato com as células recombinantes e cultivaram juntamente com fibroblastos de pacientes MPS I (Baldo *et al*, 2012a). Neste ensaio, as microcápsulas reestabeleceram a atividade enzimática nas células deficientes e os níveis de IDUA permaneceram elevados durante 45 dias. Posteriormente, o mesmo tipo de microcápsula foi implantado no peritônio de camundongos MPS I (Baldo *et al*, 2012b), onde houve uma correção parcial no acúmulo de GAG nos tecidos e um aumento transitório na atividade enzimática.

Apesar dos resultados obtidos até o momento serem apenas parcialmente satisfatórios, a microencapsulação celular parece ser uma alternativa promissora no tratamento de doenças lisossômicas como a MPS I. A base dessa abordagem terapêutica é a mesma da TRE, mas sem a necessidade de administrações enzimáticas semanais, já que as células encapsuladas produzem a enzima por um longo período. Além disso, pode ser considerada mais segura que a terapia gênica convencional devido ao fato de que células ficam isoladas em microesferas que não permitem seu contato direto com o hospedeiro. No entanto, mais estudos são necessários para aperfeiçoar este sistema, como o uso de diferentes vias de administração ou de diferentes microcápsulas.

OBJETIVOS

1. *Objetivo geral*

Produzir microcápsulas APA com células recombinantes superexpressando IDUA e testar seu efeito no tratamento do modelo animal de MPS I.

2. *Objetivos específicos*

- Produzir microcápsulas APA com células geneticamente modificadas superexpressando IDUA.
- Verificar a liberação da enzima pelas células encapsuladas *in vitro*.
- Implantar as microcápsulas na via subcutânea de camundongos MPS I e avaliar o tratamento após 120 dias.
- Implantar as microcápsulas no epíplon de camundongos MPS I e avaliar o tratamento após 60 dias.
- Retirar as microcápsulas dos animais após os tratamentos e analisar a possível presença de vascularização, infiltrado inflamatório e fibrose na superfície das cápsulas.

PARTE II

CAPÍTULO I

Subcutaneous implantation of recombinant microencapsulated cells overexpressing α-L-iduronidase increases enzyme levels in Mucopolysaccharidosis type I mice

Artigo a ser submetido para a revista Cytotherapy

Full title: Subcutaneous implantation of recombinant microencapsulated cells overexpressing α-L-iduronidase increases enzyme levels in mucopolysaccharidosis type I mice

Running title: Recombinant microencapsulated cells for MPS I treatment

Authors and Affiliations:

Barbara Zambiasi Martinelli, BSc [1,2]

Guilherme Baldo, PhD [1,3]

Giuseppe Ávila Testa[1]

Talita Giacomet de Carvalho, MSc [1,4]

Ursula Matte, PhD [1,4]

Roberto Giugliani, PhD [1,4]

[1] Gene Therapy Center, Hospital de Clínicas de Porto Alegre, Brazil

[2] Postgraduate Program in Biochemistry, Universidade Federal do Rio Grande do Sul, Porto Alegre, Brazil

[3] Postgraduate Program in Physiology, Universidade Federal do Rio Grande do Sul, Porto Alegre, Brazil

[4] Postgraduate Program in Genetics and Molecular Biology, Universidade Federal do Rio Grande do Sul, Porto Alegre, Brazil

Corresponding author:

Roberto Giugliani, MD, PhD

E-mail: rgiugliani@hcpa.ufrgs.br

Gene Therapy Center, Hospital de Clínicas de Porto Alegre

Rua Ramiro Barcelos, 2350

90035-903 - Porto Alegre, RS

Telephone: 55 51 3359 8838

Fax: 55 51 3359 8010

Abstract

Background aims: Mucopolysaccharidosis type I (MPS I) is caused by a deficiency of α-L-iduronidase (IDUA), resulting in accumulation of glycosaminoglycans (GAG). The microencapsulation of recombinant cells is a promising gene/cell therapy approach that could overcome the limitations of the current available treatments. **Methods**: Alginate-poly-L-lysine-alginate microcapsules enclosing genetically modified Baby Hamster Kidney cells overexpressing IDUA were produced and implanted in the subcutaneous space of 4-month-old MPS I mice (*Idua*$^{-/-}$). The treatment was performed in two groups of MPS I mice and evaluated 24 h and 120 days post-implantation. Untreated MPS I and normal mice were used as controls. Microcapsules were retrieved and analyzed after treatment. **Results**: Increased IDUA in the liver, kidney and heart was detected 24 h post-implantation. In a long-term treatment, serum enzyme was slightly increased in the first 45 days. After 120 days, higher IDUA activity was detected in the liver, kidney and heart, GAG accumulation was reduced in the kidney and a re-organization of the hepatic parenchyma was visualized. Microcapsules analysis showed blood vessels around them, as well as inflammatory cells and a fibrotic layer. **Conclusions:** Microencapsulated cells were able to ameliorate some aspects of the disease, indicating their potential as a treatment. To achieve better performance of the microcapsules, improvements such as the modulation of inflammatory response are suggested.

Key words: APA microcapsules, cell encapsulation, cell therapy, gene therapy, Mucopolysaccharidosis type I

Abbreviations: APA, alginate-poly-L-lysine-alginate; ERT, enzyme replacement therapy; GAG, glycosaminoglycans; IDUA, α-L-iduronidase; LSD, lysosomal storage disorder; MPS I, mucopolysaccharidosis type I; rBHK, recombinant Baby Hamster Kidney.

Introduction

Mucopolysaccharidosis type I (MPS I) is a lysosomal storage disorder (LSD) caused by mutations in the gene coding α-L-iduronidase (IDUA; EC 3.2.1.76), a lysosomal hydrolase involved in the degradation of the glycosaminoglycans (GAG) heparan and dermatan sulfate [1]. The consequent accumulation of these substrates throughout the cells leads to a chronic, progressive and multisystemic pathological condition. MPS I manifests early in childhood and displays a wide range of clinical manifestations with varying degrees of cardiorespiratory, musculoskeletal and central nervous system commitment [2–4].

Current available treatments for MPS I patients consist in hematopoietic stem cell transplantation (HSCT) and enzyme replacement therapy (ERT). Although their widespread application and clinical benefits, some shortcomings have been noted. HSCT needs to be performed early in life; it is associated with high morbidity and mortality and requires a compatible donor [5]. ERT is the most used treatment for this disorder, but it is also limited considering that the enzyme does not reach several affected organs such as brain, joints and heart valves, weekly infusions are necessary and the drug has a high cost [4]. Both treatments are based on the fact that systemic released lysosomal enzymes can be taken up by mannose-6-phosphate receptors present in the cells. Once internalized, the enzymes reach the lysosomes and degrade the accumulated storage material [6]. Using the same principle, gene therapy is a promising method to overcome the hurdles of ERT and HSCT, as it has a potential to provide a stable source of the enzyme with direct and effective delivery to targeted organs [6,7]. LSDs are a good model for such therapy, as they are monogenic disorders and even small increases in enzyme levels (10-20%) can greatly improve clinical outcome [7].

Cell microencapsulation technology is a gene/cell therapy system for the delivery of biologically active compounds. It consists in the immobilization of genetically modified cells within a polymeric semipermeable membrane, which allows the exchange of metabolites and nutrients between the cells and the external environment and it also prevents contact of host immune system [8,9]. The microenvironment can provide biochemical, cellular, and physical conditions that guide cellular processes, such as differentiation, proliferation, and migration [10]. Thereby, this device permits a localized and controlled release of the desired therapeutic factor in a sustained way, being an interesting approach for treating LSDs such as MPS I, since the enzyme secreted by the recombinant cells can be taken up by surrounding deficient cells [8,9]. In the past few years, several studies have reported cell encapsulation as a potential and promising treatment for LSDs [11–13], cardiac diseases [14], diabetes [15], cancer [16] and neurodegenerative diseases such as Alzheimer and Parkinson Diseases [17,18].

To achieve the aforementioned advantages of this technology, the election of an adequate biomaterial and the site for microcapsules implantation are important issues to be taken into account. Among a variety of natural and synthetic polymers that have been used for cell encapsulation, alginate is one of the most frequently employed biomaterial due to its positive features such as good biocompatibility and easy gelling properties [19,20]. This biomaterial creates three-dimensional structures when it reacts with divalent cations such as Ca^{2+} [21]. Moreover, the alginate composition has been optimized by the combination with poly-L-lisine (PLL), a polycation used to provide strength to the microcapsule and adjust their permeability. Alginate-PLL-alginate (APA) microcapsules are composed by an alginate core surrounded by a PLL layer that at the same time is covered by an outer alginate membrane, forming a system that has been the most widely used for microcapsule formation with a variety of applications, showing suitable

mechanical strength and resistance to swelling [19,22]. Regarding the implantation site, the preferred areas have been the intraperitoneal and the subcutaneous space [19]. Notably, the subcutaneous space provides an easy access for implantation, since the microcapsules are injected in a minimally invasive manner into a target tissue, thus avoiding surgery. In addition, this method avoids the dissemination of the beads, making easier their localization and posterior retrieval for evaluation [23].

Previously, we developed a baby hamster kidney (BHK) cell line genetically modified to overexpress IDUA [24], and alginate microcapsules containing these recombinant cells were able to correct the enzyme deficiency of fibroblasts from MPS I patients *in vitro* [11]. Also, experiments *in vivo* were performed implanting microencapsulated cells in the peritoneum of MPS I mouse model [25]. However, the treatment was able to achieve only a partial correction of the pathology. Once cell microencapsulation is a noteworthy approach to be considered for MPS I therapy, we decided to restructure the microcapsule layers and to implant the devices in a site considered more suitable for our purpose. Thus, in the present study we produced APA microcapsules containing recombinant cells overexpressing IDUA, which was implanted in the subcutaneous space of MPS I mouse model in order to evaluate their potential efficiency as a treatment.

Methods

Animals

We used *Idua*$^{-/-}$ mice (MPS I mice, kindly provided by Dr Elizabeth Neufeld, UCLA) on a C57BL/6 background [26] and their normal littermates to perform the experiments. Animals were maintained in conventional housing under a 12 h light/12 h

dark cycle with controlled temperature (19 ± 1 ° C) and humidity (50 ± 10%). At the end of experiments, mice were anesthetized by isoflurane inhalation and killed by cervical dislocation. The study was approved by the ethics review board of Hospital de Clínicas de Porto Alegre (Permit Number: 12-0311) and all procedures were performed in accordance to National and International Animal Ethic Guidelines.

Cell line and APA microcapsules production

We used a Baby Hamster Kidney (BHK) cell line transfected with the plasmid pR-IDUA and the recombinant cells (rBHK) overexpressing IDUA were selected for encapsulation [24]. Culture medium was collected to measure the enzyme activity and then rBHK cells were immobilized into APA microcapsules using an encapsulation unit, type J1 (Nisco, Zurich, Switzerland) attached to a JMS syringe pump. The cells were harvested and re-suspended in 1.5% Ultra-Pure Low Vicosity Guluronic (UP LVG) alginate solution (FMC Nova Matrix, Norway) at 8.3 x 10^7 cells/mL. The suspension was extruded through a 27-G needle using an infusion rate of 40 mL/h and an air flow of 4 L/min. Droplets fell into 80 mM $CaCl_2$ solution forming spherical hydrogel beads containing embedded cells. They were maintained in agitation for 7 min for complete ionic gelation and then were ionically crosslinked with 0.05% poly-L-lysine hydrobromide (PLL; Sigma-Aldrich, USA) for 5 min, followed by a coating with 0.1% sodium alginate solution during 5 min. Cell encapsulation was performed under sterile conditions and all solutions were sterilized by filtration. The resulting capsules were separated in amounts corresponding to a volume of 300 μL of alginate solution and maintained under normal culture conditions (DMEM supplemented with 10% fetal bovine serum at 37 ° C and 5% CO_2) for 24 h prior to implantation. After this time, medium was collected to evaluate the

IDUA released by the encapsulated cells. We also analyzed the morphology of APA microcapsules under an optical microscope.

Experimental design

For the treatment, recombinant cells overexpressing IDUA were encapsulated and evaluated pre-implantation. After evaluation, they were implanted in the subcutaneous tissue (treated group, n=8) of 4-moths-old MPS I mice. Three animals were killed 24 h later and the remaining animals were killed at day 120 post-implantation. Urine and blood samples were collected periodically over the treatment to measure GAG levels and IDUA activity, respectively. After cervical dislocation, liver, heart and kidney were harvested in order to perform IDUA activity assay, biochemical and histological GAG evaluation and capsules were explanted for histological analysis. Control groups consisted of age-matched untreated MPS I and normal mice (4-5/group).

APA microcapsules implantation

The microcapsules were implanted in the dorsal subcutaneous area of 4-month-old MPS I mice. To do so, animals were maintained under anesthesia by isoflurane inhalation and an amount of capsules corresponding to 300 μL of cell suspension (2.5×10^7 cells/animal) was carefully injected subcutaneously using a 14-G catheter (Medex, USA).

IDUA activity

The IDUA activity was measured in the culture medium collected before encapsulation, 24 h post-encapsulation and in the tissues and serum from the animals. Tissues were previously homogenized in distilled water, centrifuged, and the supernatant was collected for the assay, while the other samples were directly used. IDUA activity

assay was performed incubating the samples with the fluorescent substrate 4-methylumbelliferyl-alpha-L–iduronide (Glycosynth, Warrington, UK) at 37°C for 1 h in a formate buffer pH 3.5. Protein content of the tissues was measured using the Lowry method. Results were calculated as nmol/h/mL for serum and medium. For tissues, results were calculated as nmol/h/mg protein and expressed as a percentage of normal activity.

GAG quantification

Tissue and urinary GAG content was biochemically measured using the dymethyl blue assay. Briefly, 25 µL of sample supernatant were mixed with dymethyl blue solution (0.3 mol/L Dymethyl blue with 2 mol/L Tris) and absorbance was detected at 530 nm. Tissues were previously homogenized in phosphate buffer pH 6.5 containing papain 300 µg/mL, and the supernatant was used in the assay. The total tissue protein quantification was determined with the Lowry assay and results were expressed as µg GAG/mg protein; in the graphs they were shown as a percentage of normal levels. Urinary GAGs was measured without previous preparation of the sample and results were expressed as µg GAG/mg creatinine.

Histological analysis

Liver, kidney, heart and the microcapsules were fixed in 10% formalin solution, embedded in paraffin blocks and serially sectioned for histological analysis. To verify the presence of GAG accumulation, tissue sections were stained for Alcian blue using hematoxylin-eosin (H&E) as counterstain. The capsules were stained for H&E to examine the structure of the tissue surrounding the beads and the Sirius red staining, which

specifically stains collagen fibers, was performed to analyze fibrosis induction. Stained sections were evaluated by light microscopic examination (Olympus BX51) and photographic images were taken using Olympus DP71 camera.

Statistical analysis

Statistical analysis was performed by GraphPad Prism (version 5.01) using Student's t test. The comparisons were made between normal and MPS I groups. Statistically significant differences among groups were considered when $p<0.05$.

Results

Cells and capsules analyses before implantation

To verify the metabolic activity of the rBHK cells used in this study, we evaluated the IDUA production pre and post-encapsulation. Before encapsulation, the selected cells released IDUA in the medium at a rate of 251.9 nmol/h/mL. Then, they were immobilized in APA microcapsules and 24 h later the enzyme activity in the medium was measured again. The IDUA produced at this time by an amount of microcapsules separated to be further injected in the animals was 158.9 nmol/h/mL, corresponding to 63% of the non-encapsulated cells activity. In addition, APA microcapsules were visualized under an optical microscope, showing a spherical morphology without irregularities on their surface (Fig. 1).

Treatment evaluation

Four-months-old MPS I mice were treated with APA-microcapsules implanted in the subcutaneous tissue. In a short-term experiment, 3 animals were killed 24 h post-

implantation. As shown in the figure 2A, after 24 h the beads were able to release IDUA *in vivo*, increasing IDUA activity levels in the liver (an average of 4-fold of untreated mice, p=0.0207), kidney (2.4-fold, p=0.0015) and heart (7-fold, p=0.0021). In the serum, just a slight increase in the enzyme activity was detected, without statistical significance (Fig. 2B).

A long-term treatment was performed and animals were monitored over 120 days. IDUA activity was measured in the serum and, compared to pre-treatment levels, an increase was detected at days 15 (p= 0.0327), 30 (p= 0.0147) and 45 (p= 0.0491), but it was not different from untreated mice after this point (Fig. 3A). Urinary GAG levels remained elevated and no differences were detected at any time (Fig. 3 B).

Animals were killed after 120 days of treatment and the liver, kidney and heart were collected. IDUA activity assay was performed and we observed higher levels in the liver (4.8-fold, p=0.0014), kidney (5.3-fold p=0.0018) and heart (5.5-fold, p=0.0222) of treated MPS I mice when compared to untreated animals (Fig. 3C). These results correspond to 6.3%, 13% and 7.5% of the IDUA activity in normal mice. The biochemical measurement of GAG storage revealed an average reduction of 34% in the liver (p= 0.07) and 32% in the kidney (p=0.001), comparing treated mice with untreated at same age (8 months). No reduction was observed in the heart (p=0.2) (Fig. 3D).

In order to visualize the tissue GAG content, the liver, kidney and heart from treated and untreated MPS I mice, as well normal controls, were submitted to histological analysis using Alcian blue stain. Untreated MPS I tissues (Fig. 4B, E and H) presented a quite evident GAG accumulation, while blue cells were not observed in healthy tissues (Fig. 4A, D and G). In untreated MPS I liver, a vacuolized structure in the parenchyma is remarkable at 8 months of age (Fig. 4B). Interestingly, the treatment using APA

microcapsules was able to reorganize this architecture in some extent (Fig. 4C). In both liver and kidney, the amount of cells containing GAG storage was reduced in some areas, but a considerable accumulation was still present overall (Fig. 4C and F). The heart did not present evidences of reduction in the GAG content (Fig. 4I).

Capsules analyses after a long-term treatment

The implanted APA-microcapsules were easily recovered from the subcutaneous tissue at day 120 post-implantation. On retrieval, they were aggregated as a cluster, forming an irregular structure (Fig. 5A). Using H&E staining, it was revealed an immune response by the presence of inflammatory infiltrate and host cells such as macrophages around the capsules (Fig. 5B and C). Also, we recognized endothelial cells and some blood capillaries often containing red blood cells in the proximity of the implants (Fig. 5D and E). By Sirius Red staining it was possible to visualize the formation of a fibrotic layer with collagen deposition surrounding the capsules (Fig. 5F).

Discussion

Cell microencapsulation has been considered a promising possibility for the long-term treatment of several pathologies, including LSDs [8]. Since it could alleviate the shortcomings of conventional treatments, a nonviral gene therapy based on encapsulated cells overexpressing IDUA is an attractive alternative to MPS I therapy as it seeks to provide a continuous release of the enzyme. Our study reports the production of APA microcapsules and their application for the treatment of MPS I mouse model.

Firstly, microcapsules were evaluated *in vitro* to determine their suitability for the following *in vivo* assays. We observed that cells were correctly adapted to the biopolymer and all capsules showed a uniform and spherical morphology without irregularities on their surface. This evaluation consists in the fact that besides the biomaterial employed the morphology is also important for a great biocompatibility [27]. Additionally, IDUA was detected in the culture medium at 24 h post-encapsulation, indicating that the APA microcapsule's permselective membrane allows the diffusion of the enzyme and, consequently, they are viable for *in vivo* implantation.

Encapsulated cells were implanted in MPS I mice and we observed that after 24 h the enzyme could be released and taken up by deficient cells, increasing IDUA levels in the liver, kidney and heart. This result suggests the rapid functionality of the rBHK cells immobilized in APA microcapsules *in vivo*. **S**uch a rapid correction was not expected because the subcutaneous space is not considered a site able to provide an early neovascularization [28]. One possibility for this finding is that higher levels of IDUA were initially released from the microcapsules and an amount of enzyme was taken up even with a poor blood supply at this time point.

In order to analyze the functionality of the microcapsules in a prolonged period of time, a group of mice were kept for up to 120 days. IDUA levels were detected in the serum in the first 45 days of treatment, confirming that the enzyme was being released from the capsules. However, a decrease in serum IDUA levels was observed after this time. The reasons for this decline may include the immune response against the capsules (as shown by H&E stain in the figure 5), the transgene silencing or even cell death inside the capsules.

Despite the reduction in serum enzyme levels at day 120 post-implantation, we detected IDUA activity in the liver, kidney and heart of treated mice, indicating that a continuous release of the enzyme was provided by APA microcapsules, even though it was not observed in the blood circulation. In the kidney, 13% of the normal enzyme activity provided a reduction of 32% in the GAG content, and in the liver 6.3% of normal activity reduced 34% of GAG levels. Previously, findings of MPS I mice treated with microcapsules intraperitoneally also showed a partial correction of GAG storage in the organs [25]. Nonetheless, our result was difficult to be confirmed by histology, since considerable amounts of GAG are still visualized in the cells. Untreated MPS I mice showed an evident cell vacuolization in the hepatic tissue, which is a hallmark of LSDs and progressively increase with time [29]. Interestingly, it was possible to visualize a reduction of the cytoplasmic inclusions and a re-organization of the parenchyma in 8-month-old MPS I mice. This result is similar to the results observed in a study using encapsulated cells for MPS II treatment [30]. Urinary GAG levels did not decrease over the time and it was suggested that their normalization requires the complete correction of tissue GAG content [30].

Microcapsules were retrieved from the subcutaneous space for histological analysis after treatment. We observed the formation of some blood vessels around the microcapsules aggregate, which might be helpful to improve the access of oxygen and nutrients by the cells and the uptake of the released enzyme [22]. Similarly, the presence of blood capillaries around the capsules was previously showed by other studies at 2 weeks and 130 days post-implantation [22,31], evidencing the ability of the subcutaneous space to provide a suitable blood supply due to a neovascularization process over time.

An immune reaction was revealed by the presence of inflammatory cells within the beads. Likewise, we found a fibrotic overgrowth in the surface of the capsules. Fibrotic

process is a widely accepted metric of biocompatibility evaluation of materials and a hinder in the diffusion of cell nutrients and therapeutic products across the capsule membrane is associated to fibrosis [32]. Thus, the fibrotic layer observed could be preventing the release of IDUA from the microcapsules over time, but just in some extend, since the enzyme activity levels were detected after 120 days of implantation. A high level of biocompatibility is essential assuming that one aim of the encapsulation is to protect the enclosed cells from the host's immune response. However, even in ultrapure alginates, as the one we used, some residual impurities may be present, thereby compromising the biocompatibility [33]. It is important to be noted that although microcapsules are immunoprotective, they are not meant to prevent immune responses which could occur due to leakage of antigens, breakage of microspheres, protrusion of cells, and responses associated with the surgery [20]. Moreover, it was reported the development of neutralizing antibodies against IDUA after treatment with ERT [34], as well as with gene therapy [25,35,36], suggesting that an immune reaction to the enzyme could be partially impairing the efficacy of our treatment, although we did not measure that.

In conclusion, our results indicate that even in the presence of an immune response, a reasonable amount of IDUA was taken up by the vessels present in the tissue surrounding the microcapsules, allowing the enzyme to reach the peripheral organs. Further improvements in this system are needed to reduce GAG levels to normal values and increase the treatment efficacy.

Acknowledgments: This work was supported by grants from Conselho Nacional de Desenvolvimento Cientifico (CNPq) and from Fundo de Incentivo à Pesquisa do Hospital de Clinicas de Porto Alegre (FIPE-HCPA). The authors thank the Animal Facility of Hospital de Clínicas de Porto Alegre for the assistance provided.

Disclosure of interests: The authors have no conflict of interest to disclose.

References

[1] Matte U, Yogalingam G, Brooks D. Identification and characterization of 13 new mutations in mucopolysaccharidosis type I patients. Mol Genet Metab 2003;78:37–43.

[2] Muenzer J. Overview of the mucopolysaccharidoses. Rheumatology 2011;50:v4–12.

[3] Clarke L a, Wraith JE, Beck M, Kolodny EH, Pastores GM, Muenzer J, et al. Long-term efficacy and safety of laronidase in the treatment of mucopolysaccharidosis I. Pediatrics 2009;123:229–40.

[4] Giugliani R, Federhen A, Rojas MVM, Vieira T, Artigalás O, Pinto LL, et al. Mucopolysaccharidosis I, II, and VI: Brief review and guidelines for treatment. Genet Mol Biol 2010;33:589–604.

[5] Boelens JJ, Prasad VK, Tolar J, Wynn RF, Peters C. Current international perspectives on hematopoietic stem cell transplantation for inherited metabolic disorders. Pediatr Clin North Am 2010;57:123–45.

[6] Tomanin R, Zanetti A, Zaccariotto E, D'Avanzo F, Bellettato CM, Scarpa M. Gene therapy approaches for lysosomal storage disorders, a good model for the treatment of mendelian diseases. Acta Paediatr 2012;101:692–701.

[7] Baldo G, Giugliani R, Matte U. Gene delivery strategies for the treatment of mucopolysaccharidoses. Expert Opin Drug Deliv 2014;11:449–59.

[8] Matte U, Lagranha VL, de Carvalho TG, Mayer FQ, Giugliani R. Cell microencapsulation: a potential tool for the treatment of neuronopathic lysosomal storage diseases. J Inherit Metab Dis 2011;34:983–90.

[9] Orive G, Santos E, Pedraz JL, Hernández RM. Application of cell encapsulation for controlled delivery of biological therapeutics. Adv Drug Deliv Rev 2014;67-68C:3–14.

[10] Vermonden T, Fedorovich NE, van Geemen D, Alblas J, van Nostrum CF, Dhert WJ a, et al. Photopolymerized thermosensitive hydrogels: synthesis, degradation, and cytocompatibility. Biomacromolecules 2008;9:919–26.

[11] Baldo G, Quoos Mayer F, Burin M, Carrillo-Farga J, Matte U, Giugliani R. Recombinant encapsulated cells overexpressing alpha-L-iduronidase correct

enzyme deficiency in human mucopolysaccharidosis type I cells. Cells Tissues Organs 2012;195:323–9.

[12] Nakama H, Ohsugi K, Otsuki T. Encapsulation cell therapy for mucopolysaccharidosis type VII using genetically engineered immortalized human amniotic epithelial cells. Tohoku J Exp Med 2006;219:23–32.

[13] Piller Puicher E, Tomanin R, Salvalaio M, Friso a, Hortelano G, Marin O, et al. Encapsulated engineered myoblasts can cure Hurler syndrome: preclinical experiments in the mouse model. Gene Ther 2012;19:355–64.

[14] Paul A, Ge Y, Prakash S, Shum-Tim D. Microencapsulated stem cells for tissue repairing: implications in cell-based myocardial therapy. Regen Med 2009;4:733–45.

[15] Calafiore R, Basta G. Clinical application of microencapsulated islets: actual prospectives on progress and challenges. Adv Drug Deliv Rev 2014;67-68:84–92.

[16] Goren A, Gilert A, Meyron-Holtz E. Alginate encapsulated cells secreting Fas-ligand reduce lymphoma carcinogenicity. Cancer Sci 2012;103:116–24.

[17] Garcia P, Youssef I, Utvik JK, Florent-Béchard S, Barthélémy V, Malaplate-Armand C, et al. Ciliary neurotrophic factor cell-based delivery prevents synaptic impairment and improves memory in mouse models of Alzheimer's disease. J Neurosci 2010;30:7516–27.

[18] Klinge PM, Harmening K, Miller MC, Heile A, Wallrapp C, Geigle P, et al. Encapsulated native and glucagon-like peptide-1 transfected human mesenchymal stem cells in a transgenic mouse model of Alzheimer's disease. Neurosci Lett 2011;497:6–10.

[19] Santos E, Pedraz JL, Hernández RM, Orive G. Therapeutic cell encapsulation: ten steps towards clinical translation. J Control Release 2013;170:1–14.

[20] Rokstad AM a, Lacík I, de Vos P, Strand BL. Advances in biocompatibility and physico-chemical characterization of microspheres for cell encapsulation. Adv Drug Deliv Rev 2014;67-68:111–30.

[21] Mørch Y a, Donati I, Strand BL, Skjåk-Braek G. Effect of Ca2+, Ba2+, and Sr2+ on alginate microbeads. Biomacromolecules 2006;7:1471–80.

[22] Murua A, Castro M de, Orive G. In vitro characterization and in vivo functionality of erythropoietin-secreting cells immobilized in alginate-poly-L-lysine-alginate microcapsules. Biomacromolecules 2007;8:3302–7.

[23] Acarregui A, Pedraz JL, Blanco FJ, Hernández RM, Orive G. Hydrogel-based scaffolds for enclosing encapsulated therapeutic cells. Biomacromolecules 2013;14:322–30.

[24] Mayer FQ, Baldo G, de Carvalho TG, Lagranha VL, Giugliani R, Matte U. Effects of cryopreservation and hypothermic storage on cell viability and enzyme activity in recombinant encapsulated cells overexpressing alpha-L-iduronidase. Artif Organs 2010;34:434–9.

[25] Baldo G, Mayer FQ, Martinelli B, Meyer FS, Burin M, Meurer L, et al. Intraperitoneal implant of recombinant encapsulated cells overexpressing alpha-L-iduronidase partially corrects visceral pathology in mucopolysaccharidosis type I mice. Cytotherapy 2012;14:860–7.

[26] Ohmi K, Greenberg DS, Rajavel KS, Ryazantsev S, Li HH, Neufeld EF. Activated microglia in cortex of mouse models of mucopolysaccharidoses I and IIIB. Proc Natl Acad Sci U S A 2003;100:1902–7.

[27] Hernández RM a, Orive G, Murua A, Pedraz JL. Microcapsules and microcarriers for in situ cell delivery. Adv Drug Deliv Rev 2010;62:711–30.

[28] Vériter S, Gianello P, Dufrane D. Bioengineered sites for islet cell transplantation. Curr Diab Rep 2013;13:745–55.

[29] Heard JM, Bruyère J, Roy E, Bigou S, Ausseil J, Vitry S. Storage problems in lysosomal diseases. Biochem Soc Trans 2010;38:1442–7.

[30] Friso A, Tomanin R, Alba S, Gasparotto N, Puicher EP, Fusco M, et al. Reduction of GAG storage in MPS II mouse model following implantation of encapsulated recombinant myoblasts. J Gene Med 2005;7:1482–91.

[31] Vériter S, Mergen J, Goebbels R-M, Aouassar N, Grégoire C, Jordan B, et al. In vivo selection of biocompatible alginates for islet encapsulation and subcutaneous transplantation. Tissue Eng Part A 2010;16:1503–13.

[32] Tam SK, de Haan BJ, Faas MM, Hallé J-P, Yahia L, de Vos P. Adsorption of human immunoglobulin to implantable alginate-poly-L-lysine microcapsules: effect of microcapsule composition. J Biomed Mater Res A 2009;89:609–15.

[33] Dusseault J, Tam SK, Ménard M, Polizu S, Jourdan G, Yahia L, et al. Evaluation of alginate purification methods: effect on polyphenol, endotoxin, and protein contamination. J Biomed Mater Res A 2006;76:243–51.

[34] Beck M. Therapy for lysosomal storage disorders. IUBMB Life 2010;62:33–40.

[35] Ciron C, Desmaris N, Colle M-A, Raoul S, Joussemet B, Vérot L, et al. Gene therapy of the brain in the dog model of Hurler's syndrome. Ann Neurol 2006;60:204–13.

[36] Di Domenico C, Villani G. Gene therapy for a mucopolysaccharidosis type I murine model with lentiviral-IDUA vector. Hum Gene Ther 2005;90:81–90.

Legends of figures

Figure 1. Microscopic view of APA microcapsules containing recombinant rBHK cells before implantation. Magnification 100x.

Figure 2. Results from 24 h treatment. (A) Serum and (B) tissue IDUA activity levels 24 h post-implantation.

Figure 3. Results from 120-days treatment. (A) Serum IDUA activity over 120 days compared to day 0. Student's t-test. * $p<0.05$. (B) Urinary GAG levels over 120 days compared to day 0. (C) Tissue IDUA activity after 120 days of treatment. (D) Tissue GAG levels after 120 days of treatment.

Figure 4. Histologic analysis of tissues 120 days post-implantation. Liver, kidney and heart were stained for Alcian blue. GAG storage is represented by blue cells (arrows). (A, D and G) Normal tissues. (B, E and H) Untreated MPS I tissues. (C, F and I) Tissues from treated MPS I mice after 120 days of APA microcapsules implantation. Magnification 400x.

Figure 5. Analysis of APA microcapsules 120 days post-implantation. (A) Macroscopic aspect of microcapsules on retrieval. They were aggregated and forming an irregular structure. (B) Histologic analysis (H&E stain) indicating the capsule within embedded rBHK cells and the inflammatory infiltrate. Magnification 200x. (C) Inflammatory infiltrate containing macrophages (arrows) and multinucleated giant cell (arrowhead) surrounding and attached to the capsule, evidencing an immune reaction. Magnification 400x. (D and E) Blood vessels and endothelial cells (arrows) present in the proximity of the capsule. Magnification 400x. (F) Histologic analysis (Sirius red stain) indicating a fibrotic overgrowth and collagen deposition around the capsules (arrow). Magnification 400x.

Figures

Figure 1

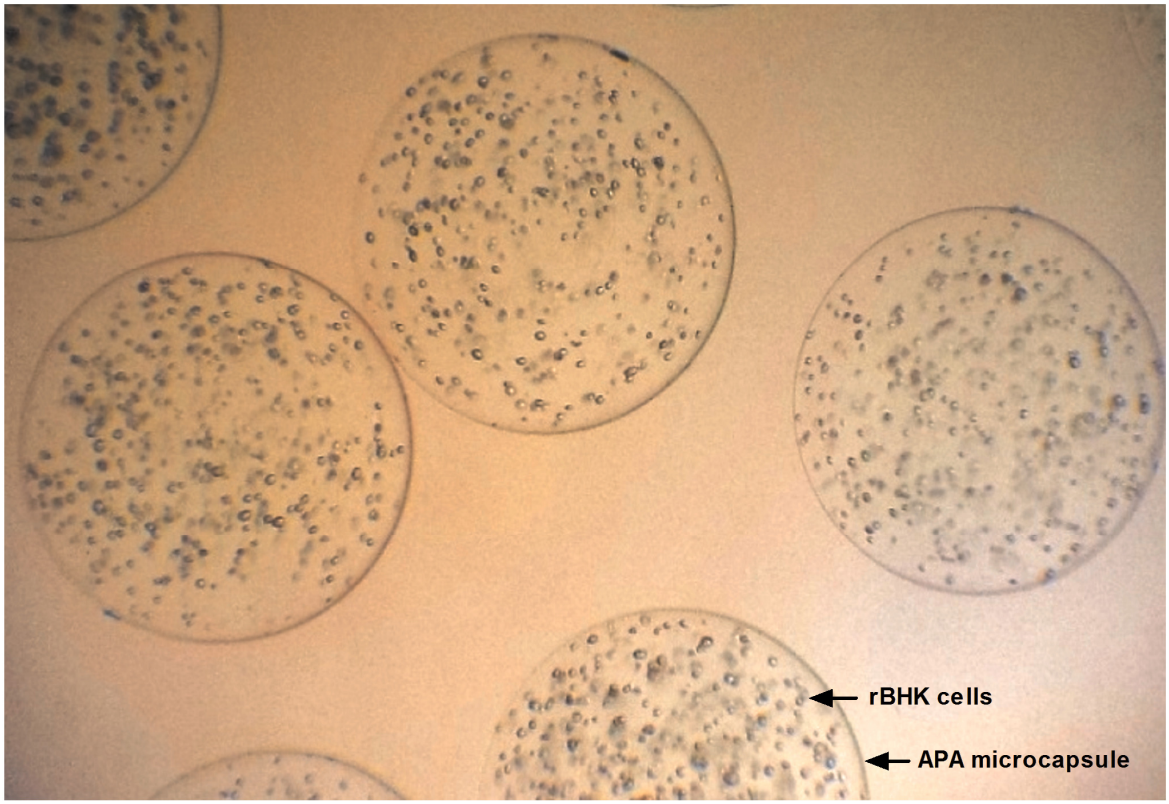

Figure 2

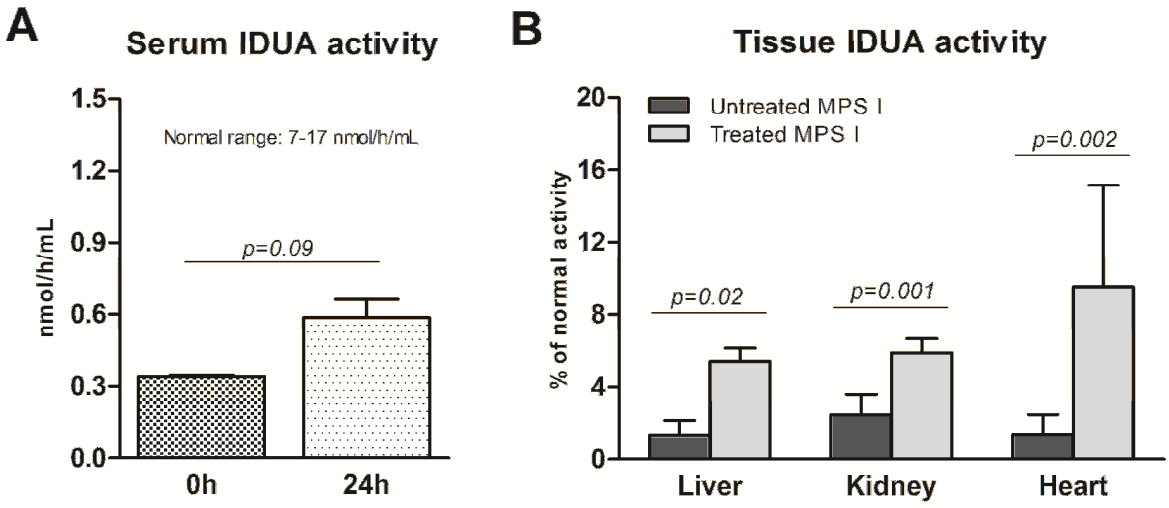

Figure 3

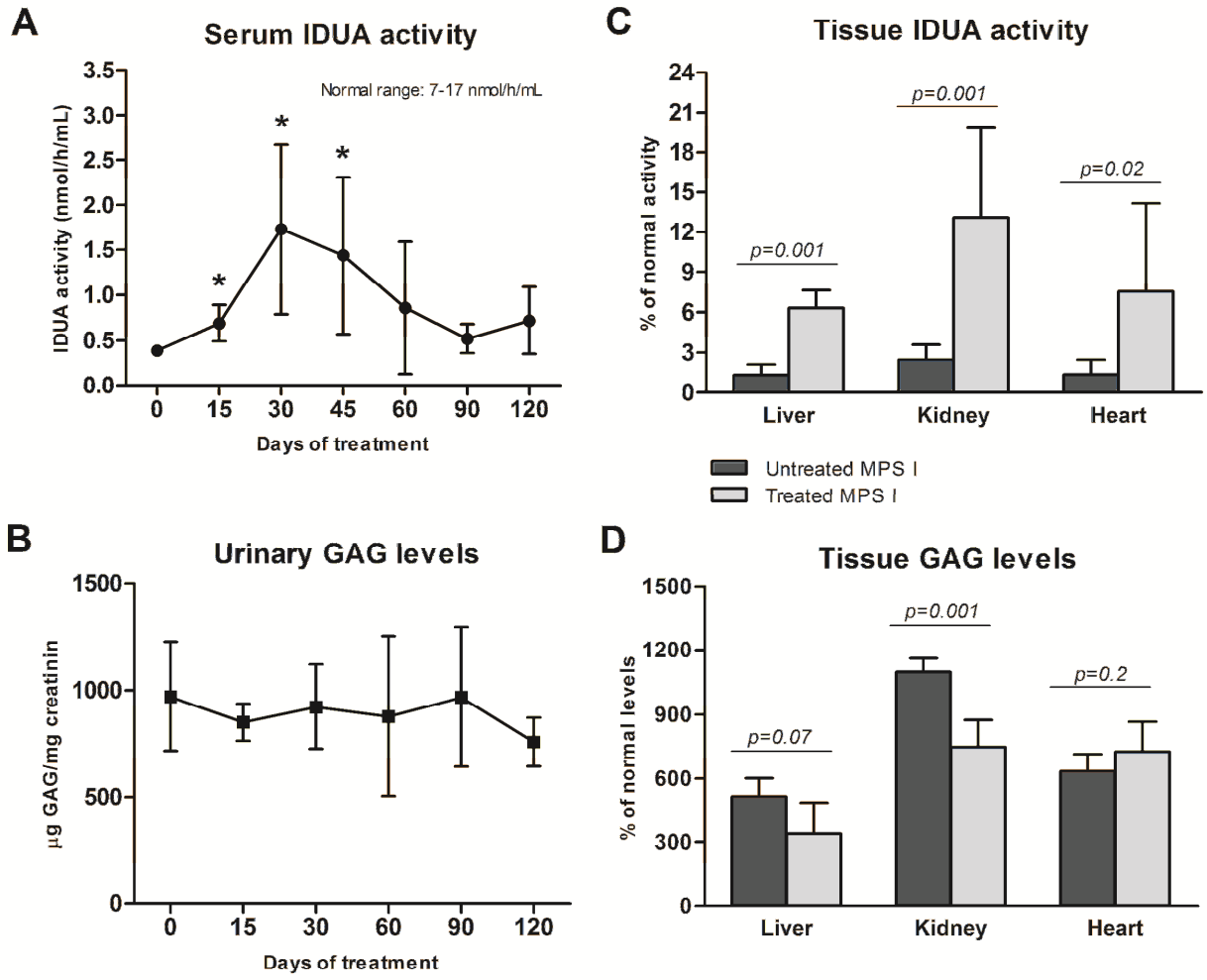
A
Serum IDUA activity
Normal range: 7-17 nmol/h/mL
IDUA activity (nmol/h/mL)
3.5
3.0
2.5
2.0
1.5
1.0
0.5
0.0
*
*
*
0
15
30
45
60
90
120
Days of treatment
C
Tissue IDUA activity
% of normal activity
24
21
18
15
12
9
6
3
0
p=0.001
p=0.001
p=0.02
Liver
Kidney
Heart
Untreated MPS I
Treated MPS I
B
Urinary GAG levels
µg GAG/mg creatinin
1500
1000
500
0
0
15
30
60
90
120
Days of treatment
D
Tissue GAG levels
% of normal levels
1500
1200
900
600
300
0
p=0.07
p=0.001
p=0.2
Liver
Kidney
Heart

Figure 4

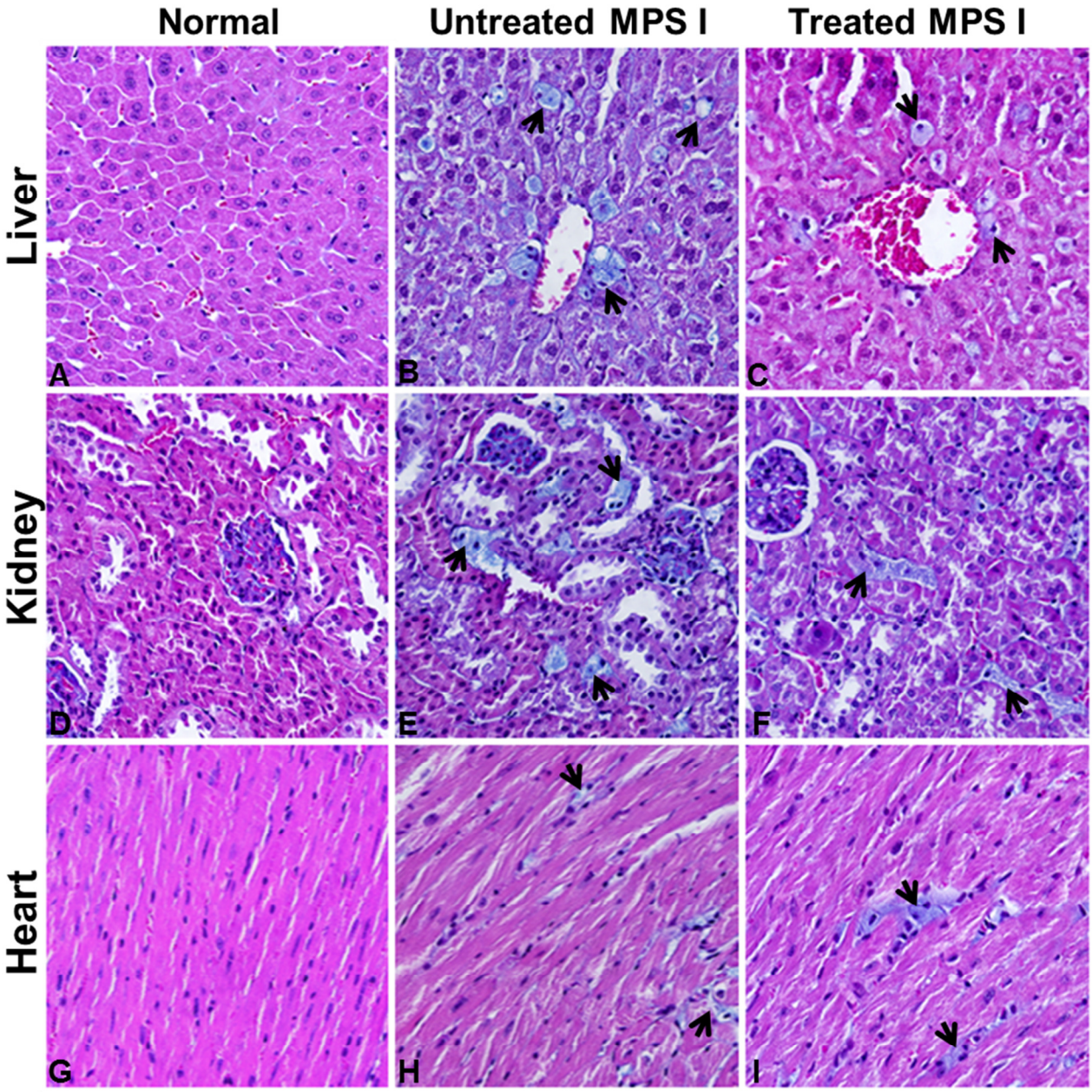
Normal
Untreated MPS I
Treated MPS I
Liver
Kidney
Heart
A
B
C
D
E
F
G
H
I

Figure 5

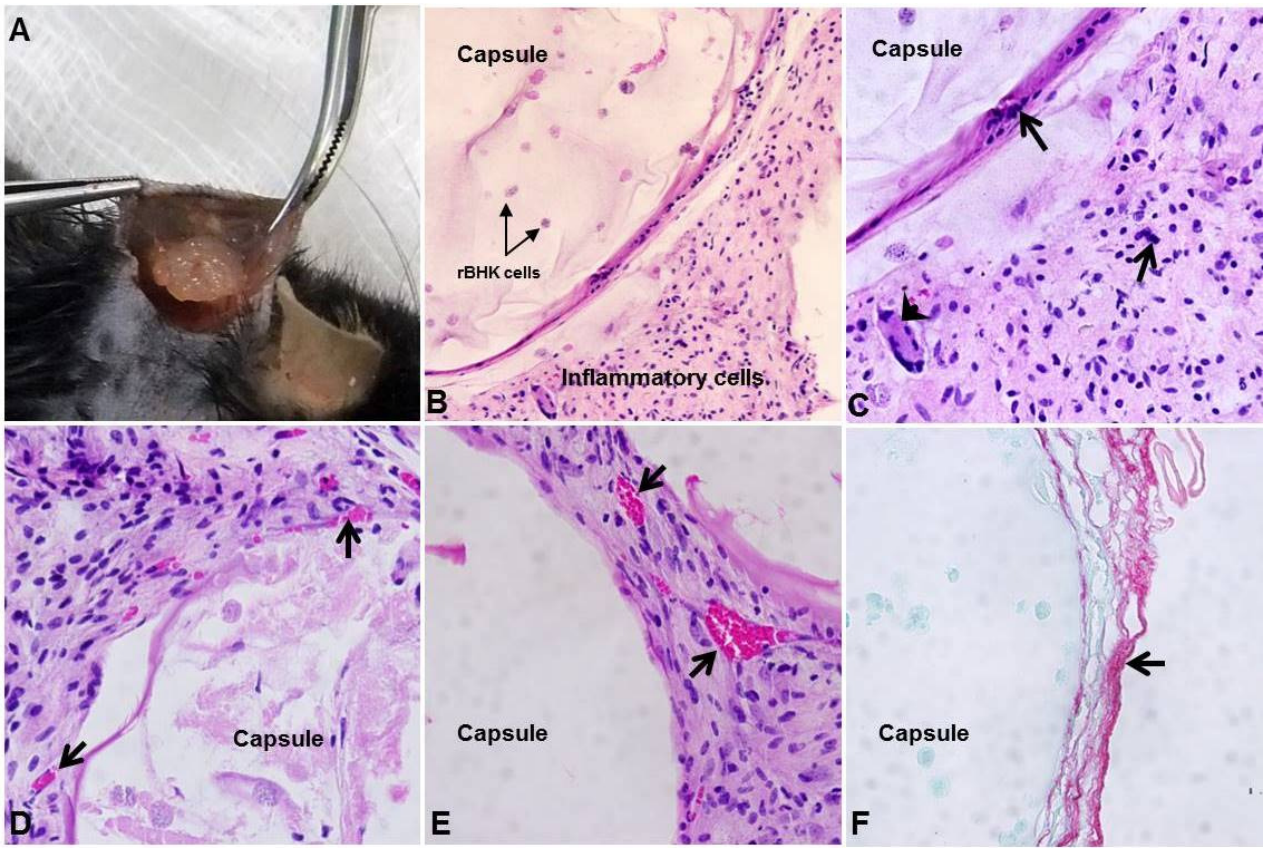
A
Capsule
rBHK cells
Inflammatory cells
B
Capsule
C
Capsule
D
E
Capsule
F
Capsule

CAPÍTULO II

Omentum is a safe site for microcapsule implant in rodents: study on the Mucopolysaccharidosis type I model

Artigo a ser submetido para a revista Artificial Organs

OMENTUM IS A SAFE SITE FOR MICROCAPSULE IMPLANT IN RODENTS: STUDY ON THE MUCOPOLYSACCHARIDOSIS TYPE I MODEL

Authors:

Barbara Zambiasi Martinelli[1,2],

Guilherme Baldo[1,3]

Nelson Alexandre Kretzmann Filho[1]

Ursula Matte[1,4]

Roberto Giugliani[1,4]

[1] Gene Therapy Center, Hospital de Clínicas de Porto Alegre, Brazil

[2] Biochemistry Department, Universidade Federal do Rio Grande do Sul, Porto Alegre, Brazil

[3] Physiology Department, Universidade Federal do Rio Grande do Sul, Porto Alegre, Brazil

[4] Genetics Department, Universidade Federal do Rio Grande do Sul, Porto Alegre, Brazil

Corresponding author:

Ursula Matte

umatte@hcpa.ufrgs.br

Gene Therapy Center, Hospital de Clínicas de Porto Alegre

Rua Ramiro Barcelos, 2350

Porto Alegre, RS

90035-903

Telephone: 55 51 3359 8838

Fax: 55 51 3359 8010

Abstract

Mucopolysaccharidosis type I (MPS I) occurs due to a deficiency of α-L-iduronidase (IDUA), leading to the accumulation of glycosaminoglycans (GAG). One promising approach for the treatment is the cell microencapsulation, a gene/cell based therapy where cells are genetic engineered to overexpress the enzyme of interest. The ideal implantation site was not yet determined and we considered the omentum a good candidate, since its high vascular density could provide adequate conditions to the cells and improve the taken up of the enzyme. Thus, we aimed to evaluate the efficiency of microencapsulated cells testing the omentum as the implant site. Recombinant cells overexpressing IDUA were immobilized in alginate-poli-L-lysine-alginate microespheres and implanted in an omentum pouch of 4-month-old MPS I mice. Some animals were killed 24 h post-implantation and increased IDUA activity levels were detected in the liver (7.9-fold of untreated mice), kidney (2.3-fold) and heart (6-fold). To verify the functionality in a long period, the treatment was also performed over 60 days. After this time, the omentum pouch was retrieved and we observed the presence of blood vessels throughout the pouch. Increased levels of IDUA activity were observed in the heart (4.5-fold) of treated mice, while the increase in the liver (2.6-fold, $p=0.08$) and kidney (4.2-fold, $p=0.056$) was not statistically significant. Histologic analysis and biochemical measurement of GAG in the tissues did not reveal differences between treated and untreated MPS I mice. Interestingly, we observed less cell vacuolization in the liver, as well as reorganization in the hepatic parenchyma. Our results showed that an adequate environment for the capsules was provided by the omentum. However, the release and taken up of the enzyme was efficient only in a short period, indicating that modifications in the technique could lead to a better performance.

Introduction

Mucopolysaccharidosis type I (MPS I) is a lysosomal storage disease (LSD) caused by a deficiency in α-L-iduronidase (IDUA; EC 3.2.1.76), which hydrolyzes terminal iduronic acid residues from the glycosaminoglycans (GAG) heparan sulfate (HS) and dermatan sulfate (DS), resulting in the accumulation of these substrates [1]. Consequently, several biochemical and physiological processes are affected, leading to a chronic and multisystemic pathological condition [2]. Treatments currently available for MPS I patients are hematopoietic stem cell transplantation (HSCT) and enzyme replacement therapy (ERT). Although their widespread application and clinical benefits, some shortcomings have been noted [3,4]. Therefore, the search for alternative strategies is highly desirable. Gene therapy based systems are promising methods to overcome the hurdles of ERT and HSCT, as it has a potential to provide constant delivery of a therapeutic product to targeted organs [5]. One strategy is the microencapsulation of genetically modified cells overexpressing the enzyme IDUA.

Cell microencapsulation is a biotechnological approach aiming an optimized delivery of biologically active compounds and has been applied in several fields of biomedicine, such as the treatment of neurological diseases, chronic anemia, bone defects, diabetes, lisosomal diseases, heart diseases and cancer [6–8]. In this system, a semi-permeable hydrogel membrane is used to encapsulate cells, preventing their direct contact with host immune cells while allowing exchange of nutrients and oxygen between the microcapsules and the extra-capsular environment [6,7]. The capsule can provide adequate conditions for the cells to survive, thus the enclosed cells are able to constantly synthesize and release the desired therapeutic compounds, as a somatic non-autologous gene therapy approach.

MPS I is a suitable candidate for this therapy because it is a monogenic disease and the clinical outcome can be improved with a small increase in the enzyme levels [5]. Since lysosomal enzymes can be released and taken up by mannose-6-phosphate receptors (M6PR) present in the cell surface, cells genetically engineered to overexpress IDUA can be immobilized in microcapsules, and these capsules can be surgically implanted *in situ* and used as a treatment. The enzyme secreted by the recombinant cells can be taken up by surrounding deficient cells. Once internalized, the enzyme reaches the lysosomes and degrades the accumulated storage material [7].

To date, a variety of biomaterials have been employed in the field of cell microencapsulation. Among them, alginate is by far the most frequently used polymer due to its advantages, including good biocompatibility, relatively low cost and easy gelation properties [9,10]. Alginate is a naturally occurring anionic polysaccharide polymer that creates three-dimensional structures when it reacts with ionic cross-linking agents, such as divalent cations (i.e., Ca^{2+}) [10]. Aditionally, the polyelectrolyte complexation of alginate capsules with a polycation, normally poly-L- lysine (PLL), is widely employed in order to increase the mechanical stability and adjust the permeability of the microcapsules. Considering that the positive charges of PLL are immunogenic, an additional alginate coat is necessary [11]. This type of microcapsule is commonly referred to as alginate-poly-L-lysine-alginate (APA) microcapsules.

Most of the studies implant the microcapsules in the subcutaneous space or intraperitoneally, but the omentum has been suggested as an alternative site for implantation. The omentum is well vascularized and has been described as a rich source of angiogenic factors [12,13], which may provide a better environment for the microcapsules. Another characteristic is that the layered structure of the omentum allows pouch formation, where microcapsules can be implanted and easily retrieved [14].

Our group developed a baby hamster kidney (BHK) cell line genetically modified to overexpress IDUA [15]. The microencapsulation of the recombinant cells was able to correct the enzyme deficiency of fibroblasts from MPS I patients *in vitro* [16], but less successful results were observed *in vivo* after microcapsules implantation in the peritoneum of MPS I mouse model [17]. Therefore in this work we aimed to produce APA microcapsules enclosing BHK cells overexpressing IDUA and to access the omentum as the implant site in order to treat MPS I mice.

Methods

Animals

We used *Idua*$^{-/-}$ mice (MPS I mice, kindly provided by Dr Elizabeth Neufeld, UCLA) on a C57BL/6 background [18] and their normal littermates to perform the experiments. Animals were genotyped at day 21 and maintained in conventional housing under a 12 h light/12 h dark cycle with controlled temperature (19 ± 1 ° C) and humidity (50 ± 10%). At the end of experiments, mice were anesthetized by isoflurane inhalation and killed by cervical dislocation. The study was approved by the authors' institutional ethics review board and all procedures were performed in accordance to National and International Animal Ethic Guidelines.

Experimental design

Recombinant cells overexpressing IDUA were encapsulated and implanted in the omentum (treated group, n=9) of 4-moths-old MPS I mice. Three animals were killed 24 h later and the remaining animals were killed at day 60 post-implantation. Urine and blood samples were collected periodically over the treatment to measure GAG levels and and

IDUA activity, respectively. After sacrifice, liver, heart and kidney were harvested in order to perform IDUA activity assay, biochemical and histological GAG evaluation, and capsules were explanted to histological analysis. Control groups consisted of untreated MPS I and normal mice of same age (4-5/group).

Cell line and APA microcapsules production

We used a Baby Hamster Kidney (BHK) cell line transfected with the plasmid pR-IDUA to generate recombinant BHK cells (rBHK) overexpressing IDUA (Mayer 2010). Previous to encapsulation, the culture medium of the selected cells was collected in order to measure the enzyme activity at this point and compare with the enzyme produced by the same amount of cells after encapsulation. The rBHK cells were immobilized into APA microcapsules using an encapsulation unit, type J1 (Nisco, Zurich, Switzerland) attached to a JMS syringe pump. The cells were harvested and re-suspended in 1.5% Ultra-Pure Low Vicosity Guluronic (UP LVG) alginate solution (FMC Nova Matrix, Norway) at 8.3 x 10^7 cells/mL. The suspension was extruded through a 27-G needle using an infusion rate of 40 mL/h and an air flow of 4L/min. Droplets fell into 80 mM $CaCl_2$ solution forming spherical hydrogel beads containing embedded cells. They were maintained in agitation for 7 min for complete ionic gelation and then were ionically crosslinked with 0.05% poly-L-lysine hydrobromide (PLL; Sigma-Aldrich, USA) for 5 min, followed by a coating with 0.1% sodium alginate solution during 5 min. Cell encapsulation was performed under sterile conditions and all solutions were sterilized by filtration before their use. The morphology of the resulting capsules was analyzed under an optical microscope and then maintained under normal culture conditions (DMEM supplemented with 10% fetal bovine serum at 37 ° C and 5% CO_2) for 24 h prior to implantation. At this time, medium was

collected to evaluate the IDUA released by the encapsulated cells and the implantation procedure was then performed.

APA microcapsules implantation

An amount of capsules corresponding to 100 μL of cell was implanted in the omentum of 4-months-old MPS I mice. Under general anesthesia with isoflurane inhalation, mice underwent a mini-laparotomy and the greater omentum was identified and spread out. Frequent irrigation with saline was ensured to prevent the omentum from drying up. APA microcapsules were placed on the surface of the surgically exposed omentum and a pouch was created by a purse-string suturing along the edges of the omentum and then tying the sutures. The omentum pouch was carefully positioned back in the peritoneal cavity and the surgical incision was closed using a standard surgical technique.

IDUA activity

The IDUA activity was measured in the culture medium collected before encapsulation, 24 h post-encapsulation and in the tissues and serum from the animals. Tissues were previously homogenized in distilled water, centrifuged, and the supernatant was collected for the assay, while serum samples were directly used. IDUA activity assay was performed incubating the samples with the fluorescent substrate 4-methylumbelliferyl-alpha-L–iduronide (Glycosynth, Warrington, UK) at 37 ° C for 1 h in a formate buffer pH 3.5. Protein content of the tissues was measured using the Lowry method. Results were expressed as nmol/h/mg protein and in the graphs they were shown as a percentage of normal activity. For serum, results were calculated as nmol/h/mL.

GAG quantification

Tissue and urinary GAG content was measured using the dymethyl blue assay. Briefly, 25 µL of sample supernatant were mixed with dymethyl blue solution (Dymethyl blue 0.3 mol/L with 2 mol/L Tris) and absorbance was detected at 530 nm. Tissues were previously homogenized in phosphate buffer pH 6.5 containing papain 300 µg/mL, and the supernatant was used in the assay. The total tissue protein quantification was determined with the Lowry assay and results were expressed as µg GAG/mg protein; in the graphs they were shown as a percentage of normal levels. Urinary GAGs was measured without previous preparation of the sample and results were expressed as µg GAG/mg creatinine.

Histological analysis

Liver, kidney, heart and the microcapsules were fixed in 10% formalin solution, embedded in paraffin blocks and serially sectioned for histological analysis. To verify the presence of GAG accumulation, tissue sections were stained for Alcian blue using hematoxylin-eosin (H&E) as counterstain.

Statistical analysis

Statistical analysis was performed by GraphPad Prism (version 5.01) using Student's t test. The comparisons were made between normal and MPS I groups. Statistically significant differences among groups were considered when $p<0.05$.

Results

Before encapsulation, rBHK cells released IDUA in the medium at an average of 75.4 nmol/h/mL. Then, they were immobilized in APA microcapsules and 24 h post-encapsulation the enzyme activity in the medium was measured again. The average of IDUA produced at this time by an amount of microcapsules separated to be implanted in the animals was 43.9 nmol/h/mL, corresponding to 58% of the non-encapsulated cells activity. The implantation in MPS I mice was performed and an omentum pouch was formed to enclose the capsules, as shown in figure 1A. At day 60 post-implantation, the omentum pouch was recovered. On retrieval, it was possible to visualize the beads through the thin omentum and numerous vessels were present around it (Fig. 1B). The macroscopic view of the capsules showed a transparent membrane, which did not evidence a fibrotic layer (Fig. 1C).

Treatment evaluation

Three animals were killed 24 h post-implantation, whereas the rest of animals were kept for 60 days. In these animals, serum IDUA activity was monitored and an increase was observed at days 7 ($p= 0.04$) and 15 ($p= 0.008$) (Fig. 2A). Although serum IDUA levels was not detected in the first 24 hours, increased IDUA activity in the liver (an average of 7.9-fold of untreated mice, $p=0.047$), kidney (2.3-fold, $p=0.008$) and heart (6-fold, $p=0.039$) was observed (Fig. 2B). After 60 days of treatment, higher levels of enzyme activity were observed in the heart (4.5-fold, $p=0.002$) of treated MPS I mice when compared to untreated animals, while the increase in the liver (2.6-fold, $p=0.08$) and kidney (4.2-fold, $p=0.056$) was statistically borderline (Fig. 2B).

A slight reduction in urinary GAG levels was observed at day 7 ($p= 0.038$) but they remained elevated over the treatment. The biochemical measurement of GAG storage in the tissues after 60 days did not reveal differences between treated and untreated MPS I mice at same age (16% reduction in the liver, $p= 0.65$, 3.7% in the kidney, $p=0.85$, and 6% in the kidney, $p=0.79$, data not shown). Histological analysis using Alcian blue stain was performed to visualize the GAG content in the tissues (Fig. 3). Interestingly, treatment with APA microcapsules was able to reorganize the architecture of hepatic tissue and less cell vacuolization was observed (Fig. 3C). However, a great amount of GAG content was still observed in the cells of all tissues of treated MPS I mice.

Discussion

In this work, we used microencapsulated rBHK cells overexpressing IDUA implanted in the omentum of MPS I mice as a treatment for this disease. Previously to implantation, APA microcapsules were evaluated, showing an adequate morphology and IDUA release rate. The reduction in the release rate following encapsulation was expected and has been previously reported [15,19,20]. It probably occur due to the stressing process of encapsulation that leads to alterations in cell metabolism, which is expected to be improved after a few days [16].

A short-term functionality of the rBHK cells immobilized in APA microcapsules was observed. After 24 h of implantation, increased levels of IDUA were detected in the tissues, confirming that the enzyme was released from the capsules, reached the circulation, and could be taken up by the tissues. Over 60 days, the microcapsules were maintained in the omentum pouch of MPS I mice. Serum IDUA levels were slightly increased in the first 15 days of treatment, but it was transient and undetectable after this

point. On the other hand, at day 60 post-implantation, we detected higher enzyme activity in the heart, and borderline results were observed in the liver and kidney. This apparent contradictory result can be explained since the enzyme from the serum is rapidly taken up by peripheral organs [21].

On retrieval of the omentum pouch, microcapsules were clearly seen with the blood vessels spread throughout the pouch indicating good integration of the blood supply to the microcapsules. Nevertheless, just a discrete taken up of the secreted enzyme was observed, and it may not be sufficient to ensure the delivery of enough enzyme to the whole tissue. The treatment did not reduce the GAG content as observed by biochemical and histologic analyses and it probably reflects the low levels of enzyme achieved in the tissues. However, the hepatic parenchyma showed reorganization and less cell vacuolization, suggesting that a slight increase in IDUA activity could be sufficient to correct this aspect. Another possibility is that the transient increase in IDUA levels observed at 24 h was able to temporarily reduce tissue GAG storage, but they increased again over the time. In addition, an aspect not tested in our work that could be reducing IDUA availability is the production of antibodies against the enzyme. It was also observed after treatment with capsules in the peritoneum of MPS I mice [17] as well as in several patients treated with ERT [4], suggesting that the immune response may be not only to the microcapsule itself but also to the enzyme.

The ability of the omentum to rapidly increase and maintain vessel density around microcapsules was expected to improve transport resulting in enhanced cell function. However, our results showed that the treatment was only efficient for a short period. Although the adequate environment provided by the omentum, where a closed relation between encapsulated cells and the systemic circulation was observed, APA microcapsules were not able to constantly release IDUA to most tissues analyzed over a

60 days treatment. Nevertheless, this approach was able to show a transient correction, and modifications on the technique could lead to a better performance.

References

1. Matte U, Yogalingam G, Brooks D. Identification and characterization of 13 new mutations in mucopolysaccharidosis type I patients. *Mol. Genet. Metab.* 2003;78:37–43.

2. Giugliani R. Mucopolysacccharidoses: From understanding to treatment, a century of discoveries. *Genet. Mol. Biol.* 2012;35:924–31.

3. Boelens JJ, Prasad VK, Tolar J, Wynn RF, Peters C. Current international perspectives on hematopoietic stem cell transplantation for inherited metabolic disorders. *Pediatr. Clin. North Am.* 2010;57:123–45.

4. Valayannopoulos V, Wijburg F a. Therapy for the mucopolysaccharidoses. *Rheumatology*. 2011;50 Suppl 5:v49–59.

5. Baldo G, Giugliani R, Matte U. Gene delivery strategies for the treatment of mucopolysaccharidoses. *Expert Opin. Drug Deliv.* 2014;11:449–59.

6. Hernández RM a, Orive G, Murua A, Pedraz JL. Microcapsules and microcarriers for in situ cell delivery. *Adv. Drug Deliv. Rev.* 2010;62:711–30.

7. Matte U, Lagranha VL, de Carvalho TG, Mayer FQ, Giugliani R. Cell microencapsulation: a potential tool for the treatment of neuronopathic lysosomal storage diseases. *J. Inherit. Metab. Dis.* 2011;34:983–90.

8. Scharp DW, Marchetti P. Encapsulated islets for diabetes therapy: history, current progress, and critical issues requiring solution. *Adv. Drug Deliv. Re.* 2014;67-68:35–73.

9. Lee K, Mooney D. Alginate: properties and biomedical applications. *Prog. Polym. Sci*. 2012 ;37:106–26.

10. De Vos P, Lazarjani HA, Poncelet D, Faas MM. Polymers in cell encapsulation from an enveloped cell perspective. *Adv. Drug Deliv. Rev.*; 2014;67-68:15–34.

11. Santos E, Pedraz JL, Hernández RM, Orive G. Therapeutic cell encapsulation: ten steps towards clinical translation. *J. Control. Release*. 2013 ;170:1–14.

12. Platell C, Cooper D, Papadimitriou JM, Hall JC. The omentum. *World J. Gastroenterol*. 2000;6:169–76.

13. Khanna O, Huang J-J, Moya ML, Wu C-W, Cheng M-H, Opara EC, et al. FGF-1 delivery from multilayer alginate microbeads stimulates a rapid and persistent increase in vascular density. *Microvasc. Res.*; 2013;90:23–9.

14. Bartholomeus K, Jacobs-Tulleneers-Thevissen D, Shouyue S, Suenens K, In't Veld P a, Pipeleers-Marichal M, et al. Omentum is better site than kidney capsule for growth, differentiation, and vascularization of immature porcine β-cell implants in immunodeficient rats. *Transplantation* 2013;96:1026–33.

15. Mayer FQ, Baldo G, de Carvalho TG, Lagranha VL, Giugliani R, Matte U. Effects of cryopreservation and hypothermic storage on cell viability and enzyme activity in recombinant encapsulated cells overexpressing alpha-L-iduronidase. *Artif. Organs* 2010;34:434–9.

16. Baldo G, Quoos Mayer F, Burin M, Carrillo-Farga J, Matte U, Giugliani R. Recombinant encapsulated cells overexpressing alpha-L-iduronidase correct enzyme deficiency in human mucopolysaccharidosis type I cells. *Cells Tissues Organs* 2012;195:323–9.

17. Baldo G, Mayer FQ, Martinelli B, Meyer FS, Burin M, Meurer L, et al. Intraperitoneal implant of recombinant encapsulated cells overexpressing alpha-L-iduronidase partially corrects visceral pathology in mucopolysaccharidosis type I mice. *Cytotherapy* 2012;14:860–7.

18. Ohmi K, Greenberg DS, Rajavel KS, Ryazantsev S, Li HH, Neufeld EF. Activated microglia in cortex of mouse models of mucopolysaccharidoses I and IIIB. *Proc. Natl. Acad. Sci.* U. S. A. 2003;100:1902–7.

19. Lagranha VL, Baldo G, de Carvalho TG, Burin M, Saraiva-Pereira ML, Matte U, et al. In vitro correction of ARSA deficiency in human skin fibroblasts from metachromatic leukodystrophy patients after treatment with microencapsulated recombinant cells. *Metab. Brain Dis.* 2008;23:469–84.

20. Murua A, Castro M de, Orive G. In vitro characterization and in vivo functionality of erythropoietin-secreting cells immobilized in alginate-poly-L-lysine-alginate microcapsules. *Biomacromolecules* 2007;8:3302–7.

21. Cotugno G, Tessitore A. Different serum enzyme levels are required to rescue the various systemic features of the mucopolysaccharidoses. *Hum. Gene Ther* 2010;569:555–69.

Figures

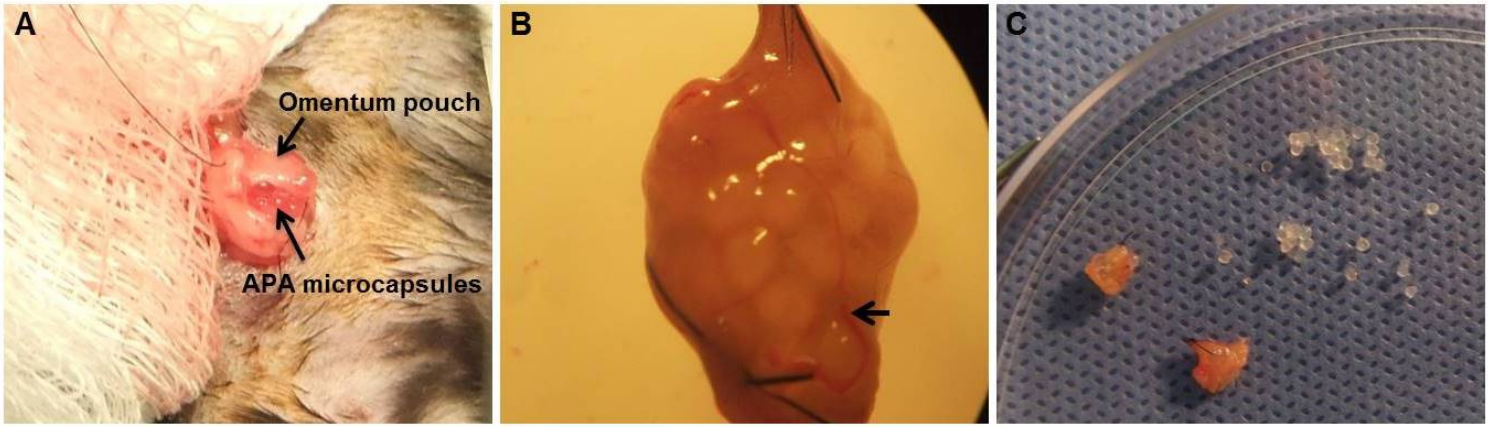

Figure 1. (A) Omentum pouch formation and capsules during the implantation procedure. (B) The omentum pouch on retrieval, arrow indicates blood vessels. (C) Macroscopic aspect of the microcapsules on retrieval.

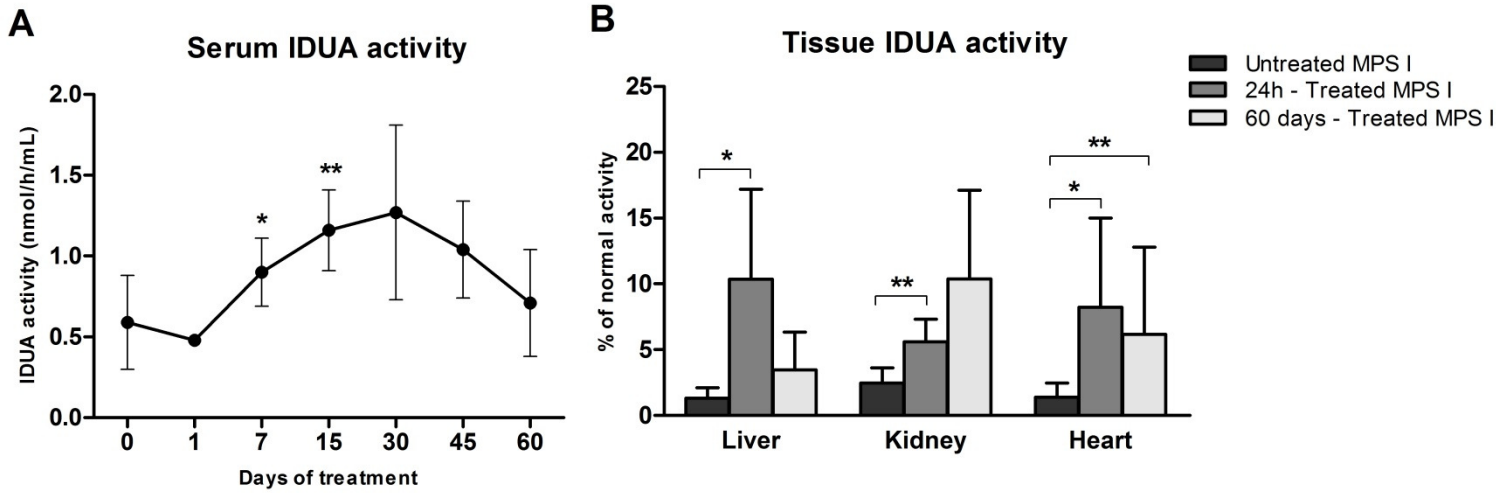

Figure 2. Serum and tissue IDUA activity. (A) Serum IDUA activity over treatment. (B) Tissue IDUA activity levels 24h and 60 days post-implantation. Student's t-test *, $p<0.05$ and ** $p<0,01$ compared to Untreated.

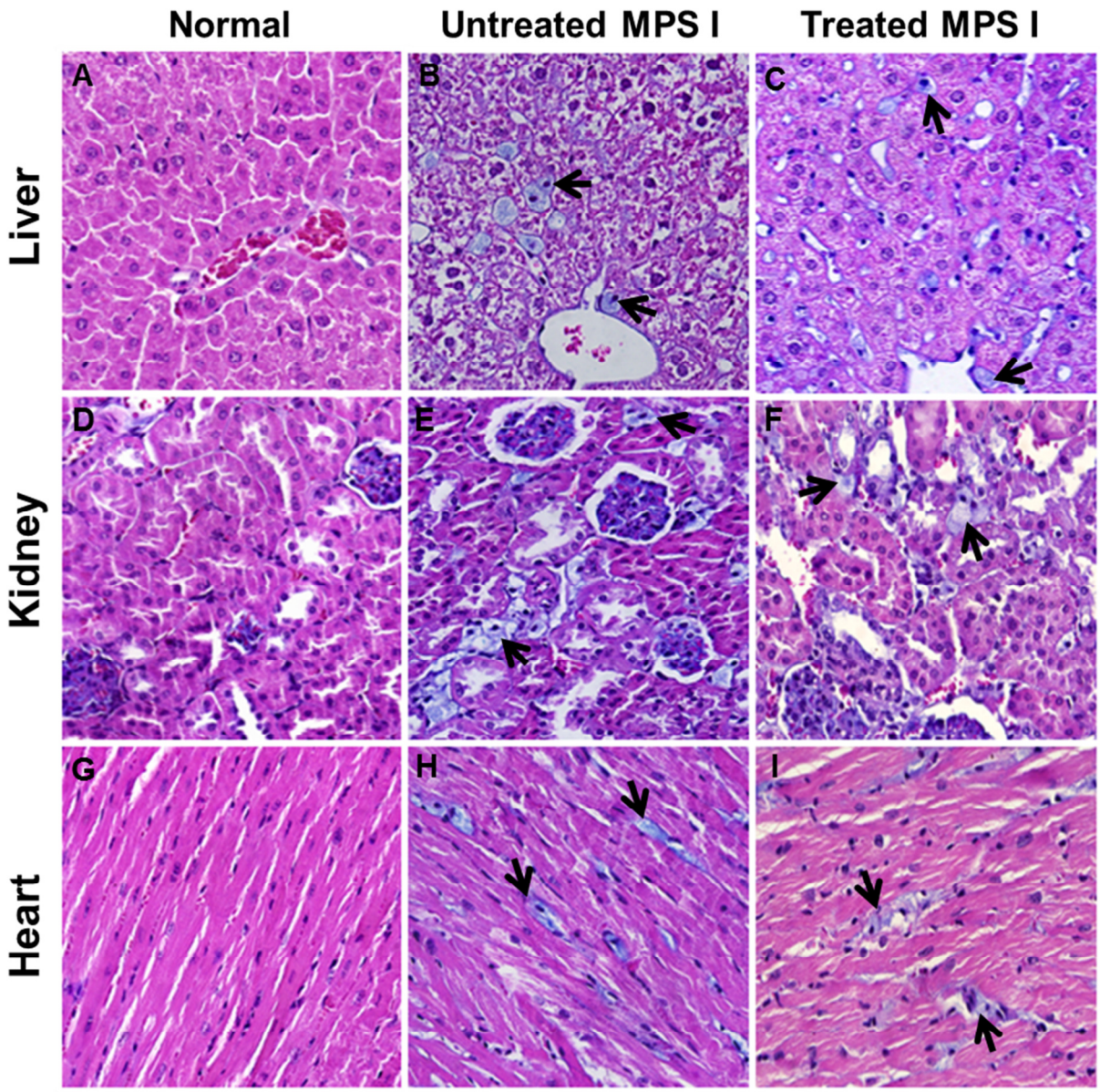

Figure 3. Histological analysis of tissues. Liver, kidney and heart were stained for Alcian blue and GAG storage is represented by blue cells (arrows). (A, D and G) Normal tissues. (B, E and H) Untreated MPS I tissues. (C, F and I) Tissues from MPS I mice after 60 days of APA microcapsules implantation. Magnification 40x.

PARTE III

DISCUSSÃO

A MPS I é uma DL causada pela deficiência da enzima IDUA e caracterizada pelo acúmulo de GAG não degradados. Consequentemente, diversos processos bioquímicos e fisiológicos são afetados, levando a uma condição patológica crônica, multisistêmica e com manifestações clínicas variadas. Os tratamentos atualmente utilizados em pacientes com MPS I consistem no TCTH e na TRE. Apesar dos benefícios, também há diversas limitações (Boelens *et al*, 2010; Giugliani *et al*, 2010).

Portanto, torna-se necessário o estudo de novas abordagens terapêuticas a fim de melhorar a eficiência do tratamento e a qualidade de vida dos pacientes. Doenças lisossômicas, como a MPS I, são excelentes candidatas ao tratamento com terapia gênica, pois são doenças mendelianas clássicas causadas pela deficiência de apenas um gene, não são reguladas por mecanismos complexos e uma atividade enzimática de apenas 15-20% dos níveis normais tem eficácia clínica (Beck, 2010), embora maiores quantidades de enzima sejam necessárias para a correção de alguns sistemas do organismo (Cotugno & Tessitore, 2010). Uma técnica que parece ser promissora é a microencapsulação celular, onde células recombinantes superexpressando a IDUA são imobilizadas em um biopolímero e utilizadas como uma fonte contínua de produção e liberação enzimática.

Em estudos anteriores do nosso grupo, a linhagem celular BHK foi transfectada com um plasmídeo pREP-9 contendo o gene da IDUA (Mayer *et al*, 2010). Essas células recombinantes (rBHK) foram encapsuladas em microesferas de alginato e testadas *in vitro* (Baldo *et al*, 2012a). O co-cultivo das cápsulas com fibroblastos de pacientes com MPS I reestabeleceu a atividade enzimática durante 45 dias e reduziu o acúmulo de GAG, sugerindo que a enzima foi produzida e processada corretamente, chegando ao compartimento lisossômico das células deficientes. Com base nos resultados promissores observados *in vitro*, a utilização das microcápsulas superexpressando IDUA para o

tratamento da MPS I foi testada no modelo animal. A disponibilidade de camundongos *Idua*$^{-/-}$, um modelo amplamente usado em estudos sobre a MPS I, tornou possível a investigação da funcionalidade das microcápsulas *in vivo*, de modo que diferentes aspectos relacionados ao biomaterial, dose de células e local de implantação podem ser testados e ajustados para atingir um tratamento bem sucedido.

Os primeiros experimentos realizados *in vivo*, utilizando cápsulas apenas com alginato e implantadas no peritônio de camundongos, não mostraram resultados tão promissores quanto o esperado após as observações *in vitro* (Baldo *et al*, 2012b). Neste tratamento, houve redução nos níveis de GAG no rim e foi detectado um aumento na atividade de IDUA apenas no coração dos camundongos MPS I. A análise das microcápsulas mostrou a presença de células inflamatórias e fibrose na superfície capsular e anticorpos anti-IDUA foram detectados no soro dos animais, de modo que essa resposta imune pode ter sido a principal causa da pouca eficiência na correção da doença. O local de administração das cápsulas pode ter interferido, pois, apesar de ser bastante utilizado para esse fim, o peritônio é um ambiente pro-inflamatório, o procedimento para a implantação é invasivo e as cápsulas ficam espalhadas, o que não permite uma revascularização próximo a elas para melhorar a captação da enzima (Opara *et al*, 2010; Vériter *et al*, 2013). Além disso, o alginato utilizado não era purificado e a possível presença de impurezas pode ter comprometido a biocompatibilidade das cápsulas (Dusseault *et al*, 2006).

Assim, seria importante verificar alterações que pudessem ser feitas a fim de obter melhores resultados. A produção de microcápsulas APA, onde há uma cobertura adicional utilizando PLL, é uma forma de ajustar a permeabilidade da membrana da cápsula e também melhorar sua resistência mecânica (Santos *et al*, 2013). Além disso, a utilização

de um alginato ultra-purificado e a escolha de outros locais para o implante podem fornecer um ambiente mais adequado para as células encapsuladas.

Portanto, neste trabalho utilizamos células rBHK superexpressando IDUA imobilizadas em microcápsulas APA, as quais foram usadas no tratamento de camundongos MPS I. Para isso, escolhemos dois locais de implantação, a via subcutânea e o epíplon (omento), devido a suas características. O implante na via subcutânea é feito através de uma injeção simples e pouco invasiva, diminuindo a possibilidade de um processo inflamatório exacerbado e facilitando a retirada das cápsulas (Acarregui *et al*, 2013; Santos *et al*, 2013). Além disso, as microcápsulas ficam unidas, sendo possível uma vascularização ao longo do tempo. O epíplon possui naturalmente uma boa vascularização, é rico em fatores angiogênicos e seu tecido permite a formação de "bolsas", de modo que as microcápsulas não se dispersam e o microambiente é adequado para as células (Bartholomeus *et al*, 2013; Khanna *et al*, 2013), uma vez que a proximidade com os vasos sanguíneos facilita a troca de metabólitos bem como a captação da enzima liberada.

Previamente ao processo de implantação a quantidade de IDUA produzida pelas células rBHK não encapsuladas foi comparada com a liberação da enzima após encapsulação, *in vitro*. A quantidade de células e cápsulas usada para essa análise foi igual ao implantado em cada camundongo. Como resultado, foi possível observar que após a encapsulação, a atividade de IDUA era aproximadamente 50-60% da atividade das células não encapsuladas. Uma redução após a encapsulação era esperada e é normal que ocorra, conforme estudos demonstrando que após a encapsulação a atividade pode ser de 35-45% da inicial (Lagranha *et al*, 2008; Murua *et al*, 2007). Assim, as microcápsulas APA apresentaram uma liberação adequada da enzima antes de serem utilizadas no tratamento dos animais.

Microcápsulas APA foram implantadas em camundongos MPS I com 4 meses de idade, os quais foram mortos 24 h depois para avaliar a capacidade de liberação da enzima *in vivo* em curto prazo. Observou-se um aumento nos níveis de IDUA no fígado, rim e coração dos animais tratados, quando comparados a camundongos que não receberam o tratamento. Isso mostra que em um curto período de tempo, a enzima é produzida e liberada pelas microcápsulas, atinge a circulação e é captada pelos tecidos de forma adequada. Porém, não foi observado um aumento na atividade enzimática no soro. Estudos relataram que tanto no HSCT quanto na ERT os níveis enzimáticos no soro dos pacientes diminuem rapidamente após a infusão intravenosa, mas ainda podem ser detectados nos tecidos após uma semana (Cotugno & Tessitore, 2010). Portanto, o fato de a atividade enzimática não ter sido detectada no soro provavelmente ocorre devido à rápida captação pelos tecidos periféricos.

A TRE, o tratamento mais utilizado para a MPS I, requer a administração enzimática semanalmente ou quinzenalmente, tornando necessária a investigação de dispositivos capazes de liberar a enzima por longos períodos. Portanto, experimentos em longo prazo foram realizados, onde alguns camundongos foram tratados com microcápsulas no tecido subcutâneo por 120 dias e outros animais tiveram as cápsulas implantadas no epíplon por 60 dias.

Em relação ao tratamento feito através da via subcutânea, após 120 dias foi possível detectar uma atividade enzimática elevada nos 3 órgãos analisados (fígado, rim e coração), indicando que a enzima continuou sendo produzida e liberada pelas cápsulas. A presença marcante de vasos sanguíneos em torno das cápsulas provavelmente contribuiu para isso, pois possibilitou uma boa captação da enzima. Outro parâmetro utilizado para avaliar o efeito do tratamento consiste na observação do acúmulo de GAG nos tecidos. A dosagem bioquímica mostrou uma diminuição de 32% nos níveis de GAG no rim dos

camundongos tratados em relação a animais não tratados. No fígado, apesar de não ser estatisticamente significativa, houve uma redução de 34%. Nesses órgãos, também foi observada a maior elevação da atividade enzimática, mostrando uma relação entre níveis de IDUA e correção do acúmulo de GAG. Resultados parecidos foram mostrados em camundongos MPS I com microcápsulas na cavidade peritoneal (Baldo *et al*, 2012b). No entanto, a redução não foi facilmente observada pela análise histológica dos tecidos. Apesar de um pouco menos evidente no fígado e no rim, muitas células ainda apresentaram acúmulo de GAG. Além de células azuis que correspondem ao acúmulo de GAG nos tecidos, uma característica da MPS I, bem como de outras DL, é a presença de células vacuolizadas e com grânulos, o que tende a progredir com o curso da doença (Heard *et al*, 2010). Notavelmente, pode-se observar que nos camundongos tratados o parênquima hepático está reorganizado e a presença de vacúolos e inclusões citoplasmáticas diminuiu. Uma correção no aspecto dos tecidos também foi relatada em camundongos MPS II (Friso *et al*, 2005), onde além do fígado, houve uma melhora na aparência do rim e do baço após tratamento com mioblastos recombinantes microencapsulados.

Outro grupo de camundongos MPS I recebeu o tratamento com microcápsulas implantadas no epíplon, onde foi feita uma "bolsa" a fim de acomodar as microcápsulas. Após 60 dias de tratamento, os órgãos foram avaliados e a atividade enzimática estava elevada apenas no coração dos animais tratados, mas resultados muito próximos à significância foram encontrados também no fígado e no rim. A dosagem bioquímica do conteúdo de GAG nos tecidos, bem como a análise histológica, não mostrou diferenças no acúmulo entre animais tratados e não tratados, sugerindo que a pequena elevação nos níveis de IDUA não foi suficiente para reduzir a quantidade de GAG. Apesar disso, uma melhora em relação à vacuolização do tecido hepático também foi observada, como

anteriormente mencionada em relação ao tratamento pela via subcutânea. Não sabemos se as diferenças entre os tratamentos se devem apenas a via de implantação, pois a comparação direta entre os resultados não pode ser feita, uma vez que tanto a quantidade de microcápsulas/células implantadas em cada animal quanto o tempo de tratamento foram diferentes.

Em ambos os tratamentos, a elevação nos níveis de IDUA no soro dos animais foi transitória, o que parece estar relacionado à rápida captação pelos órgãos. No entanto, se fosse possível detectar níveis elevados de enzima no soro, poderia ser devido a uma maior liberação pelas cápsulas, o que provavelmente levaria a uma correção mais considerável no acúmulo de GAG. Além disso, os níveis de GAG urinários não diminuíram, sugerindo que seriam necessários níveis mais elevados de IDUA e uma correção maior no acúmulo de GAG teciduais para que também houvesse diminuição na excreção de GAG pela urina. É interessante notar que em ensaios de terapia gênica com vetores virais os níveis séricos da enzima são geralmente maiores e estão diretamente relacionados com os níveis de GAG, especialmente em órgãos de difícil acesso (Chung *et al*, 2007; Cotugno & Tessitore, 2010).

Uma vez que em estudos prévios detectamos a presença de infiltrado inflamatório nas microcápsulas após implante intraperitoneal (Baldo *et al*, 2012b) e intramuscular (de Carvalho, 2008), neste trabalho também analisamos as microcápsulas ao fim do tratamento. Ambos os locais de implantação proporcionaram uma boa vascularização ao redor das cápsulas, seja pelo tempo que elas ficaram implantadas, no caso da via subcutânea, ou pela existência prévia de um grande suprimento vascular, no caso do epíplon. A presença de uma resposta inflamatória, com macrófagos e células gigantes multinucleadas nas proximidades e também aderidas à superfície capsular foi observada, bem como a formação de fibrose com depósito de colágeno recobrindo as cápsulas.

Fibrose, infiltração e adesão de células inflamatórias do hospedeiro na superfície das cápsulas são parâmetros geralmente utilizados para avaliar a biocompatibilidade das cápsulas (Rokstad *et al*, 2014).

Uma resposta imune com adsorção de proteínas sobre microcápsulas é comum e geralmente ocorre como consequência do procedimento cirúrgico. A inflamação ocorre logo após o implante e tende a diminuir após algumas semanas, mas 2-10% da quantidade de macrófagos e fibroblastos permanecem na superfície da cápsula (Anderson *et al*, 2008). Quando a quantidade de macrófagos é elevada, ocorre a sua fusão e formação de células gigantes multinucleadas que persistem por toda a vida útil do implante, levando a uma inflamação crônica e formação de uma camada fibrótica com colágeno (Anderson *et al*, 2008). Além do procedimento de implantação, o desencadeamento da resposta imune pode ter ocorrido pelo biomaterial utilizado. No geral, os alginatos podem conter impurezas como endotoxinas e polifenóis, os quais influenciam a biocompatibilidade das microcápsulas (Dusseault *et al*, 2006). Isso não é esperado para um alginato ultra puro, como o que utilizamos, mas algumas impurezas residuais ainda podem estar presentes mesmo em alginatos ultra purificados (Dusseault *et al*, 2006), o que influenciaria na resposta inflamatória.

A formação de uma camada de colágeno e crescimento de células em torno das microcápsulas compromete a difusão através da membrana (Dang *et al*, 2013), podendo dificultar a passagem da IDUA para o meio extra-capsular. A atividade enzimática nos tecidos teve um aumento significativo, mas mesmo assim foi baixa, de modo que essa resposta inflamatória pode ser uma barreira impedindo que grandes quantidades de enzima sejam liberadas e, consequentemente, apenas uma pequena melhora pôde ser observada pelos parâmetros avaliados. Outro ponto a ser ressaltado é que a produção de anticorpos contra a IDUA ocorre em muitos pacientes tratados com TRE, bem como em modelos

animais da doença (Valayannopoulos 2011), sugerindo que a resposta imune pode não ter sido apenas contra as microcápsulas, mas também contra a enzima. Trabalhos usando células microencapsuladas ou outras formas de terapia gênica relataram que camundongos MPS I desenvolvem anticorpos contra a IDUA, mas os níveis são parecidos com os encontrados em camundongos tratados com TRE. Assim, a neutralização não é total e as terapias perdem apenas parte da sua eficiência (Baldo *et al*, 2012b; Piller Puicher *et al*, 2012).

A resposta inflamatória é evidente e continua sendo um problema para o tratamento, tanto neste estudo como em outros trabalhos onde microcápsulas foram implantadas em modelos animais, constituindo o maior desafio para o uso da tecnologia de microencapsulação celular. Dessa forma, estratégias para prevenir a adesão de células e adsorção de proteínas no biomaterial, a fim de impedir o desencadeamento de uma resposta inflamatória exacerbada, podem ser úteis para melhorar o desempenho da terapia. Nosso grupo está estudando a utilização de microcápsulas e anti-inflamatórios em combinação, estratégia que apresentou resultados satisfatórios em vários estudos. Como exemplo, pode-se citar a melhora na função de ilhotas co-encapsuladas com curcumina ou desametasona (Dang *et al*, 2013), bem como uma maior liberação de eritropoietina por células encapsuladas administradas no espaço subcutâneo juntamente com microesferas contendo dexametasona (Murua *et al*, 2011).

A partir dos resultados apresentados, pode-se concluir que o implante de células recombinantes microencapsuladas para o tratamento da MPS I teve resultados parcialmente satisfatórios em relação ao aumento da atividade de IDUA e redução de GAG observado após o implante na via subcutânea, bem como a diminuição da vacuolização das células hepáticas. No entanto, em ambas as vias de implantação uma resposta imune foi desencadeada, possivelmente prejudicando a funcionalidade das

microcápsulas. Assim, torna-se importante a investigação de métodos que possam melhorar a biocompatibilidade e aumentar a eficiência da liberação e captação da enzima. Há estudos que obtiveram sucesso com o uso dessa abordagem terapêutica tanto em estudos pré-clínicos quanto clínicos e, portanto, é válido o aperfeiçoamento da técnica para o tratamento da MPS I, já que as microcápsulas podem ser implantadas em órgãos de difícil acesso pela TRE, como as articulações e o SNC.

CONCLUSÕES

- As microcápsulas APA apresentaram uma morfologia adequada e a liberação de IDUA pelas células rBHK após a encapsulação foi satisfatória.
- As células microencapsuladas implantadas na via subcutânea de camundongos MPS I foram capazes de corrigir alguns aspectos da doença, uma vez que após 120 dias de tratamento a atividade de IDUA estava elevada no fígado, rim e coração dos animais tratados, o acúmulo de GAG diminuiu parcialmente no rim e no fígado e as células hepáticas apresentaram menor vacuolização. Apesar disso, não houve melhora no coração em relação à quantidade de GAG acumulados, a atividade no soro teve apenas um leve e transitório aumento, bem como uma leve diminuição dos GAG urinários nos primeiros dias de tratamento.
- As células microencapsuladas implantadas no epíplon de camundongos MPS I não corrigiram a deficiência enzimática (exceto no coração) e o acúmulo de GAG teciduais após 60 dias de tratamento. Os níveis de IDUA no soro aumentaram discretamente e os GAG urinários não diminuíram ao longo do tratamento.
- A análise histológica das microcápsulas retiradas dos animais após o tratamento mostrou a presença de vasos sanguíneos nas proximidades das cápsulas, bem como uma resposta imune evidenciada por um infiltrado inflamatório contendo macrófagos e uma camada fibrótica na superfície capsular.

REFERÊNCIAS

Acarregui, A., Pedraz, J.L., Blanco, F.J., Hernández, R.M., Orive, G., 2013. Hydrogel-based scaffolds for enclosing encapsulated therapeutic cells. Biomacromolecules 14, 322–30.

Anderson, J.M., Rodriguez, A., Chang, D.T., 2008. Foreign body reaction to biomaterials. Semin. Immunol. 20, 86–100. Augst, A.D., Kong, H.J., Mooney, D.J., 2006. Alginate hydrogels as biomaterials. Macromol. Biosci. 6, 623–33.

Baldo, G., Giugliani, R., Matte, U., 2014. Gene delivery strategies for the treatment of mucopolysaccharidoses. Expert Opin. Drug Deliv. 11, 449–59.

Baldo, G., Mayer, F.Q., Martinelli, B., Meyer, F.S., Burin, M., Meurer, L., Tavares, A.M.V., Giugliani, R., Matte, U., 2012a. Intraperitoneal implant of recombinant encapsulated cells overexpressing alpha-L-iduronidase partially corrects visceral pathology in mucopolysaccharidosis type I mice. Cytotherapy 14, 860–7.

Baldo, G., Quoos Mayer, F., Burin, M., Carrillo-Farga, J., Matte, U., Giugliani, R., 2012b. Recombinant encapsulated cells overexpressing alpha-L-iduronidase correct enzyme deficiency in human mucopolysaccharidosis type I cells. Cells Tissues Organs 195, 323–9.

Barsoum, S.C., Milgram, W., Mackay, W., Coblentz, C., Delaney, K.H., Kwiecien, J.M., Kruth, S. a, Chang, P.L., 2003. Delivery of recombinant gene product to canine brain with the use of microencapsulation. J. Lab. Clin. Med. 142, 399–413.

Bartholomeus, K., Jacobs-Tulleneers-Thevissen, D., Shouyue, S., Suenens, K., In't Veld, P. a, Pipeleers-Marichal, M., Pipeleers, D.G., Hellemans, K., 2013. Omentum is better site than kidney capsule for growth, differentiation, and vascularization of immature porcine β-cell implants in immunodeficient rats. Transplantation 96, 1026–33.

Beck, M., 2010. Therapy for lysosomal storage disorders. IUBMB Life 62, 33–40.

Beck, M., Arn, P., Giugliani, R., Muenzer, J., Okuyama, T., Taylor, J., Fallet, S., 2014. The natural history of MPS I: global perspectives from the MPS I Registry. Genet. Med.

Bidarra, S.J., Barrias, C.C., Granja, P.L., 2014. Injectable alginate hydrogels for cell delivery in tissue engineering. Acta Biomater. 10, 1646–62.

Bishop, J.R., Schuksz, M., Esko, J.D., 2007. Heparan sulphate proteoglycans fine-tune mammalian physiology. Nature 446, 1030–7.

Boelens, J.J., Prasad, V.K., Tolar, J., Wynn, R.F., Peters, C., 2010. Current international perspectives on hematopoietic stem cell transplantation for inherited metabolic disorders. Pediatr. Clin. North Am. 57, 123–45. d

Brooks, D. a, Muller, V.J., Hopwood, J.J., 2006. Stop-codon read-through for patients affected by a lysosomal storage disorder. Trends Mol. Med. 12, 367–73.

Calafiore, R., Basta, G., 2014. Clinical application of microencapsulated islets: actual prospectives on progress and challenges. Adv. Drug Deliv. Rev. 67-68, 84–92.

Chang, T., 1964. Semipermeable microcapsules. Science (80). 146, 1–2.

Cheng, S.H., 2014. Gene therapy for the neurological manifestations in lysosomal storage disorders. J. Lipid Res.

Chung, S., Ma, X., Liu, Y., Lee, D., Tittiger, M., Ponder, K.P., 2007. Effect of neonatal administration of a retroviral vector expressing alpha-L-iduronidase upon lysosomal storage in brain and other organs in mucopolysaccharidosis I mice. Mol. Genet. Metab. 90, 181–92.

Clarke, L. a, Russell, C.S., Pownall, S., Warrington, C.L., Borowski, a, Dimmick, J.E., Toone, J., Jirik, F.R., 1997. Murine mucopolysaccharidosis type I: targeted disruption of the murine alpha-L-iduronidase gene. Hum. Mol. Genet. 6, 503–11.

Clarke, L. a, Wraith, J.E., Beck, M., Kolodny, E.H., Pastores, G.M., Muenzer, J., Rapoport, D.M., Berger, K.I., Sidman, M., Kakkis, E.D., Cox, G.F., 2009. Long-term efficacy and safety of laronidase in the treatment of mucopolysaccharidosis I. Pediatrics 123, 229–40.

Cotugno, G., Tessitore, A., 2010. Different serum enzyme levels are required to rescue the various systemic features of the mucopolysaccharidoses. Hum. Gene Ther. 569, 555–569.

D'Aco, K., Underhill, L., Rangachari, L., Arn, P., Cox, G.F., Giugliani, R., Okuyama, T., Wijburg, F., Kaplan, P., 2012. Diagnosis and treatment trends in mucopolysaccharidosis I: findings from the MPS I Registry. Eur. J. Pediatr. 171, 911–9.

Dang, T.T., Thai, A. V, Cohen, J., Slosberg, J.E., Siniakowicz, K., Doloff, J.C., Ma, M., Hollister-Lock, J., Tang, K.M., Gu, Z., Cheng, H., Weir, G.C., Langer, R., Anderson, D.G., 2013. Enhanced function of immuno-isolated islets in diabetes therapy by co-encapsulation with an anti-inflammatory drug. Biomaterials 34, 5792–801.

De Carvalho, T.G., 2008. Células microencapsuladas em alginato de cálcio: avaliação de parâmetros *in vitro* e *in vivo* [senior thesis] Porto Alegre, RS: Universidade Federal do Rio Grande do Sul.

De Vos, P., Bucko, M., Gemeiner, P., Navrátil, M., Svitel, J., Faas, M., Strand, B.L., Skjak-Braek, G., Morch, Y. a, Vikartovská, A., Lacík, I., Kolláriková, G., Orive, G., Poncelet, D., Pedraz, J.L., Ansorge-Schumacher, M.B., 2009. Multiscale requirements for bioencapsulation in medicine and biotechnology. Biomaterials 30, 2559–70.

De Vos, P., Lazarjani, H.A., Poncelet, D., Faas, M.M., 2014. Polymers in cell encapsulation from an enveloped cell perspective. Adv. Drug Deliv. Rev. 67-68, 15–34.

Delgadillo, V., O'Callaghan, M.D.M., Artuch, R., Montero, R., Pineda, M., 2011. Genistein supplementation in patients affected by Sanfilippo disease. J. Inherit. Metab. Dis. 34, 1039–44.

Donati, I., Paoletti, S., 2009. Alginates: Biology and Applications, Microbiology Monographs. Springer Berlin Heidelberg, Berlin, Heidelberg.

Dusseault, J., Tam, S.K., Ménard, M., Polizu, S., Jourdan, G., Yahia, L., Hallé, J.-P., 2006. Evaluation of alginate purification methods: effect on polyphenol, endotoxin, and protein contamination. J. Biomed. Mater. Res. A 76, 243–51.

Friso, A., Tomanin, R., Alba, S., Gasparotto, N., Puicher, E.P., Fusco, M., Hortelano, G., Muenzer, J., Marin, O., Zacchello, F., Scarpa, M., 2005. Reduction of GAG storage in MPS II mouse model following implantation of encapsulated recombinant myoblasts. J. Gene Med. 7, 1482–91.

Gandhi, N.S., Mancera, R.L., 2008. The structure of glycosaminoglycans and their interactions with proteins. Chem. Biol. Drug Des. 72, 455–82. d

Garcia, P., Youssef, I., Utvik, J.K., Florent-Béchard, S., Barthélémy, V., Malaplate-Armand, C., Kriem, B., Stenger, C., Koziel, V., Olivier, J.-L., Escanye, M.-C., Hanse, M., Allouche, A., Desbène, C., Yen, F.T., Bjerkvig, R., Oster, T., Niclou, S.P., Pillot, T., 2010. Ciliary neurotrophic factor cell-based delivery prevents synaptic impairment and improves memory in mouse models of Alzheimer's disease. J. Neurosci. 30, 7516–27.

Giugliani, R., 2012. Mucopolysacccharidoses: From understanding to treatment, a century of discoveries. Genet. Mol. Biol. 35, 924–31.

Giugliani, R., Federhen, A., Rojas, M.V.M., Vieira, T., Artigalás, O., Pinto, L.L., Azevedo, A.C., Acosta, A., Bonfim, C., Lourenço, C.M., Kim, C.A., Horovitz, D., Bonfim, D., Norato, D., Marinho, D., Palhares, D., Santos, E.S., Ribeiro, E., Valadares, E., Guarany, F., de Lucca, G.R., Pimentel, H., de Souza, I.N., Correa, J., Fraga, J.C., Goes, J.E., Cabral, J.M., Simionato, J., Llerena, J., Jardim, L., Giuliani, L., da Silva, L.C.S., Santos, M.L., Moreira, M.A., Kerstenetzky, M., Ribeiro, M., Ruas, N., Barrios, P., Aranda, P., Honjo, R., Boy, R., Costa, R., Souza, C., Alcantara, F.F., Avilla, S.G. a, Fagondes, S., Martins, A.M., 2010. Mucopolysaccharidosis I, II, and VI: Brief review and guidelines for treatment. Genet. Mol. Biol. 33, 589–604.

Giugliani, R., Rojas, V.M., Martins, A.M., Valadares, E.R., Clarke, J.T.R., Góes, J.E.C., Kakkis, E.D., Worden, M.A., Sidman, M., Cox, G.F., 2009. A dose-optimization trial of laronidase (Aldurazyme) in patients with mucopolysaccharidosis I. Mol. Genet. Metab. 96, 13–9.

Goren, A., Dahan, N., Goren, E., Baruch, L., Machluf, M., 2010. Encapsulated human mesenchymal stem cells: a unique hypoimmunogenic platform for long-term cellular therapy. FASEB J. 24, 22–31.

Haskins, M., 2007. Animal models for mucopolysaccharidosis disorders and their clinical relevance. Acta Paediatr. 96, 56–62.

Heard, J.M., Bruyère, J., Roy, E., Bigou, S., Ausseil, J., Vitry, S., 2010. Storage problems in lysosomal diseases. Biochem. Soc. Trans. 38, 1442–7.

Hernández, R.M. a, Orive, G., Murua, A., Pedraz, J.L., 2010. Microcapsules and microcarriers for in situ cell delivery. Adv. Drug Deliv. Rev. 62, 711–30.

Holley, R., Deligny, A., Wei, W., 2011. Mucopolysaccharidosis type I, unique structure of accumulated heparan sulfate and increased N-sulfotransferase activity in mice lacking α-l-iduronidase. J. Biol. Chem. 286, 37515–37524.

Khanna, O., Huang, J.-J., Moya, M.L., Wu, C.-W., Cheng, M.-H., Opara, E.C., Brey, E.M., 2013. FGF-1 delivery from multilayer alginate microbeads stimulates a rapid and persistent increase in vascular density. Microvasc. Res. 90, 23–9.

Kim, Y.M., Jeon, Y.H., Jin, G.C., Lim, J.O., Baek, W.Y., 2004. Immunoisolated chromaffin cells implanted into the subarachnoid space of rats reduce cold allodynia in a model of neuropathic pain: a novel application of microencapsulation technology. Artif. Organs 28, 1059–66.

Klinge, P.M., Harmening, K., Miller, M.C., Heile, A., Wallrapp, C., Geigle, P., Brinker, T., 2011. Encapsulated native and glucagon-like peptide-1 transfected human mesenchymal stem cells in a transgenic mouse model of Alzheimer's disease. Neurosci. Lett. 497, 6–10.

Lagranha, V.L., Baldo, G., de Carvalho, T.G., Burin, M., Saraiva-Pereira, M.L., Matte, U., Giugliani, R., 2008. In vitro correction of ARSA deficiency in human skin fibroblasts from metachromatic leukodystrophy patients after treatment with microencapsulated recombinant cells. Metab. Brain Dis. 23, 469–84.

Lee, K., Mooney, D., 2012. Alginate: properties and biomedical applications. Prog. Polym. Sci. 37, 106–126.

Lim, F., Sun, a M., 1980. Microencapsulated islets as bioartificial endocrine pancreas. Science 210, 908–10.

Lim, G., Zare, S., Dyke, M. Van, Atala, A., 2010. Cell microencapsulation, in: Therapeutic Applications of Cell Microencapsulation. Springer New York, pp. 126–136.

Matte, U., Lagranha, V.L., de Carvalho, T.G., Mayer, F.Q., Giugliani, R., 2011. Cell microencapsulation: a potential tool for the treatment of neuronopathic lysosomal storage diseases. J. Inherit. Metab. Dis. 34, 983–90.

Matte, U., Yogalingam, G., Brooks, D., 2003. Identification and characterization of 13 new mutations in mucopolysaccharidosis type I patients. Mol. Genet. Metab. 78, 37–43.

Mayer, F.Q., Baldo, G., de Carvalho, T.G., Lagranha, V.L., Giugliani, R., Matte, U., 2010. Effects of cryopreservation and hypothermic storage on cell viability and enzyme activity in recombinant encapsulated cells overexpressing alpha-L-iduronidase. Artif. Organs 34, 434–9.

Mayer, F.Q., Artigalás, O.A., Lagranha, V.L., Baldo, G., Schwartz, I.V., Matte, U., Giugliani, R., 2013. Chloramphenicol enhances IDUA activity on fibroblasts from mucopolysaccharidosis I patients. Curr. Pharm. Biotechnol 14, 194-8.

McGlynn, R., Dobrenis, K., Walkley, S.U., 2004. Differential subcellular localization of cholesterol, gangliosides, and glycosaminoglycans in murine models of mucopolysaccharide storage disorders. J. Comp. Neurol. 480, 415–26.

Mørch, Y. a, Donati, I., Strand, B.L., Skjåk-Braek, G., 2006. Effect of Ca2+, Ba2+, and Sr2+ on alginate microbeads. Biomacromolecules 7, 1471–80.

Muenzer, J., 2011. Overview of the mucopolysaccharidoses. Rheumatology 50, v4–12.

Muenzer, J., 2014. Early initiation of enzyme replacement therapy for the mucopolysaccharidoses. Mol. Genet. Metab. 111, 63–72.

Muñoz-Rojas, M.V., Bay, L., Sanchez, L., van Kuijck, M., Ospina, S., Cabello, J.F., Martins, A.M., 2011. Clinical manifestations and treatment of mucopolysaccharidosis type I patients in Latin America as compared with the rest of the world. J. Inherit. Metab. Dis. 34, 1029–37.

Murua, A., Castro, M. de, Orive, G., 2007. In vitro characterization and in vivo functionality of erythropoietin-secreting cells immobilized in alginate-poly-L-lysine-alginate microcapsules. Biomacromolecules 8, 3302–3307.

Murua, A., Herran, E., Orive, G., Igartua, M., Blanco, F.J., Pedraz, J.L., Hernández, R.M., 2011. Design of a composite drug delivery system to prolong functionality of cell-based scaffolds. Int. J. Pharm. 407, 142–50.

Noh, H., Lee, J.I., 2014. Current and potential therapeutic strategies for mucopolysaccharidoses. J. Clin. Pharm. Ther. 39, 215–24.

Ohmi, K., Greenberg, D.S., Rajavel, K.S., Ryazantsev, S., Li, H.H., Neufeld, E.F., 2003. Activated microglia in cortex of mouse models of mucopolysaccharidoses I and IIIB. Proc. Natl. Acad. Sci. U. S. A. 100, 1902–7.

Opara, E.C., Mirmalek-Sani, S.-H., Khanna, O., Moya, M.L., Brey, E.M., 2010. Design of a bioartificial pancreas(+). J. Investig. Med. 58, 831–7.

Orive, G., Santos, E., Pedraz, J.L., Hernández, R.M., 2014. Application of cell encapsulation for controlled delivery of biological therapeutics. Adv. Drug Deliv. Rev. 67-68C, 3–14.

Pareta, R., McQuilling, J.P., Sittadjody, S., Jenkins, R., Bowden, S., Orlando, G., Farney, A.C., Brey, E.M., Opara, E.C., 2014. Long-term function of islets encapsulated in a redesigned alginate microcapsule construct in omentum pouches of immune-competent diabetic rats. Pancreas 43, 605–13.

Paul, A., Ge, Y., Prakash, S., Shum-Tim, D., 2009. Microencapsulated stem cells for tissue repairing: implications in cell-based myocardial therapy. Regen. Med. 4, 733–45.

Pereira, V.G., Gazarini, M.L., Rodrigues, L.C., da Silva, F.H., Han, S.W., Martins, A.M., Tersariol, I.L.S., D'Almeida, V., 2010. Evidence of lysosomal membrane permeabilization in mucopolysaccharidosis type I: rupture of calcium and proton homeostasis. J. Cell. Physiol. 223, 335–42.

Piller Puicher, E., Tomanin, R., Salvalaio, M., Friso, a, Hortelano, G., Marin, O., Scarpa, M., 2012. Encapsulated engineered myoblasts can cure Hurler syndrome: preclinical experiments in the mouse model. Gene Ther. 19, 355–64.

Platt, F.M., Boland, B., van der Spoel, A.C., 2012. The cell biology of disease: lysosomal storage disorders: the cellular impact of lysosomal dysfunction. J. Cell Biol. 199, 723–34.

Ponder, K., Haskins, M., 2007. Gene therapy for mucopolysaccharidosis 7, 1333–1345.

Prasad, V.K., Kurtzberg, J., 2010. Cord blood and bone marrow transplantation in inherited metabolic diseases: scientific basis, current status and future directions. Br. J. Haematol. 148, 356–72.

Rokstad, A.M. a, Lacík, I., de Vos, P., Strand, B.L., 2014. Advances in biocompatibility and physico-chemical characterization of microspheres for cell encapsulation. Adv. Drug Deliv. Rev. 67-68, 111–30.

Santos, E., Pedraz, J.L., Hernández, R.M., Orive, G., 2013. Therapeutic cell encapsulation: ten steps towards clinical translation. J. Control. Release 170, 1–14.

Scott, H.S., Anson, D.S., Orsborn, a M., Nelson, P. V, Clements, P.R., Morris, C.P., Hopwood, J.J., 1991. Human alpha-L-iduronidase: cDNA isolation and expression. Proc. Natl. Acad. Sci. U. S. A. 88, 9695–9.

Sifuentes, M., Doroshow, R., Hoft, R., Mason, G., Walot, I., Diament, M., Okazaki, S., Huff, K., Cox, G.F., Swiedler, S.J., Kakkis, E.D., 2007. A follow-up study of MPS I patients treated with laronidase enzyme replacement therapy for 6 years. Mol. Genet. Metab. 90, 171–80.

Sugawara, K., Saito, S., Ohno, K., Okuyama, T., Sakuraba, H., 2008. Structural study on mutant alpha-L-iduronidases: insight into mucopolysaccharidosis type I. J. Hum. Genet. 53, 467–74.

Terlato, N.J., Cox, G.F., 2003. Can mucopolysaccharidosis type I disease severity be predicted based on a patient's genotype? A comprehensive review of the literature. Genet. Med. 5, 286–94.

Thomas, J. a, Beck, M., Clarke, J.T.R., Cox, G.F., 2010. Childhood onset of Scheie syndrome, the attenuated form of mucopolysaccharidosis I. J. Inherit. Metab. Dis. 33, 421–7.

Tomatsu, S., Montaño, A.M., Oguma, T., Dung, V.C., Oikawa, H., de Carvalho, T.G., Gutiérrez, M.L., Yamaguchi, S., Suzuki, Y., Fukushi, M., Sakura, N., Barrera, L., Kida, K., Kubota, M., Orii, T., 2010. Dermatan sulfate and heparan sulfate as a biomarker for mucopolysaccharidosis I. J. Inherit. Metab. Dis. 33, 141–50.

Valayannopoulos, V., Wijburg, F. a, 2011. Therapy for the mucopolysaccharidoses. Rheumatology (Oxford). 50 Suppl 5, v49–59.

Vériter, S., Gianello, P., Dufrane, D., 2013. Bioengineered sites for islet cell transplantation. Curr. Diab. Rep. 13, 745–55.

Wang, D., Shukla, C., Liu, X., Schoeb, T.R., Clarke, L. a, Bedwell, D.M., Keeling, K.M., 2010. Characterization of an MPS I-H knock-in mouse that carries a nonsense mutation analogous to the human IDUA-W402X mutation. Mol. Genet. Metab. 99, 62–71.

Zhang, Y., Wang, W., Xie, Y., Yu, W., Teng, H., Liu, X., Zhang, X., Guo, X., Fei, J., Ma, X., 2007. In vivo culture of encapsulated endostatin-secreting Chinese hamster ovary cells for systemic tumor inhibition. Hum. Gene Ther. 18, 474–81.

ANEXOS

PRODUÇÃO CIENTÍFICA RELACIONADA

Durante o período do mestrado, um artigo foi elaborado e 2 foram publicados, além da dissertação. Estes trabalhos envolvem diferentes aspectos da MPS I e estão em anexo.

ANEXO I

Reduced NCAM gene expression and increased GFAP protein expression may contribute to the neuropathology of Mucopolysaccharidosis type I

Martinelli BZ, Mayer FQ, Baldo G, Wink MR, Fernandes MC, Giugliani R, Matte U.

Abstract

Mucopolysaccharidosis type I (MPS I) is a lysosomal storage disease caused by a deficiency of α-L-iduronidase (IDUA), resulting in accumulation of heparan sulfate (HS) and affecting several metabolic pathways. In order to gain insight into the neuropathophysiology of MPS I, we evaluated the expression of genes coding proteins that could be impaired by HS storage and the astrocyte response under this condition. Thus, brain cortex and hippocampus from 6-month-old MPS I and normal mice were used to analyze the gene expression of neural cell adhesion molecule (*NCAM*), growth associated protein-43 (*GAP-43*), fibroblast growth factor-2 (*FGF-2*) and fibroblast growth factor receptor-1 (*FGFR-1*) by quantitative-PCR reactions. Immunohistochemistry was performed to evaluate glial fibrilar acidic protein (*GFAP*) positive cells in the tissues. The results demonstrate that *NCAM* mRNA levels were reduced in both cortex (0.65-fold normal) and hippocampus (0.6-fold normal) of MPS I mice. There was an increase in *GAP-43* levels in hippocampus (1.37-fold normal) but not in the cortex. *FGFR-1* was increased in both cortex (1.19-fold normal) and hippocampus (1.37-fold normal), and no difference in *FGF-2* expression was detected. The number of GFAP-positive cells was higher in the cortex (7.7-fold normal) and hippocampus (1.4-fold normal) of MPS I mice, with darker staining and more profuse ramifications. Considering the altered pattern of expression observed, our study suggests possible pathways that could contribute to the neuropathology of MPS I, although more precise molecular mechanisms need to be verified.

1. Introduction

Mucopolysaccharidosis type I (MPS I) is a lysosomal storage disease (LSD) caused by a deficiency of the lysosomal hydrolase α-L-iduronidase (IDUA), with impairment in the degradation of the glycosaminoglycans (GAGs) heparan sulfate (HS) and dermatan sulfate (DS), leading to a progressive and multisystemic disease with a wide range of manifestations (Giugliani et al., 2010; Matte et al., 2003). The neuropathology in LSDs is noted by the accumulation of primary and secondary storage products, affecting metabolic pathways in the central nervous system (CNS; Heard et al., 2010; Wilkinson et al., 2012). However, the mechanisms by which lysosomal storage of GAGs can lead to neurological damage are not yet clarified.

HS and the its proteoglycans (HSPGs) at the cell surface and within the extracellular matrix bind a plethora of ligands and are essential for cell signaling and distribution of growth factors and cytokines (Bishop et al., 2007). In CNS, HSPGs interact with fibroblast growth factor-2 (FGF-2), increasing its affinity for FGF receptor-1 (FGFR-1). The induction of FGF-2/FGFR-1 system by HS chains results in activation of various signal transduction pathways and have a critical role in neurogenesis, axonal guidance, and synapse formation (Reuss and von Bohlen und Halbach, 2003; Zechel et al., 2010). FGFR-1 is also the main partner of neural cell adhesion molecule (NCAM), a regulator of intracellular signaling involved in cell adhesion and neurite outgrowth, synaptic plasticity, learning and memory consolidation (Kiselyov, 2010; Sandi, 2004). NCAM-mediated activation of FGFR-1 was shown to be associated with increased growth-associated protein (GAP-43, also known as neuromodulin) phosphorylation (Korshunova and Mosevitsky, 2010).

The neurological dysfunction in MPS I mice has been reported to involve neuroinflammation, gliosis and memory deficits (Baldo et al., 2012; Pan et al., 2008; Reolon et al., 2006). A previous study from our group has shown CNS pathology quite evident at 6 months of age in the mouse model, glial fibrilar acid protein (GFAP), a classical marker for activated astrocytes, increased at 8 months (Baldo et al., 2012). GFAP overexpression is an indication of reactive gliosis and is known to be induced by multiple factors such as brain damage, aging and disease (Middeldorp and Hol, 2011; Sofroniew and Vinters, 2010).

Trying to gain insight into the neuropathophysiology of MPS I, we analyzed gene expression of *NCAM*, *GAP-43*, *FGF-2* and *FGFR-1*, four genes coding proteins that could

be impaired by HS accumulation, in the CNS of 6-month-old MPS I mice and normal littermates.

2. Material and methods

2.1. Animals

Male *Idua*$^{-/-}$ mice (MPS I group, n=4) on a C57BL/6 background (Ohmi et al., 2003) and their normal littermate controls (normal group, n=5) were used in this study. Animals were maintained in conventional housing under a 12h light/12h dark cycle with controlled temperature (19 ± 1 ° C) and humidity (50 ± 10%). At 6 months old, they were killed by cervical dislocation after isoflurane anesthesia. The brain was obtained and cortex and hippocampus were isolated and divided in two parts. One part of each tissue was maintained at -80°C for gene expression analysis, and the other part was fixed in buffered formalin for immunohystochemistry analysis. The study was approved by the authors' institutional ethics review board and was conducted in accordance with the National Guidelines on Animal Care.

2.2. RT-qPCR

Total RNA was isolated from cortex and hippocampus following the manufacturer's protocol using Trizol® (Invitrogen, USA) and was quantified using NanoDrop (NanoDrop Technologies, USA). The conversion to cDNA was made using M-MLV Reverse Transcriptase (Invitrogen, USA).

Gene expression of *NCAM, FGF-2, FGFR-1* and *GAP-43* was performed by the comparative CT (ΔΔCT) method (Livak and Schmittgen, 2001) and Glyceraldehyde 3-phosphate dehydrogenase (*GAPDH*) was the reference gene. Primers pairs used for each gene are described on Table 1. Quantitative PCR reactions were performed on the MXPro Program (Stratagene – GE Healthcare Life Sciences, USA) using SYBR Green Master Mix (Invitrogen, USA) at 60°C annealing temperature for all genes.

2.3. Immunohistochemistry

For detection of GFAP in cortex and hippocampus, immunohistochemistry was performed by peroxidase-based ADVANCE™ HRT kit (DAKO, USA) using the specific primary antibody at 1:700 dilution. To detect reactive cells, the tissues were analyzed by

counting positive GFAP cells ($GFAP^+$) in 5 random high power fields by a researcher blinded for the groups.

2.4. Data analysis

Statistical analysis was performed by Predictive Analytics SoftWare (PASW, version 18.0) and GraphPad Prism (version 5.01) using Student's t test. The comparisons were made between normal and MPS I groups. Statistical differences among groups were considered when $p<0.05$.

3. Results

Quantitative real-time PCR analysis was used to determine *NCAM*, *GAP-43*, *FGF-2* and *FGFR-1* gene expression in cortex and hippocampus from MPS I and normal groups (Fig.1). The *NCAM* mRNA levels were reduced in both cortex (0.65-fold normal, p=0.027) and hippocampus (0.6-fold normal, p=0.0053) of MPS I mice (Fig.1A). There was an increase in *GAP-43* mRNA levels in hippocampus (1.37-fold normal, p=0.002) and no significant difference was observed in cortex (p=0.068) (Fig.1B). *FGFR-1* mRNA was increased in both cortex (1.19-fold normal, p=0.042) and hippocampus (1.37-fold normal, p=0.0002) (Fig.1C). *FGF-2* mRNA levels in cortex and hippocampus did not show differences between normal and MPS I groups (Fig.1D).

In order to investigate if cortex and hippocampus of MPS I mice show alterations in astrocytes, immunohistochemistry was used to evaluate the distribution of GFAP-positive ($GFAP^+$) cells from MPS I and normal mice. GFAP-immunostained cells in MPS I group showed darker staining and more ramifications than the normal group (Fig. 2). The number of GFAP+ cells was higher in the cortex (7.7-fold normal, p=0.003) and hippocampus (1.4-fold normal, p=0.01) of MPS I group, indicating the presence of activated astrocytes.

4. Discussion

MPS I is a progressive and multisystemic disease caused by a deficiency of the lysosomal hydrolase IDUA. Due to the impaired turnover of GAGs, the primary accumulation of HS and secondary storage of other compounds affect many different cell

types, causing abnormalities in a variety of cellular functions (Heard et al., 2010). Moreover, the HS accumulated in MPS I is abnormally sulfated, which impairs signal transduction pathways, since the degree and pattern of HS sulfation determines growth factors binding and function (Gallagher, 2006, Holley et al., 2011; Pan et al., 2005).

Here we showed a modest increase in the expression of *FGFR-1* in both cortex and hippocampus of MPS I mice but no differences in *FGF-2* levels. Similarly, the mouse model of MPS IIIB, at same age and also characterized by HS accumulation, did not present differences in *FGF-2* levels in both frontal cortex and hippocampus, but it was reduced in the caudal cortex (Li et al., 2002). Conflicting with our findings, FGFR-1 levels were reduced in these brain structures (Li et al., 2002). Although alterations in *FGF-2* expression were not observed here, a study showed the impaired FGF-2 function in proliferation and survival of multipotent adult progenitor cells from MPS I patients (Pan et al., 2005).

HS is also involved in NCAM function (Senkov et al., 2012), regulating cell adhesion, neurite outgrowth, stress modulation, learning and memory (Dityatev et al., 2004; Gascon et al., 2007; Sandi, 2004). For the first time, NCAM expression is analyzed in MPS, and our results showed a considerable reduction in *NCAM* mRNA levels in both cortex and hippocampus of MPS I mice. Studies both *in vitro* and *in vivo* have reported that NCAM signaling cascade can be initiated by the direct interaction with its major partner FGFR-1, and a deficiency in NCAM causes reduced FGFR activation (Aonurm-Helm et al., 2010; Kiselyov, 2010; Walmod et al., 2004). In addition, we observed that *GAP-43* mRNA levels are higher in MPS I hippocampus than in normal littermates. GAP-43 is the major protein of the growth cone, implicated in morphogenic activity and is important for NCAM-induced neuritogenesis, a process where FGFR-1 activation by NCAM initiates a signaling cascade resulting in phosphorylation of GAP-43, leading to stabilization of the actin cytoskeleton and neurite outgrowth (Korshunova and Mosevitsky, 2010). Thus, the increased expression of FGFR-1 could be a compensatory mechanism to maintain the aforementioned process in the case of reduced NCAM expression.

The accumulation of HS was previously related to the synaptic plasticity and the neuropathology of MPS IIIB in studies showing lower levels of synaptophysin and its enhanced degradation, increased neurite outgrowth and GAP-43 mRNA and protein expression with age (Hocquemiller et al., 2010; Li et al., 2002; Vitry et al., 2009). Since the deleterious role of GAP-43 overexpression was observed on memory (Holahan et al., 2007), the increased GAP-43 mRNA levels in hippocampus of MPS I mice, even

moderate, are consistent with the impaired spatial learning and memory noted in MPS I mice (Baldo et al., 2012; Pan et al., 2008; Reolon et al., 2006). Moreover, cognition, memory formation and neural plasticity in the hippocampus are also modulated by *NCAM* (Gascon et al., 2007; Sandi, 2004; Venero and Herrero, 2006) and NCAM activity-dependent remodeling of synapses involve interactions with HS proteoglycans (Dityatev et al., 2004; Senkov et al., 2012), suggesting that the cognitive impairment in MPS I could be related to NCAM and GAP-43 altered expression.

As a consequence of the altered expression pattern and the well-characterized storage compounds in MPS I, perturbed homeostasis in CNS are expected. Astrocytes undergo a series of changes in response to pathological insults, being considered a hallmark of CNS conditions (Halassa and Haydon, 2010). Changes in their morphology and increased *GFAP* expression are characteristics of reactive gliosis, a process highly associated with neuroinflammation, brain injury, aging and neurodegeneration (Middeldorp and Hol, 2011; Sofroniew and Vinters, 2010). We found high levels of GFAP protein expression in cortex and hippocampus of MPS I group, indicating that important alterations in astrocyte function may happen in MPS I. Previously, an increase in GFAP expression was reported in cortex of MPS I mice at 8 months of age (Baldo et al., 2012) and MPS I and MPS IIIB at 3, 4 and 9 months (Ohmi et al., 2003; Wilkinson et al., 2012), confirming the involvement of storage products in MPS neuroinflammation.

Astrocyte-neuron interactions via NCAM modulate the astrocyte proliferation and reduce the microglial activation (Chang et al., 2000; Krushel et al., 1998), indicating that reduced *NCAM* expression may contribute to neuroinflammation along with GFAP in MPS I. GFAP and NCAM/FGFR-1 relation and function have been evidenced by studies using a NCAM-derived peptide, identified as FG loop (FGL), which interacts with the binding site of FGFR-1, mimicking their action (Aonurm-Helm et al., 2010; Kraev et al., 2011; Walmod et al., 2004). It was reported that FGL treatment reduces astrocytes GFAP immunoreactivity and microglial cell density in hippocampus, restore cognitive function and averts neuropathology in ageing models due to its anti-inflammatory properties (Downer et al., 2010; Ojo et al., 2011), suggesting that the neuroinflammation observed in MPS I could be related to decreased NCAM expression.

In conclusion, altered *NCAM, FGFR-1, GAP-43* and GFAP pattern expression was observed in the MPS I mouse model, suggesting their contribution to the neuropathology of this disease, although more precise molecular mechanisms need to be verified.

References

Aonurm-Helm, A., Berezin, V., Bock, E., Zharkovsky, A., 2010. peptide, restores disrupted fibroblast growth factor receptor (FGFR) phosphorylation and FGFR mediated signaling in neural cell adhesion molecule (NCAM)-deficient. Brain Res. 1309, 1–8.

Baldo, G., Mayer, F.Q., Martinelli, B., Dilda, A., Meyer, F., Ponder, K.P., Giugliani, R., Matte, U., 2012. Evidence of a progressive motor dysfunction in Mucopolysaccharidosis type I mice. Behav. Brain Res. 233, 169–75.

Bishop, J.R., Schuksz, M., Esko, J.D., 2007. Heparan sulphate proteoglycans fine-tune mammalian physiology. Nature 446, 1030–7.

Chang, R.C., Hudson, P., Wilson, B., Liu, B., Abel, H., Hemperly, J., Hong, J.S., 2000. Immune modulatory effects of neural cell adhesion molecules on lipopolysaccharide-induced nitric oxide production by cultured glia. Brain Res. Mol. Brain Res. 81, 197–201.

Dityatev, A., Dityateva, G., Sytnyk, V., Delling, M., Toni, N., Nikonenko, I., Muller, D., Schachner, M., 2004. Polysialylated neural cell adhesion molecule promotes remodeling and formation of hippocampal synapses. J. Neurosci. 24, 9372–82.

Downer, E.J., Cowley, T.R., Lyons, A., Mills, K.H.G., Berezin, V., Bock, E., Lynch, M. a, 2010. A novel anti-inflammatory role of NCAM-derived mimetic peptide, FGL. Neurobiol. Aging 31, 118–28.

Gascon, E., Vutskits, L., Kiss, J., 2007. Polysialic acid–neural cell adhesion molecule in brain plasticity: From synapses to integration of new neurons. Brain Res. Rev. 56, 101–118.

Giugliani, R., Federhen, A., Rojas, M.V.M., Vieira, T., Artigalás, O., Pinto, L.L., Azevedo, A.C., Acosta, A., Bonfim, C., Lourenço, C.M., Kim, C.A., Horovitz, D., Bonfim, D., Norato, D., Marinho, D., Palhares, D., Santos, E.S., Ribeiro, E., Valadares, E., Guarany, F., de Lucca, G.R., Pimentel, H., de Souza, I.N., Correa, J., Fraga, J.C., Goes, J.E., Cabral, J.M., Simionato, J., Llerena, J., Jardim, L., Giuliani, L., da Silva, L.C.S., Santos, M.L., Moreira, M.A., Kerstenetzky, M., Ribeiro, M., Ruas, N., Barrios, P., Aranda, P., Honjo, R., Boy, R., Costa, R., Souza, C., Alcantara, F.F., Avilla, S.G. a, Fagondes, S., Martins, A.M., 2010. Mucopolysaccharidosis I, II, and VI: Brief review and guidelines for treatment. Genet. Mol. Biol. 33, 589–604.

Halassa, M.M., Haydon, P.G., 2010. Integrated brain circuits: astrocytic networks modulate neuronal activity and behavior. Annu. Rev. Physiol. 72, 335–55.

Heard, J.M., Bruyère, J., Roy, E., Bigou, S., Ausseil, J., Vitry, S., 2010. Storage problems in lysosomal diseases. Biochem. Soc. Trans. 38, 1442–7.

Hocquemiller, M., Vitry, S., Bigou, S., Bruyère, J., Ausseil, J., Heard, J.M., 2010. GAP43 overexpression and enhanced neurite outgrowth in mucopolysaccharidosis type IIIB cortical neuron cultures. J. Neurosci. Res. 88, 202–13.

Holahan, M.R., Honegger, K.S., Tabatadze, N., Routtenberg, A., 2007. GAP-43 gene expression regulates information storage. Learn. Mem. 14, 407–15. doi:10.1101/lm.581907

Kiselyov, V., 2010. NCAM and the FGF-Receptor. Adv. Exp. Med. Biol. 663, 67–79.

Korshunova, I., Mosevitsky, M., 2010. Role of the Growth-Associated Protein GAP-43 in NCAM-Mediated Neurite Outgrowth. Adv. Exp. Med. Biol., Advances in Experimental Medicine and Biology 663, 169–182.

Kraev, I., Henneberger, C., Rossetti, C., Conboy, L., Kohler, L.B., Jennings, A., Venero, C., Popov, V., Rusakov, D., Stewart, M.G., Bock, E., Berezin, V., Sandi, C., 2011. A peptide mimetic targeting trans-homophilic NCAM binding sites promotes spatial learning and neural plasticity in the hippocampus. PLoS One 6, e23433.

Krushel, L. a, Tai, M.H., Cunningham, B. a, Edelman, G.M., Crossin, K.L., 1998. Neural cell adhesion molecule (N-CAM) domains and intracellular signaling pathways involved in the inhibition of astrocyte proliferation. Proc. Natl. Acad. Sci. U. S. A. 95, 2592–6.

Li, H.H., Zhao, H.-Z., Neufeld, E.F., Cai, Y., Gómez-Pinilla, F., 2002. Attenuated plasticity in neurons and astrocytes in the mouse model of Sanfilippo syndrome type B. J. Neurosci. Res. 69, 30–8.

Livak, K.J., Schmittgen, T.D., 2001. Analysis of relative gene expression data using real-time quantitative PCR and the 2(-Delta Delta C(T)) Method. Methods 25, 402–8.

Matte, U., Yogalingam, G., Brooks, D., Leistner, S., Schwartz, I., Lima, L., Norato, D.Y., Brum, J.M., Beesley, C., Winchester, B., Giugliani, R., Hopwood, J.J., 2003. Identification and characterization of 13 new mutations in mucopolysaccharidosis type I patients 78, 37–43.

Middeldorp, J., Hol, E.M., 2011. GFAP in health and disease. Prog. Neurobiol. 93, 421–43.

Ohmi, K., Greenberg, D.S., Rajavel, K.S., Ryazantsev, S., Li, H.H., Neufeld, E.F., 2003. Activated microglia in cortex of mouse models of mucopolysaccharidoses I and IIIB. Proc. Natl. Acad. Sci. U. S. A. 100, 1902–7.

Ojo, B., Rezaie, P., Gabbott, P.L., Cowely, T.R., Medvedev, N.I., Lynch, M. a, Stewart, M.G., 2011. A neural cell adhesion molecule-derived peptide, FGL, attenuates glial cell activation in the aged hippocampus. Exp. Neurol. 232, 318–28.

Pan, D., Sciascia, A., Vorhees, C. V, Williams, M.T., 2008. Progression of multiple behavioral deficits with various ages of onset in a murine model of Hurler syndrome. Brain Res. 1188, 241–53.

Reolon, G.K., Braga, L.M., Camassola, M., Luft, T., Henriques, J.A.P., Nardi, N.B., Roesler, R., 2006. Long-term memory for aversive training is impaired in Idua(-/-) mice, a genetic model of mucopolysaccharidosis type I. Brain Res. 1076, 225–30.

Reuss, B., von Bohlen und Halbach, O., 2003. Fibroblast growth factors and their receptors in the central nervous system. Cell Tissue Res. 313, 139–57.

Sandi, C., 2004. Stress, cognitive impairment and cell adhesion molecules. Nat. Rev. Neurosci. 5, 917–30.

Senkov, O., Tikhobrazova, O., Dityatev, A., 2012. PSA-NCAM: synaptic functions mediated by its interactions with proteoglycans and glutamate receptors. Int. J. Biochem. Cell Biol. 44, 591–5.

Sofroniew, M. V, Vinters, H. V, 2010. Astrocytes: biology and pathology. Acta Neuropathol. 119, 7–35.

Venero, C., Herrero, A., 2006. Hippocampal up-regulation of NCAM expression and polysialylation plays a key role on spatial memory. Eur. J. Neurosci. 23, 1585–1595.

Vitry, S., Ausseil, J., Hocquemiller, M., Bigou, S., Dos Santos Coura, R., Heard, J.M., 2009. Enhanced degradation of synaptophysin by the proteasome in mucopolysaccharidosis type IIIB. Mol. Cell. Neurosci. 41, 8–18.

Walmod, P.S., Kolkova, K., Berezin, V., Bock, E., 2004. Zippers make signals: NCAM-mediated molecular interactions and signal transduction. Neurochem. Res. 29, 2015–35.

Wilkinson, F.L., Holley, R.J., Langford-Smith, K.J., Badrinath, S., Liao, A., Langford-Smith, A., Cooper, J.D., Jones, S. a, Wraith, J.E., Wynn, R.F., Merry, C.L.R., Bigger, B.W., 2012. Neuropathology in mouse models of mucopolysaccharidosis type I, IIIA and IIIB. PLoS One 7, e35787.

Zechel, S., Werner, S., Unsicker, K., von Bohlen und Halbach, O., 2010. Expression and functions of fibroblast growth factor 2 (FGF-2) in hippocampal formation. Neuroscientist 16, 357–73.

Tables

Table 1: Primer pairs used to gene expression analysis.

	Forward (5' – 3')	***Reverse (5' – 3')***
NCAM	GTGAAGAAAAGACTCTGGATG	TGGAGCTTGGGAGCATATTG
GAP-43	AACAAGCCGATGTGCCTGC	CAGCGTCTTTCTCCTCCTCA
FGFR-1	TCTACACACACCAGAGCGATG	ATGACCCTCCTTCAGCAGC
FGF-2	GAGAAGAGCGACCCACACG	GGCACACACTCCCTTGATAGA
GAPDH	CCCATCACCATCTTCCAGG	CATATTTGGCAGCTTTCTCC

Figures

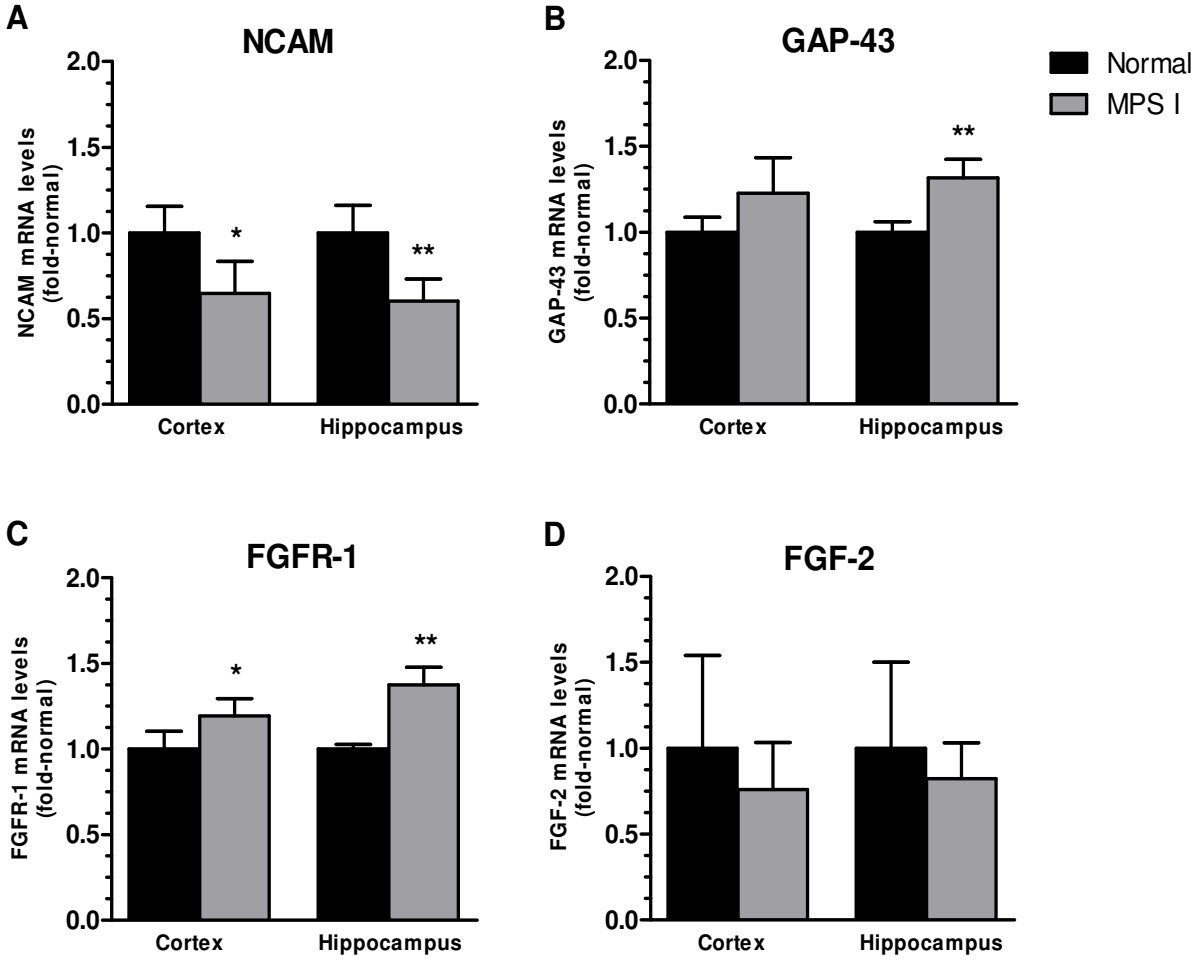

Fig. 1: NCAM (A), GAP-43 (B), FGFR-1(C) and FGF-2 (D) mRNA levels in cortex and hippocampus of normal (n=5) and MPS I mice (n=4). Gene expression was performed by the comparative CT (ΔΔCT) method and GAPDH was the reference gene. * $p< 0.05$; ** $p< 0.01$ Student's t test.

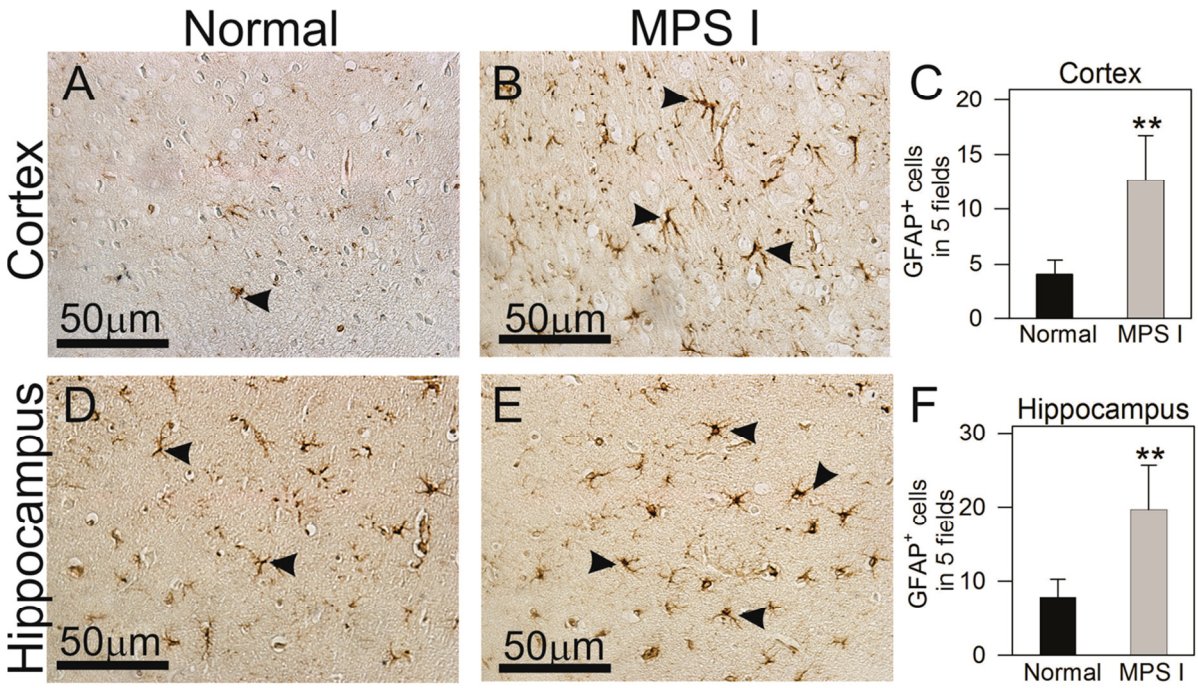

Fig. 2: Glial fibrilary acidic protein (GFAP) immunohistochemistry. Representative sections from normal (A and D; n=5) and MPS I (B and E; n=4) mouse brains. Number of positive cells was counted in 5 fields (40X magnification) in mouse cortex (C) and hippocampus (F). Arrows indicate positive cells for GFAP immunohistochemistry, evidencing glial activation in MPS I mice. ** $p < 0.01$ Student's t test.

ANEXO II

Molecular Genetics and Metabolism 109 (2013) 33–40

Contents lists available at SciVerse ScienceDirect

Molecular Genetics and Metabolism

journal homepage: www.elsevier.com/locate/ymgme

Enzyme replacement therapy started at birth improves outcome in difficult-to-treat organs in mucopolysaccharidosis I mice

Guilherme Baldo [a,b], Fabiana Q. Mayer [a], Bárbara Z. Martinelli [a,b], Talita G. de Carvalho [a,c], Fabiola S. Meyer [d], Patrícia G. de Oliveira [e], Luise Meurer [f], Ângela Tavares [g], Ursula Matte [a,c,*], Roberto Giugliani [a,b,c,h]

[a] Centro de Terapia Gênica, Hospital de Clinicas de Porto Alegre, RS, Brazil
[b] Programa de Pós-graduação em Ciências Biológicas: Bioquímica, UFRGS, Porto Alegre, RS, Brazil
[c] Programa de Pós-graduação em Genética e Biologia Molecular, UFRGS, Porto Alegre, RS, Brazil
[d] Unidade de Experimentação Animal, Hospital de Clinicas de Porto Alegre, RS, Brazil
[e] Laboratório de Doenças Auto-imunes, Hospital de Clínicas de Porto Alegre, RS, Brazil
[f] Unidade de Patologia Experimental, Hospital de Clínicas de Porto Alegre, RS, Brazil
[g] Programa de Pós-graduação em Fisiologia, UFRGS, Porto Alegre, RS, Brazil
[h] Departamento de Genética, UFRGS, Porto Alegre, RS, Brazil

ARTICLE INFO

Article history:
Received 17 January 2013
Received in revised form 9 March 2013
Accepted 9 March 2013
Available online 16 March 2013

Keywords:
Mucopolysaccharidosis I
Enzyme replacement therapy
Hurler Syndrome
Blood–brain-barrier

ABSTRACT

Since we previously observed that in patients with mucopolysaccharidosis (MPS) the storage of undegraded glycosaminoglycans (GAG) occurs from birth, in the present study we aimed to compare normal, untreated MPS I mice (knockout for alpha-L-iduronidase-IDUA), and MPS I mice treated with enzyme replacement therapy (ERT, Laronidase, 1.2 mg/kg every 2 weeks) started from birth (ERT-neo) or from 2 months of age (ERT-ad). All mice were sacrificed at 6 months. Both treatments were equally effective in normalizing GAG levels in the viscera but had no detectable effect on the joint. Heart function was also improved with both treatments. On the other hand, mice treated from birth presented better outcomes in the difficult-to-treat aortas and heart valves. Surprisingly, both groups had improvements in behavior tests, and normalization of GAG levels in the brain and IDUA injection resulted in detectable levels of enzyme in the brain tissue 1 h after administration. ERT-ad mice developed significantly more anti-IDUA-IgG antibodies, and mice that didn't develop antibodies had better performances in behavior tests, indicating that development of antibodies may reduce enzyme bioavailability. Our results suggest that ERT started from birth leads to better outcomes in the aorta and heart valves, as well as a reduction in antibody levels. Some poor vascularized organs, such as the joints, had partial or no benefit and ancillary therapies might be needed for patients. The results presented here support the idea that ERT started from birth leads to better treatment outcomes and should be considered whenever possible, a observation that gains relevance as newborn screening programs are being considered for MPS and other treatable lysosomal storage disorders.

1. Introduction

Mucopolysaccharidosys type I (MPS I) is a disorder characterized by deficiency of the lysosomal hydrolase alpha-L-iduronidase (IDUA) and storage of undegraded glycosaminoglycans (GAG) heparan sulphate and dermatan sulphate. The disease spectrum varies from the severe Hurler syndrome (OMIM #67014) to the attenuated Scheie syndrome (OMIM # 67016). The Hurler form presents severe mental retardation in addition to other systemic manifestations (organomegaly, heart enlargement, joint stiffness) which are also found in the attenuated forms of the disease [1].

Enzyme replacement therapy (ERT) is available for MPS I patients since early 2000s, and it is currently the most used treatment for this disorder [2]. It relies on the ability of deficient cells to internalize a systemic delivered enzyme using the mannose-6-phosphate receptor [3], which reaches the lysosome and degrades the GAG.

In recent years, reports in large animal models [4] and human subjects [5,6] suggest that early introduction of ERT leads to better outcomes. For example, a multicentric clinical study with early treatment (started before 5 years of age) reported improvement in heart function, decrease in urinary GAG and normal mental development [5]. Also, studies in the MPS VII mice showed that the blood-brain-barrier (BBB) is permissive to lysosomal enzymes only during the first 2 weeks of life [7], and therefore neonatal treatment could reduce storage in the brain and possibly prevent or delay the cognitive decline. However, a

Abbreviations: CtsD, cathepsin D; ERT, enzyme replacement therapy; GAG, glycosaminoglycans; GFAP, glial fibrillary acid protein; MPS, mucopolysaccharidosis.

* Corresponding author at: Centro de Terapia Genica, Hospital de Clinicas de Porto alegre, Rua Ramiro Barcelos, 2350, Porto Alegre, RS, Brazil—90035-903. Fax: +55 51 3359 8010.
E-mail address: umatte@hcpa.ufrgs.br (U. Matte).

1096-7192/$ – see front matter © 2013 Elsevier Inc. All rights reserved.
http://dx.doi.org/10.1016/j.ymgme.2013.03.005

systematic comparison of ERT for MPS I started at birth or at young adult age was never performed.

We have recently described that in human patients with different types of MPS, GAG storage can be detected already in the placental tissue, suggesting that in those patients GAG accumulation starts in the fetal life [8]. Therefore, we decided to systematically investigate the benefits from ERT started at birth comparing to the adult period in MPS I mice.

2. Material and methods

2.1. Experimental groups

The study was approved by the authors' institutional ethics review board and mice on a C57BL/6 background (kindly donated by Dr. Elizabeth Neufeld, UCLA, USA) were used. MPS I and normal mice were genotyped by PCR as previously described [9].

We compared four groups of male mice: in the first group, MPS I mice (knockout for the IDUA gene) received ERT (Laronidase®, Genzyme, USA) from birth (ERT-neo, n = 10) at 1.2 mg/kg intravenously every two weeks. The first Laronidase injection in neonatal mice was performed via the superficial temporal vein, and subsequent injections were performed via tail vein. The total Laronidase volume was injected over 30 s. This regimen was chosen based on a previous clinical study from the group [10]. The second group received the same treatment but it was started at 60 days of age (ERT-ad, n = 8). We compared those groups to untreated MPS I mice (MPS I, n = 13) and to wild-type mice (Normal, n = 10). All animals were weighed and sacrificed at 6 months of age. In treated mice, the sacrifice was performed two weeks after the last injection.

In addition, some 4 month-old MPS I mice (n = 3–4/group) were injected with a single dose of laronidase (zero, 1.2 or 2.4 mg enzyme/kg weight) through the tail vein (maximum volume of enzyme injected was 120 μL). Animals were anesthetized, serum was collected and animals were perfused with at least 20 mL of PBS 1 h after the injection to measure enzyme activity in the brain.

2.2. IDUA activity

Tissues were homogenized with a dismembrator in distilled water. Alpha-L-iduronidase activity assay was performed incubating the protein extracts with the fluorescent substrate 4-methylumbelliferyl-alpha-L-iduronide (Glycosynth, UK) at 37 °C for 1 h in pH 3.5 formate buffer [11]. Results were expressed as fold-change, compared to MPS I untreated mice. Protein content was measured using the method described by Lowry [12].

2.3. Cathepsin D activity

Tissues were homogenized in 100 mM sodium acetate pH 5.5 containing 2.5 mM ethylenediaminetetraacetic acid, 0.1% Triton X-100, and 2.5 mM dithiothreitol. The cathepsin D (CtsD) assay was performed at pH 4 with 5 μM of the substrate 7-methoxycoumarin-4-acetyl-(Mca)-Gly-Lys-Pro-Ile-Leu-Phe-Phe-Arg-Leu-Lys-2,4 nitrophenyl (Dnp)-D-Arg-NH2, which can also be cleaved by CtsE, with Mca-Pro-Leu-OH (Enzo Life Sciences, USA) as the standard, as previously described [13].

2.4. GAG measurement

Tissues were homogenized in phosphate buffer and GAGs were measured using the dimethyl blue technique. In this technique, 25 uL of supernatant was mixed with freshly prepared dimethyl blue solution (Dimethyl blue 0.3 mol/L with 2 mol/L Tris) and absorbance was read at 530 nm. Results were expressed as percentage of normal mice. Urine samples were centrifuged and 25 μL were used for measuring GAG levels, and results were expressed as μg GAG/mg creatinine. Creatinine was measured using the Picric acid method [9].

2.5. Echocardiographic analysis

Six-month old mice were anesthetized with isofluorane and positioned on a controlled temperature bed. Animals were placed in left lateral decubitus position (45° angle) to obtain cardiac images. An EnVisor HD System, Philips Medical (Andover, MA, USA), with a 12-4 MHz transducer was used, at 2 cm depth with fundamental and harmonic imaging. Images were captured by a trained operator with experience in small animal echocardiography.

Left ventricular ejection fraction (LVEF) was calculated as: (end diastolic volume − end-systolic volume/end-diastolic volume) × 100; end-diastolic and end-systolic cavity volumes were calculated using Simpson's rule [14]. LV fraction shortening (LVFS) values were obtained using the following equation: LVFS = DD − SD/DD × 100 (diastolic diameter—DD; systolic diameter—SD). Fractional area change (FAC) was calculated as follows: FAC = diastolic area − systolic area/diastolic area. In the pulmonary valve the measures of the ejection and acceleration times were obtained using Doppler echocardiography, and their ratio was used as an index of pulmonary vascular resistance (PVR) [15].

2.6. Behavioral tests

2.6.1. Open field test

Locomotor and exploratory activities were assessed using an open field test. The test consisted of a square arena (52 × 52 cm^2) with 60 cm high walls. The floor was divided into 16 squares by parallel and intersecting lines, obtaining four centered squares and 12 periphery squares. Mice were placed in one of the corners of the open field and (a) ambulation (number of times a mouse crossed with 4 paws one of the lines in the floor), and (b) exploratory behavior (rearings) were observed during 5 min for both control and MPS I animals.

2.6.2. Repeated open field

This test is used as a measure of habituation memory [16,17]. In this test, mice are put in the open field apparatus for 5 min and activity (number of crossings and rearings) is measured. The test is repeated 30 and 60 min after the first trial to evaluate habituation to the new environment (a reduction in the activity should be observed in mice after each trial), and the results from the third trial are compared to the first one.

2.7. Histological analysis

At the time of sacrifice, mice were anesthetized, serum was collected by retro-orbital puncture and mice were sacrificed by cervical dislocation. Liver, lungs, kidneys, heart, testicles, aorta, and brain (cerebellum, cortex and hippocampus) were isolated and systematically divided in two pieces. One was flash frozen in liquid nitrogen for biochemical analysis and the other portion was fixed in buffered formalin. Thin cross sections were submitted to routine histological processing, stained with hematoxylin–eosin/alcian blue and analyzed.

Heart valves from the left ventricle (aortic and mitral valve) were obtained by sectioning the basal part of the heart. Samples were processed for histological analysis (H–E/alcian blue stain) and valve thickness was measured in at least 5 different points using a software (CellF, Olympus, Hamburg, Germany) and the average was used as a measure of the valve thickness.

Knee joints were collected and placed in buffered formalin for 2–7 days following decalcification with EDTA 14% for an additional week. Paraffin processing was performed according to routine techniques. A score was created to evaluate histological abnormalities, according to Supplementary Table 1. The higher the score, the worse

are the joints. Analyses were performed by a pathologist blinded to the groups.

Immunohistochemistry for glial fibrillary acidic protein (GFAP) was performed using specific antibody (Dako Cytomation, Polyclonal Rabbit anti-GFAP) and a secondary anti-rabbit IgG antibody conjugated to horseradish peroxidase as previously published [9]. Slides were analyzed by a researcher blinded to the groups, counting positive cells in 5 high-power fields (40×).

2.8. Antibody formation

We measured the formation of antibodies against the recombinant enzyme in serum collected at time of sacrifice. For the assay, 96-well ELISA plates were coated with 4 μg/mL of Laronidase in acid PBS overnight and blocked with 3% BSA. Diluted serum was added (1:50) and incubated for 2 h. A secondary antibody (Goat anti-mouse IgG, Sigma, USA) conjugated to peroxidase was diluted 1:1000, incubated for 3 h and revealed with TMB for 6 min. The reaction was stopped with H_2SO_4·1 M and the absorbance read at 450 nm [18].

2.9. Ethics and statistics

All experiments were approved by the ethics committee of our institution (Committee of Ethics in Research from Hospital de Clinicas de Porto Alegre—Permit number 08-658) with all procedures carried out in accordance with the recommendations in the Guide for the Care and Use of Laboratory Animals of the National Institutes of Health, monitored by our veterinary and designed to minimize animal suffering. For statistical analysis SigmaStat version 3.0 was used. Results were compared using ANOVA and Tukey or student t test, as indicated, and shown as average with errors bars indicating one standard deviation. A $p < 0.05$ was considered as statistically significant.

3. Results

3.1. Body weight and urinary GAG

No obvious adverse reactions were observed in ERT-neo or ERT-ad. MPS I mice were significantly heavier than normal mice (31.6 g vs 26 g, $p < 0.01$). Mice treated from birth presented a significant reduction in their weight, compared to MPS I untreated mice (27.2 g, $p < 0.01$) while mice treated from 2 months presented intermediate weight (30.1 g), which was not different from untreated mice (Fig. 1A). Urinary GAG presented a 56% reduction in ERT-neo mice and a 48% reduction in ERT-ad, both being significant compared to untreated MPS I ($p < 0.05$) and not different from normal mice (Fig. 1B).

3.2. GAG storage in visceral organs

Tissue GAG were extracted and quantified. GAG levels were elevated in liver (5.5-fold the normal values, $p < 0.05$ vs normal), whole kidney (cortex and medulla, 4.1-fold, $p < 0.05$), heart (2.5-fold, $p < 0.05$) and lungs (2-fold, $p < 0.05$) of untreated MPS I mice. Both ERT-neo and ERT-ad were equally effective in restoring normal GAG levels (Fig. 2A). Furthermore, histological analysis confirmed the reduction in tissue GAG in these organs and also in the testis (Fig. 2B).

3.3. Heart function

Echocardiography analysis was performed in 6-month old mice to analyze heart function. MPS I animals presented abnormalities in the left ventricle, with reduced ejection fraction, shortening fraction and fractional area change ($p < 0.05$ vs normal). Untreated mice also had a reduced AT/ET ratio in the pulmonary valve, which indicates pulmonary vascular resistance. Both treatments were able to restore normal heart function, with Neo-ERT performing slightly better (Fig. 3).

3.4. Aorta and heart valves

MPS I mice present aortic wall dilatation and heart valves thickening. MPS I mice aortas were distended (average of 33 μm in normal versus 73 μm in MPS I mice, which is 2.2-fold normal, $p < 0.01$) and had high amounts of storage, as evidenced by white vacuoles that can be visualized in H–E staining (Fig. 4A). ERT-neo aortas were 1.5-fold the normal values (average of 51 μm, not significant versus normal, $p < 0.05$ versus MPS I) while ERT-ad were 1.8-fold the normal values (average of 59 μm, $p < 0.05$ versus normal, not significant vs MPS I, Fig. 4B). Both treated groups still had some degree of storage in the aortas.

The width of heart valves from the left ventricle was also measured at 6 months (Fig. 4A). Untreated MPS I mice presented thickened heart valves, which were 3.5-fold the normal values (average value for normal valve thickness was 24 μm, versus 84 μm in MPS I mice, $p < 0.01$). ERT-neo group showed a significant reduction (average of 35 μm, which is 1.4-fold normal, $p < 0.01$ compared to MPS I and not significant versus normal), while ERT-ad presented intermediate values (average of 51 μm, 2.1-fold normal) which were not different from either normal ($p = 0.088$) or MPS I ($p = 0.052$) values (Fig. 4C). These results suggest that the heart valve is hard to correct, but ERT-neo seem to better prevent the thickening of this structure.

3.5. Behavioral analysis and brain abnormalities

Brain function was assessed using the open field test. MPS I mice have reduced crossings and rearings at the open field test, as

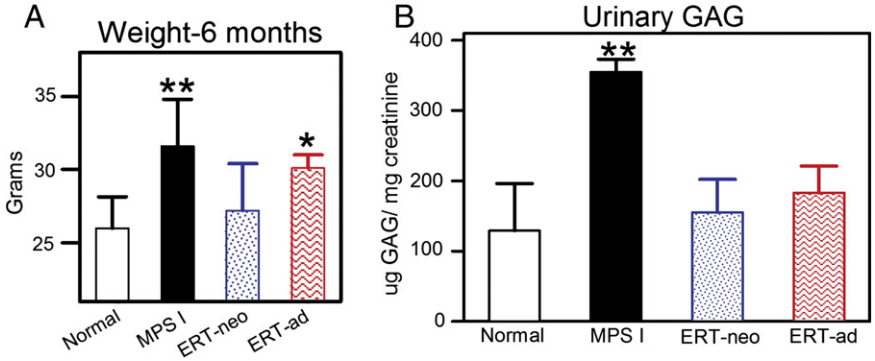

Fig. 1. Body weight and urinary GAG levels at 6 months. A) Body weight. Mice were weighed at 6 months. **$p < 0.01$ and *$p < 0.05$, compared to normal. ANOVA and Tukey *post hoc* B) Urinary GAG. Urine was collected from 6-month old mice, 2 weeks after the last Laronidase injection. *$P < 0.05$ compared to normal, ANOVA and Tukey *post hoc*.

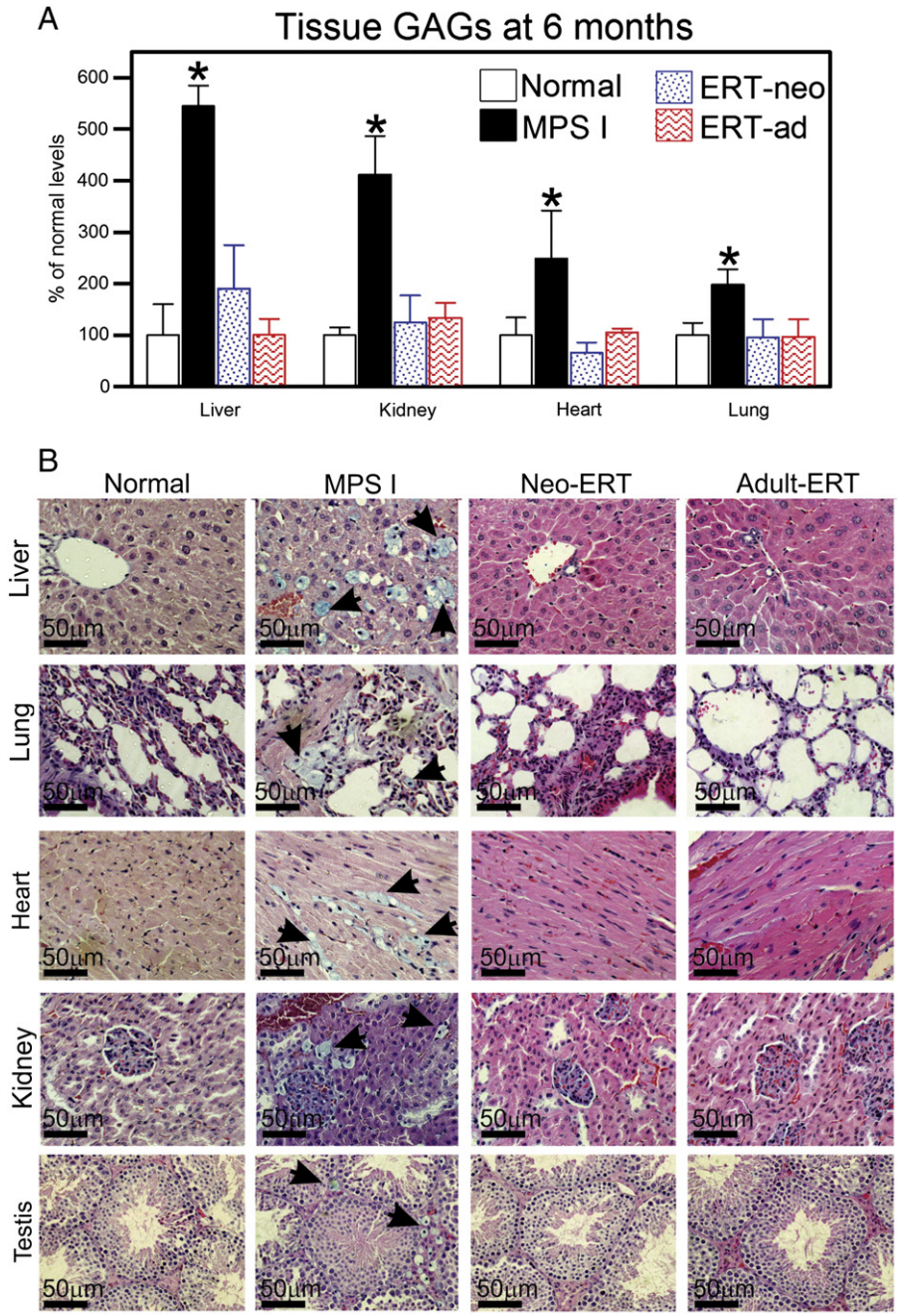

Fig. 2. Tissue GAG levels. A) Tissue GAG were measured using the dimethyl blue technique in visceral organs, and results are presented as percentage of normal levels. *P < 0.05 compared to normal levels, ANOVA and Tukey post hoc. N = 5–6/group. B) Representative histological sections stained with H–E/alcian blue (which show GAG storage in blue, indicated by black arrows) in visceral organs.

previously reported [9]. Surprisingly, both ERT-neo and ERT-ad had marked improvements in their locomotor activity and exploratory behavior (Fig. 5A). The open field can be used as a test of habituation memory if done repeated times. MPS I mice failed to habituate to the new environment, evidenced by a very small reduction in their activity comparing the first and the third trials. On the other hand, ERT-neo and ERT-ad mice habituate similarly to normal mice, and their activity in the third trial was about 60% of the first trial (Fig. 5B).

Based on these results, we measured GAG in the cortex of these mice. GAG levels were in MPS I mice were 1.8-fold the normal values ($p < 0.01$ vs normal), and both treatment reduced GAG to normal levels (Fig. 5C). Since GAG levels were not markedly elevated, we measured activity of cathepsin D, which we have found to be consistently elevated in the brains of MPS I mice and could be used as a biomarker (unpublished data). The CtsD activity in MPS I mice was 5-fold normal ($p < 0.01$ vs normal), and was reduced in ERT-neo (2.3-fold, not significant vs normal, $p < 0.05$ vs MPS I) and ERT-ad (1.8-fold, not significant versus normal, $p < 0.05$ vs MPS I) as can be visualized in Fig. 5D.

Finally, we evaluated GFAP content in the brain (Fig. 5E), since it was previously shown that brains of untreated MPS I mice have higher GFAP content, suggesting a neuroinflammatory process. GFAP content was elevated in MPS I mice (2.2-fold the normal values, $p = 0.001$) and reduced in both neonatal and adult-treated groups (1.3 and 1.4-fold normal, respectively, not significant versus normal and $p < 0.05$ versus MPS).

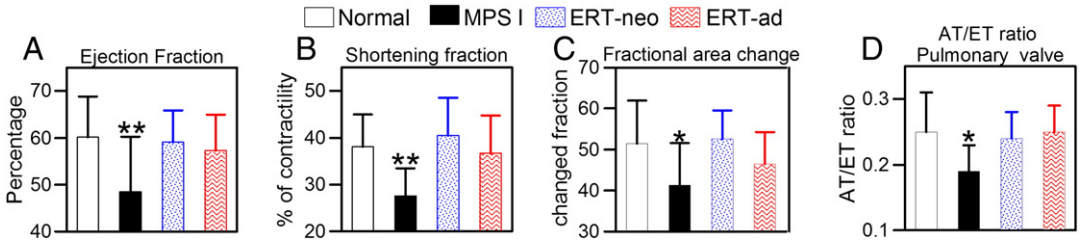

Fig. 3. Results from echocardiography. Analyses were performed in 6-month old mice as described in the Material and methods section. A) Ejection fraction. B) Shortening fraction. C) Fractional area change and D) The ratio between ejection and acceleration times measured at the pulmonary valve. The 3 first parameters suggest left ventricular dysfunction, while the AT/ET ratio suggests pulmonary hypertension in MPS I mice. *P < 0.05 compared to normal, ANOVA and Tukey. N = 6–13 animals/group.

3.6. IDUA activity in the brain

As our results from behavior and biochemical tests showed improvements, we decided to do an additional group of adult mice that were injected with 1.2 mg/kg of enzyme and sacrificed 1 h later. IDUA activity was 1.7-fold higher than in the untreated mice in the hippocampus (not significant), 1.1-fold in the cerebellum (not significant) and 3-fold in the cortex ($p < 0.05$ vs untreated). When the dose was increased twice (2.4 mg/kg of body weight) enzyme levels were markedly elevated, reaching almost normal levels in some areas, as can be seen in Fig. 5F. These results, together with the reduction in GAG levels observed in the brain cortex, suggest a benefit from the treatment on the brain disease.

3.7. Joint analysis

We have created a score to better describe the abnormalities found in MPS I knee joints using H–E stain (Supplement Table 1). These abnormalities included presence of a mild inflammatory infiltrate and loss of articular architecture, among other features. The average score of MPS I mice was significantly worse than Normal mice. In addition, both treatments were not able to improve joint aspect (Fig. 6 and Supplement Fig. 1).

3.8. Antibody formation and correlation with behavior test

We next sought to determine if treatment when started at earlier times could lead to a reduced antibody response against the enzyme. Using an ELISA assay, we could demonstrate that anti-IDUA antibodies could be detected in only 1 animal out of seven ERT-neo tested mice. On the other hand, in Ad-ERT mice, we detected antibodies in 5 out of 7 animals tested ($p < 0.05$, compared to other groups). No antibodies were detected in normal or untreated MPS I mice (Fig. 7A).

We then hypothesized that the development of antibodies against IDUA could reduce serum enzyme availability and less enzyme would reach hard-to-treat organs such as the brain. When we separated mice that developed antibodies from those who didn't (regardless when treatment was started), the mice who developed antibodies were the ones who failed to habituate to a new environment in the repeated open field test ($p < 0.05$, Fig. 7B). Other parameters, such joint disease, did not correlate with antibody levels.

4. Discussion

Several clinical studies have demonstrated improvement in biochemical and functional measures of MPS I disease after treatment with Laronidase [19,20]. Also, a clinical study performed in children younger than 5 years have shown reduction liver and heart dimensions and normal mental development [5]. In addition, a study performed in MPS I dogs has shown that a higher dose of the enzyme (1.6 mg/kg) led to normalization of GAG storage in visceral organs, synovium and the mitral valve, as well as the brain [4]. Furthermore, studies in the MPS VII mouse model have shown benefits from early treatment in several parameters as well, including brain abnormalities [7,21]. All these studies as well as our previous observation that GAG storage occurs from birth in MPS patients [8] led us to systematically investigate the benefits from neonatal treatment comparing to treatment started at adult age in MPS I mice. The dose of 1.2 mg/kg

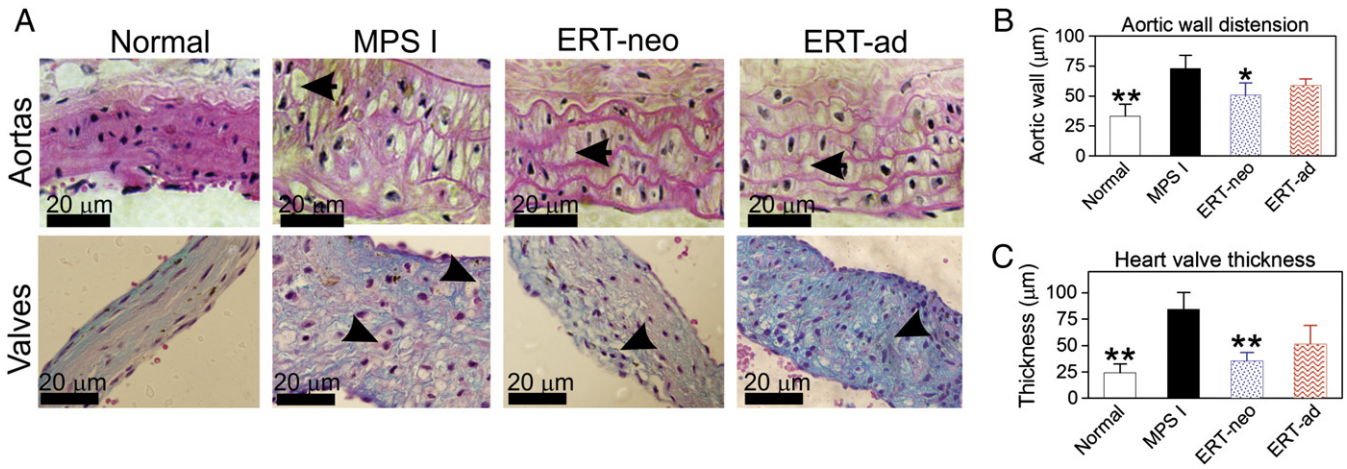

Fig. 4. Aorta and heart valves. A) Upper panels show examples of ascending aortas from normal, MPS I and ERT-treated groups stained with H–E. Note aortic wall distension in MPS I mice and GAG storage (white vacuoles, arrow). Lower panels show examples of heart valves stained with H–E/alcian blue in MPS I, normal and treated mice. Note heart valve thickening and GAG storage (arrow). B) Quantification of aortic wall distension in the 4 groups. N = 3–8 animals/group. C) Quantification of heart valve thickness. N = 3–4/group. * P < 0.05; ** P < 0.01 versus MPS I, ANOVA and Tukey post hoc.

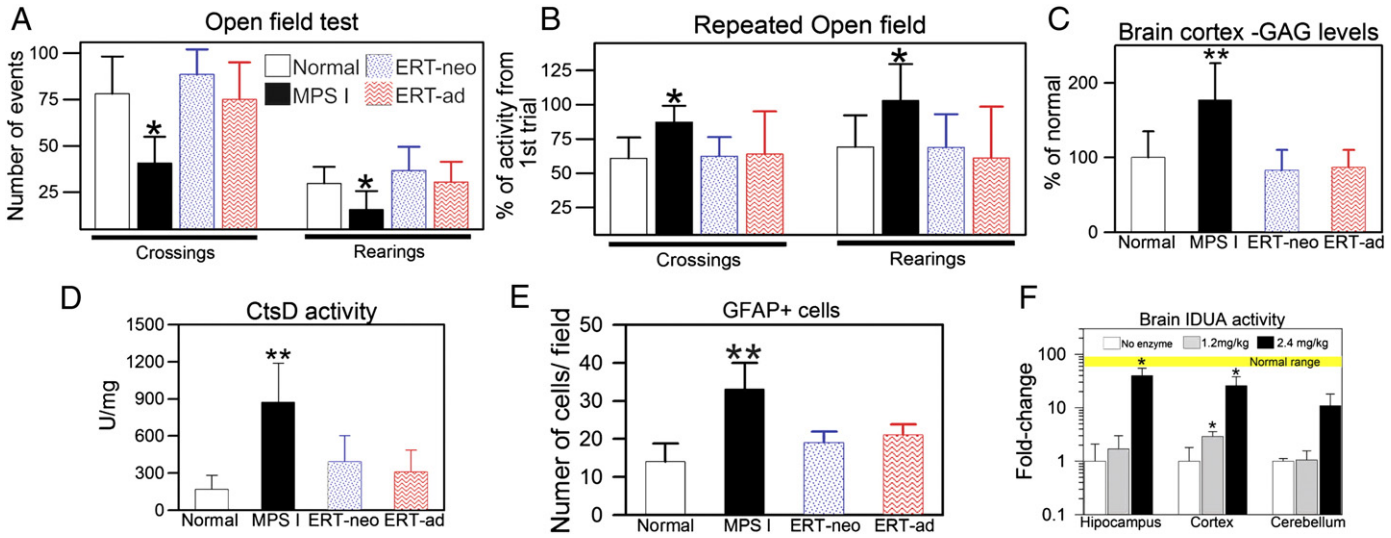

Fig. 5. Improvements in behavior and brain biochemical parameters at 6 months. A) Open field test was used as a measure of locomotor (crossings) and exploratory (rearings) activities. N = 6–9/group B) The repeated open field test is a measure of habituation (non-aversive memory). The activity in the 3rd trial was compared to the 1st trial, as results are expressed as percentage of activity from 1st trial. N = 6–9/group C) GAG levels measured in the brain cortex. N = 5–6/group D) Cathepsin D (CtsD) activity was measured at pH 4 using a fluorescent substrate. N = 5/group. E) Glial fibrilarry acid protein (GFAP) content, an indicator of neuroinflammation. F) IDUA activity in 3-month old treated mice. For this experiment, mice received a single injection of 1.2 mg/kg (n = 4) or 2.4 mg/kg (n = 3) of Laronidase, and 1 h later, brain was perfused and collected for IDUA assay, and results were compared to untreated mice (n = 3). Enzyme activity could be detected in the brain areas, suggesting that the enzyme could cross the blood–brain-barrier. Yellow line indicates normal values. IDUA levels for untreated MPS I mice ranged from 0.05 to 0.16 nmol/h/mg, and IDUA levels for normal mice ranged from 12.6 to 19.4 nmol/h/mg. Note that IDUA levels are presented in log scale.*p < 0.05; **p < 0.01, ANOVA and Tukey.

was chosen because it is the regimen proved to be efficient in patients [10] and it gives a half-life in mice of approximately 90 min, similar to that found in humans [5]. Although the 0.6 mg/kg weekly regimen and the 1.2 mg/kg dose every 2 weeks gave similar results in humans, we cannot rule out the hypothesis that some effects in mice could vary depending on the dose and frequency of the injections.

The abnormal heavier weight observed in MPS I mice may be attributed to abnormalities in liver and spleen sizes, to metabolic alterations, as well as bone disease [17,22]. Our results suggest that, when weight is evaluated, the ERT-neo mice have a better outcome than ERT-ad, although results might not be significant for ERT-ad due to a smaller number of animals analyzed. The urinary GAG levels are used as a biomarker of treatment effectiveness, and results suggest that both treatments lead to improvements.

GAG levels were elevated in visceral organs, and both treatments were equally effective in reducing them. However, results from

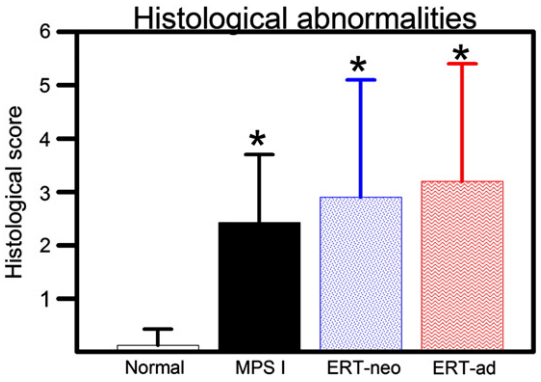

Fig. 6. Joint disease. A score was created based on the abnormalities found in untreated MPS I mice (Supplement Table 1), and no benefit was found from either ERT-neo or ERT-ad treatments (Supplement Fig. 1). *p < 0.05, ANOVA and Tukey post hoc versus normal. N = 7–10/group.

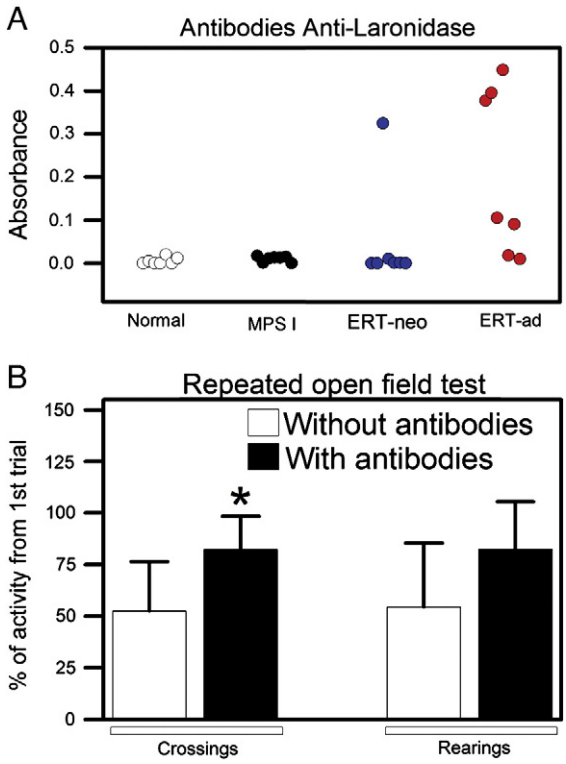

Fig. 7. Antibody formation. A) Serum IgG-anti-Laronidase antibodies in mice at 6 months. Each dot represents results from individual mice. ERT-ad developed significantly higher levels of antibodies (p < 0.05 compared to other groups, ANOVA and Tukey *post hoc*). B) Analysis of performance in repeated open field test in mice who develop antibodies and those who did not. Treated mice that developed antibodies (n = 4) were separated from those who didn't (n = 8), regardless when treatment was started, and analysis of repeated open field test suggests that the ones who develop antibodies perform worse in the test. P < 0.05 compared to animals who didn't develop antibodies, Student's t test.

previous studies have shown contradictory results regarding improvement of heart function after ERT [5,23,24]. Therefore, we evaluated several parameters using echocardiography. Both treatments were able to restore left ventricular function, as well as pulmonary hypertension parameters in mice, suggesting that ERT can prevent heart disease in MPS I.

The aorta and the heart valves in MPS have been shown to be difficult to treat by ERT, HSCT or even gene therapy [11,23–25] and therefore they are structures that need a careful evaluation. In the present work, we measured thickness of the heart valves and ascending aorta, as well as the storage in these structures. Both treatments were only partially effective in treating these aspects of the disease, however we could observe that ERT-neo had results that approached the normal group. The aortas in MPS I mice show loss of elastin and increased distension as early as 1.5 months, which is progressive [26]. We suggest that the benefit from early treatment comes from the fact that once established, the structural changes in these organs cannot be reverted, and therefore treatment should be started before the onset of symptoms. Also, these organs seem to be only partially corrected, since GAG storage was still present even in treated mice, possibly because these structures are poorly vascularized.

One of the most unexpected findings of this study is certainly the apparent improvement in brain function. It is believed that the recombinant enzyme is not able to cross the blood-brain-barrier (BBB) and reach the brain [27], although some studies suggest improvements in cognitive function in treated MPS I children [5,28]. Here, we have shown that both ERT-neo and ERT-ad groups improved in behavioral tests and reduced GAG levels in the brain cortex, however, it is important to point out that results from behavioral tests in MPS I mice need to be carefully interpreted because improvement in the function of other organs can alter the results. Therefore, we evaluated the activity of cathepsin D and GFAP, which were found to be markedly elevated in MPS I mice and reduced in both treated groups. Cathepsin D activity was measured since we have previously shown that other lysosomal enzymes are usually elevated in MPS I, and normalization of their activities is a good biochemical indicator of correction of disease [13,16]. It is interesting to notice that mice treated from 2 months also showed improvements, since at this time point abnormalities such as hypoactivity [17] as well as increased neuroinflammation [9] could already be detectable in these mice. Our results raise the question if the brain disease is complete irreversible in MPS I as initially thought. Also, these results differ from what has been previously shown for MPS VII mice, where it was suggested that only early treatment was able to improve brain pathology [7].

Based on those findings, we tested if we could detect enzyme activity the brain with the dose that we have administered (1.2 mg/kg) as well as at a higher dose (2.4 mg/kg). We found a very small increase in IDUA activity in the brain cortex with the 1.2 mg/kg dose, and a major increase in all brain regions with the higher dose 1 h after the injection. A recent study [4] in dogs have also found a reduction in GAG levels in the brain even with a smaller dose (0.58 mg/kg), suggesting that some enzyme can cross the BBB in animal models, although the process is somewhat inefficient. Since mice were sacrificed 1 h after the injection, we excluded the possibility of IDUA being taken through the BBB by immune cells, and favor the hypothesis of some other mechanism of transport, which will be evaluated in future studies. It is important to point out that although the MPS I mice were extensively perfused with PBS before organ collection, we cannot completely exclude that some IDUA activity observed in the brain could be derived from endothelial cells. However, the observations of reduced GAG levels, GFAP content and CtsD function suggest that at least a small fraction of the enzyme is crossing the BBB. Another point to be considered is that the ERT is delivered in a much quicker way in mice than it is in patients, and that may lead to differences on the biodistribution of the enzyme.

Despite marked improvements in the brain, some organs did not show any improvement. We have developed a score to evaluate the histological disease of MPS I mice (Baldo G, personal communication). In the present work we extend those findings to the ERT-treated groups, confirming that the poor vascularized joint is also difficult to correct, despite early treatment. The results in dogs have shown some improvement in skeletal disease [4], while studies in patients suggest that ERT is only able to slow the progression of the symptoms [29]. Although no deep analysis of skeletal aspects of disease was performed in the present study, our results from joint tissue suggest that bones and joints had no marked benefits from ERT. The reason for this discrepancy among species may be related to kinetics and biodistribution of the enzyme, and further studies are needed to clarify this issue. However, our results suggest that improvement in bone and joint disease might pass through ancillary therapies.

Finally, antibody levels were measured as we have previously described [18]. ERT-ad mice developed higher antibody levels than ERT-neo mice, consistent with the induction of immune tolerance in neonates, which have been described before in MPS I dogs [4]. Interestingly, mice that developed antibodies performed significantly worse in the open field habituation test, suggesting that the presence of serum antibodies might be neutralizing part of the serum IDUA, and reducing the fraction of the enzyme that crosses the BBB. Since most of MPS I patients also develop neutralizing antibodies [30,31], the early treatment could lead to a better efficacy of the therapy. We could not observe correlation of antibody levels with other parameters, such as joint disease and visceral GAG storage. We suggest that in organs such as the liver, high amounts of enzyme are available, and even if neutralizing antibodies are developed, there is still enough enzyme to revert the disease, while organs such as the joint do not get benefits from ERT simply because the enzyme does not reach these structures, regardless antibody formation.

In conclusion, our results suggest that early introduction of ERT is more effective in preventing abnormalities in the aorta and the heart valves, as well as in reducing anti-Laronidase antibodies, while other parameters do not show marked differences from late treatment. The data presents the idea that ERT started from birth leads to better treatment outcomes in some organs and should be considered whenever possible, a observation that gains relevance as newborn screening programs are being considered for the treatable LSDs.

Supplementary data to this article can be found online at http://dx.doi.org/10.1016/j.ymgme.2013.03.005.

Acknowledgments

The authors would like to thank Elizabeth Neufeld (UCLA, USA) for providing the MPS I mice. Grant support was provided by Conselho Nacional de Desenvolvimento Cientifico (CNPq), FAPERGS and Fundo de Incentivo a Pesquisa do HCPA (FIPE-HCPA).

References

[1] E.F. Neufeld, J. Muenzer, The mucopolysaccharidoses, in: C.R. Scriver, A.L. Beaudet, W.S. Sly, D. Valle (Eds.), The Metabolic and Molecular Bases of Inherited Disease, McGraw-Hill, New York, 2001, pp. 3421–3452 2.

[2] R. Giugliani, A. Federhen, M.V. Rojas, T. Vieira, O. Artigalas, L.L. Pinto, A.C. Azevedo, A. Acosta, C. Bonfim, C.M. Lourenço, C.A. Kim, D. Horovitz, D. Bonfim, D. Marinho, D. Palhares, E.S. Santos, E. Ribeiro, E. Valadares, F. Guarany, G.R. de Luca, H. Pimentel, I.N. de Souza, J.S. Correa, J.C. Fraga, J.E. Goes, J.M. Cabral, J. Simionato, J.J. Llerena, L. Jardim, L. Giugliani, L.C. da Silva, M.L. Santos, M.A. Moreira, M. Kerstenetzky, M. Ribeiro, N. Ruas, P. Barrios, P. Aranda, R. Honjo, R. Boy, R. Costa, C. Souza, F.F. Alcantara, S.G. Avilla, S. Fagondes, A.M. Martins, Mucopolysaccharidosis I, II, and VI: brief review and guidelines for treatment, Genet. Mol. Biol. 33 (2010) 589–604.

[3] U. Matte, V.L. Lagranha, T.G. de Carvalho, F.Q. Mayer, R. Giugliani, Cell microencapsulation: a potential tool for the treatment of neuronopathic lysosomal storage diseases, J. Inherit. Metab. Dis. 34 (2011) 983–990.

[4] A.D. Dierenfeld, M.F. McEntee, C.A. Vogler, C.H. Vite, A.H. Chen, M. Passage, S. Le, S. Shah, J.K. Jens, E.M. Snella, K.L. Kline, J.D. Parkes, W.A. Ware, L.E. Moran, A.J. Fales-Williams, J.A. Wengert, R.D. Whitley, D.M. Betts, A.M. Boal, E.A. Riedesel, W. Gross, N.M. Ellinwood, P.I. Dickson, Replacing the enzyme alpha-L-iduronidase at birth ameliorates symptoms in the brain and periphery of dogs with mucopolysaccharidosis type I, Sci. Transl. Med. 2 (2010) 60ra89.

[5] J.E. Wraith, M. Beck, R. Lane, A. Van der Ploeg, E. Shapiro, Y. Xue, E.D. Kakkis, N. Guffon, Enzyme replacement therapy in patients who have mucopolysaccharidosis I and are younger than 5 years: results of a multinational study of recombinant human alpha-L-iduronidase (laronidase), Pediatrics 120 (2007) e37–e46.
[6] O. Gabrielli, L.A. Clarke, S. Bruni, G.V. Coppa, Enzyme replacement therapy in a 5-month-old boy with attenuated presymptomatic MPS I: 5-year follow-up, Pediatrics 125 (2009) e183–e187.
[7] C. Vogler, B. Levy, N.J. Galvin, C. Thorpe, M.S. Sands, J.E. Barker, J. Baty, E.H. Birkenmeier, W.S. Sly, Enzyme replacement in murine mucopolysaccharidosis type VII: neuronal and glial response to beta-glucuronidase requires early initiation of enzyme replacement therapy, Pediatr. Res. 45 (1999) 838–844.
[8] G. Baldo, U. Matte, O. Artigalas, I.V. Schwartz, M.G. Burin, E. Ribeiro, D. Horovitz, T.P. Magalhaes, M. Elleder, R. Giugliani, Placenta analysis of prenatally diagnosed patients reveals early GAG storage in mucopolysaccharidoses II and VI, Mol. Genet. Metab. 103 (2011) 197–198.
[9] G. Baldo, F.Q. Mayer, B. Martinelli, A. Dilda, F. Meyer, K.P. Ponder, R. Giugliani, U. Matte, Evidence of a progressive motor dysfunction in Mucopolysaccharidosis type I mice, Behav. Brain Res. 233 (2012) 169–175.
[10] R. Giugliani, V.M. Rojas, A.M. Martins, E.R. Valadares, J.T. Clarke, J.E. Góes, E.D. Kakkis, M.A. Worden, M. Sidman, G.F. Cox, A dose-optimization trial of laronidase (Aldurazyme) in patients with mucopolysaccharidosis I, Mol. Genet. Metab. 96 (2009) 13–19.
[11] G. Baldo, F. Quoos Mayer, M. Burin, J. Carrillo-Farga, U. Matte, R. Giugliani, Recombinant encapsulated cells overexpressing alpha-L-iduronidase correct enzyme deficiency in human mucopolysaccharidosis type I cells, Cells Tissues Organs. 195 (2012) 323–329.
[12] O.H. Lowry, N.J. Rosebrough, A.L. Farr, R.J. Randall, Protein measurement with the Folin phenol reagent, J. Biol. Chem. 193 (1951) 265–275.
[13] G. Baldo, S. Wu, R.A. Howe, M. Ramamoothy, R.H. Knutsen RH, J. Fang, R.P. Mecham, Y. Liu, X. Wu, J.P. Atkinson, K.P. Ponder, Pathogenesis of aortic dilatation in mucopolysaccharidosis VII mice may involve complement activation, Mol. Genet. Metab. 104 (2011) 608–619.
[14] A.M. Tavares, A.S. da Rosa Araújo, G. Baldo, U. Matte, N. Khaper, A. Belló-Klein, L.E. Rohde, N. Clausell, Bone marrow derived cells decrease inflammation but not oxidative stress in an experimental model of acute myocardial infarction, Life Sci. 87 (2010) 699–706.
[15] J.E. Jones, L. Mendes, M.A. Rudd, G. Russo, J. Loscalzo, Y.Y. Zhang, Serial noninvasive assessment of progressive pulmonary hypertension in a rat model, Am. J. Physiol. Heart Circ. Physiol. 283 (2002) 364–371.
[16] G. Baldo, D. Wozniak, K. Ohlemiller, Y. Zhang, R. Giugliani R, K.P. Ponder, Retroviral Vector-mediated Gene Therapy to Mucopolysaccharidosis I Mice Improves Sensorimotor Impairments and Other Behavior Deficits, J Inherit Metab Dis. in press.
[17] D. Pan, A. Sciascia, C.V. Vorhees, M.T. Williams, Progression of multiple behavioral deficits with various ages of onset in a murine model of Hurler syndrome, Brain Res. 1188 (2008) 241–253.
[18] G. Baldo, F.Q. Mayer, B. Martinelli, F. Meyer, M. Burin, L. Meurer, A.M. Tavares, R. Giugliani, U. Matte, Intraperitoneal implant of recombinant encapsulated cells overexpressing alpha-L-iduronidase partially corrects visceral pathology in Mucopolysaccharidosis type I mice, Cytotherapy 14 (2012) 860–867.
[19] E.D. Kakkis, J. Muenzer, G.E. Tiller, L. Waber, J. Belmont, M. Passage, B. Izykowski, J. Phillips, R. Doroshow, I. Walot, R. Hoft, E.F. Neufeld, Enzyme replacement therapy in mucopolysaccharidosis I, N. Engl. J. Med. 344 (2001) 182–188.
[20] J.E. Wraith, L.A. Clarke, M. Beck, E.H. Kolodny, G.M. Pastores, J. Muenzer, D.M. Rapoport, K.I. Berger, S.J. Swiedler, E.D. Kakkis, T. Braakman, E. Chadbourne, K. Walton-Bowen, G.F. Cox, Enzyme replacement therapy for mucopolysaccharidosis I: a randomized, doubleblinded, placebo-controlled, multinational study of recombinant human alpha-L-iduronidase (laronidase), J. Pediatr. 144 (2004) 581–588.
[21] L.H. O'Connor, L.C. Erway, C.A. Vogler, W.S. Sly, A. Nicholes, J. Grubb, S.W. Holmberg, B. Levy, M.S. Sands, Enzyme replacement therapy for murine mucopolysaccharidosis type VII leads to improvements in behavior and auditory function, J. Clin. Invest. 101 (1998) 1394–1400.
[22] J.C. Woloszynek, T. Coleman, C.F. Semenkovich, M.S. Sands, Lysosomal dysfunction results in altered energy balance, J. Biol. Chem. 282 (2007) 35765–35771.
[23] E.A. Braunlin, I.M. Berry, C.B. Whitley, Cardiac findings after enzyme replacement therapy for mucopolysaccharidosis type I, Am. J. Cardiol. 98 (2006) 416–418.
[24] M. Sifuentes, R. Doroshow, R. Hoft, G. Mason, I. Walot, M. Diament, S. Okazaki, K. Huff, G.F. Cox, S.J. Swiedler, E.D. Kakkis, A follow-up study of MPS I patients treated with laronidase enzyme replacement therapy for 6 years, Mol. Genet. Metab. 90 (2007) 171–180.
[25] N. Watanabe, P.V. Anagnostopoulos, A. Azakie, Aortic stenosis in a patient with Hurler's syndrome after bone marrow transplantation, Cardiol. Young 21 (2011) 349–350.
[26] X. Ma, M. Tittiger, R.H. Knutsen, A. Kovacs, R. Schaller, R.P. Mecham, K.P. Ponder, Upregulation of elastase proteins results in aortic dilatation in mucopolysaccharidosis I mice, Mol. Genet. Metab. 94 (2008) 298–304.
[27] E.D. Kakkis, E. Schuchman, X. He, Q. Wan, S. Kania, S. Wiemelt, C.W. Hasson, T. O'Malley, M.A. Weil, G.A. Aguirre, D.E. Brown, M.E. Haskins, Enzyme replacement therapy in feline mucopolysaccharidosis I, Mol. Genet. Metab. 72 (2001) 199–208.
[28] R.Y. Wang, E.J. Cambray-Forker, K. Ohanian, D.S. Karlin, K.K. Covault, P.H. Schwartz, J.E. Abdenur, Treatment reduces or stabilizes brain imaging abnormalities in patients with MPS I and II, Mol. Genet. Metab. 98 (2009) 406–411.
[29] A. Tylki-Szymanska, J. Marucha, A. Jurecka, M. Syczewska, B. Czartoryska, Efficacy of recombinant human alpha-L-iduronidase (laronidase) on restricted range of motion of upper extremities in mucopolysaccharidosis type I patients, J. Inherit. Metab. Dis. 33 (2010) 151–157.
[30] R. Kakavanos, C.T. Turner, J.J. Hopwood, E.D. Kakkis, D.A. Brooks, Immune tolerance after long-term enzyme-replacement therapy among patients who have mucopolysaccharidosis I, Lancet 361 (2003) 1608–1613.
[31] K.P. Ponder, Immune response hinders therapy for lysosomal storage diseases, J. Clin. Invest. 118 (2008) 2686–2689.

ANEXO III

INTERNATIONAL JOURNAL OF Experimental Pathology

Int. J. Exp. Path. (2013), 94, 305–311

ORIGINAL ARTICLE

Characterization of joint disease in mucopolysaccharidosis type I mice

Patricia G. de Oliveira*,[1], Guilherme Baldo[†,‡,1], Fabiana Q. Mayer[‡], Barbara Martinelli[‡], Luise Meurer[§], Roberto Giugliani[†,‡], Ursula Matte[‡] and Ricardo M. Xavier*,[¶]

**Programa de pós-graduação em medicina: ciências medicas, Universidade Federal do Rio Grande do Sul, Rio Grande do Sul, Brazil, [†]Programa de pós-graduação em Ciências Biológicas: Bioquímica, Universidade Federal do Rio Grande do Sul, Rio Grande do Sul, Brazil, [‡]Centro de Terapia Gênica, Hospital de Clinicas e Porto Alegre, Porto Alegre, Brazil, [§]Serviço de Patologia, Hospital de Clinicas de Porto Alegre, Porto Alegre, Brazil and [¶]Servico de Reumatologia, Hospital de Clinicas de Porto Alegre, Porto Alegre, Brazil*

INTERNATIONAL JOURNAL OF EXPERIMENTAL PATHOLOGY

doi: 10.1111/iep.12033

Received for publication: 17 January 2013
Accepted for publication: 11 May 2013

Correspondence
Patricia G. de Oliveira
Hospital de Clínicas de Porto Alegre
Serviço de Reumatologia
Rua Ramiro Barcellos
2350, sala 645
Porto Alegre 90035-003
Brazil
Tel.: +55 51 21018340
Fax: +55 51 33313834
E-mail: patty.go@gmail.com
[1]Both authors contributed equally to this work.

SUMMARY

Mucopolysaccharidoses (MPS) are lysosomal storage disorders characterized by mutations in enzymes that degrade glycosaminoglycans (GAGs). Joint disease is present in most forms of MPS, including MPS I. This work aimed to describe the joint disease progression in the murine model of MPS I. Normal (wild-type) and MPS I mice were sacrificed at different time points (from 2 to 12 months). The knee joints were collected, and haematoxylin–eosin staining was used to evaluate the articular architecture. Safranin-O and Sirius Red staining was used to analyse the proteoglycan and collagen content. Additionally, we analysed the expression of the matrix-degrading metalloproteinases (MMPs), MMP-2 and MMP-9, using immunohistochemistry. We observed progressive joint alterations from 6 months, including the presence of synovial inflammatory infiltrate, the destruction and thickening of the cartilage extracellular matrix, as well as proteoglycan and collagen depletion. Furthermore, we observed an increase in the expression of MMP-2 and MMP-9, which could conceivably explain the degenerative changes. Our results suggest that the joint disease in MPS I mice may be caused by a degenerative process due to increase in proteases expression, leading to loss of collagen and proteoglycans. These results may guide the development of ancillary therapies for joint disease in MPS I.

Keywords
alpha-L-iduronidase, joint disease, matrix metalloproteinases, mucopolysaccharidoses type I

Mucopolysaccharidoses (MPS) are lysosomal storage disorders characterized by mutations in enzymes that degrade glycosaminoglycans (GAGs). Joint disease is present in most forms of MPS, including MPS I (Giugliani *et al.* 2010).

Mucopolysaccharidoses I occurs due to a deficiency of the enzyme alpha-L-iduronidase (IDUA), which is involved in the degradation of heparan sulphate and dermatan sulphate. Consequently, these two GAGs accumulate in the lysosomes and in the extracellular space, leading to the clinical manifestations observed. Bone and joint disease in MPS I patients is characterized by abnormal cartilage and bone development, short stature, dysostosis multiplex and degenerative joint disease (Pastores & Meere 2005).

The animal model of MPS I was created through the disruption of the *Idua* gene (Ohmi *et al.* 2003) and has been proven to be a valuable tool for the study of disease pathogenesis (Ohmi *et al.* 2003; Ma *et al.* 2008). The mice present with joint disease in later stages of life (Visigalli *et al.* 2010), but a complete description of the disease was never reported.

Therefore, in the present work, we created a score to characterize the histological abnormalities present in the knee joints of MPS I mice. This histological profile allowed us to study the age of onset of joint disease and its progression. In addition, we also attempted to suggest possible mechanisms underlying the disease.

Material and methods

Animals

All animal studies were approved by the authors' institutional review board, and MPS I mice bred on a C57BL/6 background (kindly donated by Dr. Elizabeth Neufeld, UCLA, USA) were used. Both male and female *Idua*$^{-/-}$ mice (MPS I group) and their normal littermate controls, *Idua*$^{-/+}$ and *Idua*$^{+/+}$ (wild-type group, wt), served as subjects for experiments. MPS I mice were identified by PCR (Baldo *et al.* 2012), and group sizes ranged from 6 to 11 animals at each time point. Animals were maintained in conventional housing under a 12-h light/12-h dark cycle with controlled temperature (19 ± 1 °C) and humidity (50 ± 10%) and sacrificed at 2, 4, 6, 8 or 12 months.

Ethical Approval

All experimental procedures involving animals were performed in accordance with the National Institutes of Health Guide for Care and Use of Animals and with the approval of our institutional ethics committee.

Histological analyses

Mouse knees from both rear legs were collected and placed in buffered formalin from 24 h to up to 1 week, and tissue samples were decalcified with 14% EDTA for up to 1 week. Paraffin sections (7 μm thickness) were produced and stained with haematoxylin/eosin (H–E) for articular architecture, Safranin-O for proteoglycan (PG) content and Sirius Red for the evaluation of collagen levels.

The extent of joint disease was scored, given the following abnormalities analysed with H–E staining: presence of inflammatory infiltrate (0 – absent, 1 – present); bone resorption (0 – absent, 1 – mild, 2 – moderate, 3 – severe); cartilage resorption (0 – absent, 1 – mild, 2 – moderate, 3 – severe) and fibrocartilaginous proliferation (0 – absent, 1 – mild, 2 – moderate, 3 – severe). The maximum score was 10. An example of each abnormality scored can be found in Figure 1.

Safranin is a cationic dye in which staining is proportional to proteoglycan content in normal cartilage. When analysing the Safranin-O slides for cartilage proteoglycan content, the following semi-quantitative scoring was used: 0 – normal staining of non-calcified cartilage; 1 – decreased but not complete loss of Safranin-O staining over 1–100% of the articular surface; 2 – complete loss of Safranin-O staining in the non-calcified cartilage, extending to <25% of the articular surface; 3 – complete loss of Safranin-O staining in the non-calcified cartilage, extending to 25–50% of the articular surface; 4 – complete loss of Safranin-O staining in the non-calcified cartilage, extending to 50–75% of the articular surface; and 5 – complete loss of Safranin-O staining in the non-calcified cartilage, extending to >75% of the articular surface (Schmitz *et al.* 2010). In all cases, both legs were blindly analysed by the pathologist, and the final scores were obtained from the leg featuring more severe pathology.

To evaluate the collagen content, a single batch of slides were stained with Sirius Red. Images were obtained using a digital camera that was coupled to a microscope (Zeiss, Germany). Pictures of the articular cartilage were used to obtain the total pixel values (red signal), which corresponded to the extent of collagen staining.

Growth plate alterations

The length of growth plates obtained from wt and MPS I mice was measured using the Photoshop computer program. Photographs of the tibial growth plate (H–E slides) were taken at 20× magnification and assembled to form a single picture. The length of the growth plate was measured in at least six distinct points located throughout the growth plate extension along the axis of the chondrocyte column, as indicated in Figure 4c. The average length was obtained for each animal.

Expression of matrix metalloproteinases

Immunohistochemistry for matrix metalloproteinase type 2 (MMP-2, Abbiotec, USA) and MMP-9 (Santa Cruz, USA) was performed using the primary antibody in a 1:200 dilution, incubated overnight at 4 °C. The secondary antibody (multispecies, DAKO, USA) conjugated to peroxidase was incubated in a 1:1000 dilution for 18 h, and the samples were developed with DAB. Quantification was performed on a signal per area basis, excluding areas with no tissue, using the ImageProPlus software, as previously described (Baldo *et al.* 2011b). The results were expressed as fold change from normal values (normal average pixels was considered as a value of 1).

Statistical analysis

Results for general score, growth plate abnormalities and immunohistochemistry were compared using *t*-test. P value <0.05 was considered to be significant. All analyses were performed using the SigmaStat software, version The results are presented as mean and standard deviation.

Results

Time course of histological alterations

Glycosaminoglycan storage could be visualized as early as 2 months in MPS I mice; however, no other major histological abnormalities were observed at 2 and 4 months (Figure 2b). Other alterations became detectable at 6 months (Figure 2c), when 66% (4 of 6) of MPS I mice presented with mild inflammatory infiltrate. Inflammatory cells were leucocytes, observed in the synovial membrane. Fibrocartilaginous proliferation was present in 66% (4/6) of MPS I mice, with three of the animals exhibiting mild alterations.

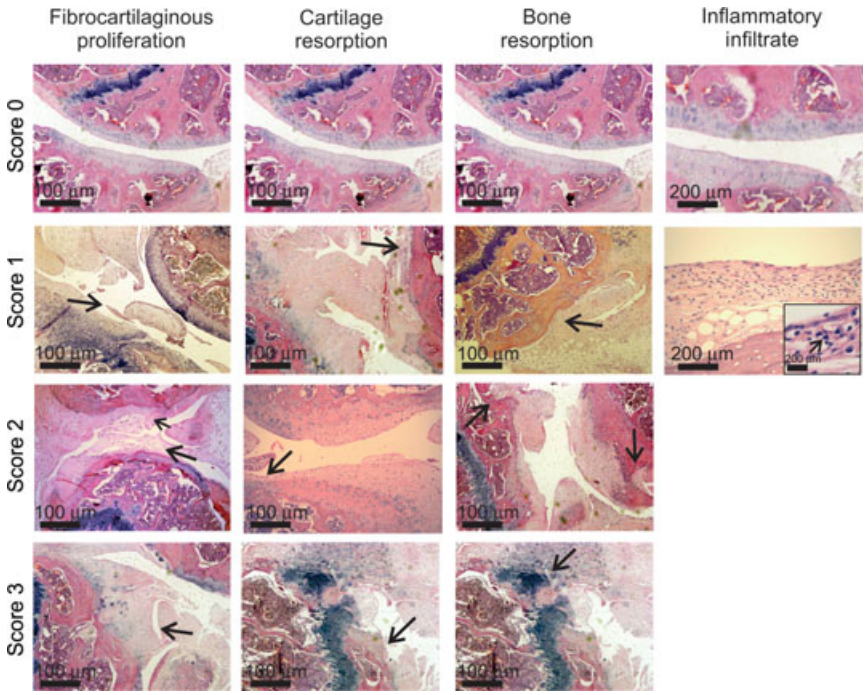

Figure 1 Example of abnormalities observed in the score used for evaluation of joint disease in MPS I mice (H–E stain). Arrows indicate the specific abnormality shown in each picture. In the inflammatory infiltrate picture grade 1, an insert of higher magnification was used to better exemplify the mononuclear cells observed in the synovium area (arrow). In some cases, the same picture was used more than once, when it contained more than one abnormality or in the case of normal architecture.

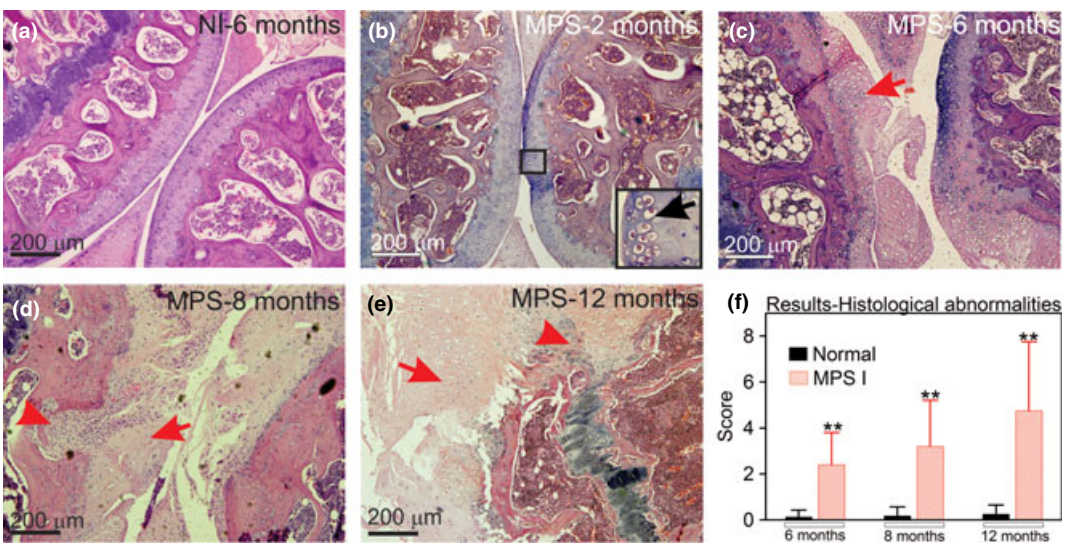

Figure 2 Aspect of knee joints using H–E stain. (a) Joint sections representative from a wt mouse at 6 months; (b) MPS I mice at 2 months, insert indicates GAG storage; (c) MPS I mouse at 6 months, with the arrow indicating damage to the articular surface; (d) MPS I mouse at 8 months, with the arrowhead representing bone resorption and the arrow indicating fibrocartilaginous proliferation; (e) MPS I mouse at 12 months, with the arrowhead showing intense bone resorption and the arrow indicating intense fibrocartilaginous proliferation; and (f) results from histological scores obtained in wt and MPS I mice joints at 6, 8 and 12 months (N = 6–11). Score was based on abnormalities described in Figure 1 and detailed in the methods section, where the higher the score, the worse the joint. The maximum score is 10. $^{**}P < 0.01$, using Student's t-test. N = 6–11 mice/group.

In contrast, cartilage resorption was mild and present in only 2 of 6 mice. Similarly, bone resorption was rare (1/6) and mild at this time point. Animals had uneven articular surfaces, and proteoglycan depletion was mild at this age. The average score for MPS I mice at 6 months was 2.3 ± 1.4 *vs.* 0.1 ± 0.3 in wt mice ($P < 0.01$, Figure 2f).

Joint alterations were even more pronounced at 8 and 12 months, with evidence of proteoglycan and collagen depletion in the cartilage matrix and underlying the bone. At 8 months, inflammatory infiltrate was still mild but present in 91% of MPS I mice (10/11). Other parameters were also present in almost all mice, including fibrocartilaginous proliferation, irregularities at the articular surface and cartilage resorption. Bone resorption was present in only one mouse. The average score for MPS I mice was 3.2 ± 2.0, whereas for wt mice, it was 0.2 ± 0.4 ($P < 0.01$, Figure 2d).

At 12 months, more striking differences were observed, including bone resorption in 50% of MPS I mice (4/8). The inflammatory infiltrate was still mild but present in 88% of the mice. Other parameters were also more prominent. The average score for MPS I mice was 4.8 ± 3.1 *vs.* 0.25 ± 0.5 in wt mice ($P < 0.01$, Figure 2e, f). The individual results for each parameter can be seen in supplement Figure S1.

A loss of cartilage proteoglycan content was progressive with age (6–12 months of age, Figure 3a–d). Collagen levels, analysed by Sirius Red stain, suggest that wt mice show con-

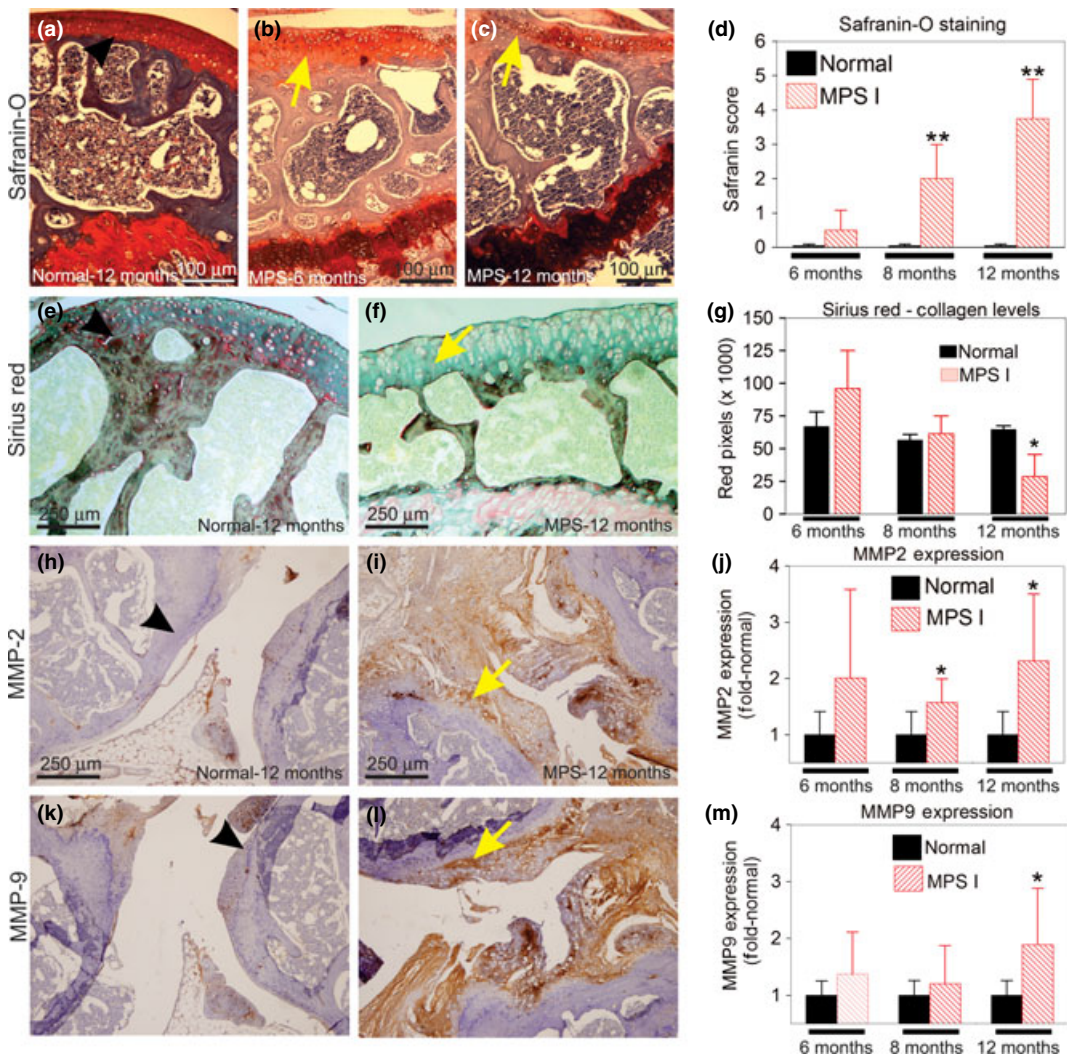

Figure 3 Mechanisms of joint degeneration in MPS I. (a-d) Safranin-O staining. (a) Representative section of a wt joint at 12 months. (b) MPS I mouse at 6 months. (c) MPS I mouse at 12 months, with loss of red signal (yellow arrow) showing loss of proteoglycans. (d) Results from the histological scores obtained with the Safranin-O stain at 6, 8 and 12 months. $^{**}P = 0.01$, using Student's *t*-test. $N = 3$–4 mice/group. (e–g) Collagen levels evaluated by Sirius Red stain. (e) Wt joint at 12 months. (f) MPS I mouse at 12 months, showing loss of red stain (yellow arrow). (g) Quantification of the red signal in wt and MPS I mice. A significant reduction in the collagen levels was observed in the MPS I mice at 12 months ($^{**}P < 0.01$, Student's *t*-test). (h–m) Immunohistochemistry for the matrix metalloproteinases (MMP). (h) MMP-2 expression in 12 months wt mouse; (i) MMP-2 expression in 12 months' MPS I mouse, yellow arrow denotes positive staining (brown areas). (j) Quantification of MMP-2 positive signal.$^{*}P < 0.05$, *t*-test. $N = 6$–9 mice/group. (k) MMP-9 expression in Wt mouse at 12 months. (l) MMP-nine expression in MPS I joint at 12 months. (m) Quantification of MMP-2 positive signal. $^{*}P < 0.05$, *t*-test. Results are shown as fold-normal, with the normal values being considered 1. Black arrows represent the normal histology, while yellow arrows represent the abnormal findings. $N = 6$–9 mice/group.

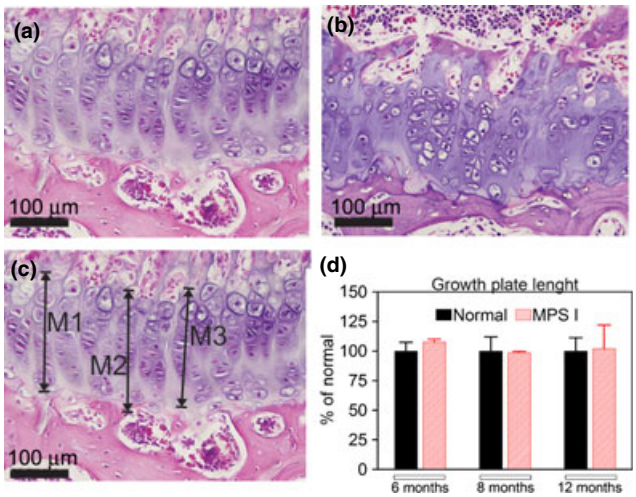

Figure 4 Measurements of the length of the growth plate. On the upper panels, an example of a growth plate from a normal (a) and a MPS I (b) mouse, with disorganization of the chondrocyte axis being shown in MPS I mice. On the lower panel, an example on how the growth plate length was measured (c) and the results for growth plate length (d) are visualized. No differences in length were found between normal and MPS I mice at any time points analysed. $N = 6$ mice/group. M, measure.

stant collagen levels from 6 to 12 months, whereas the MPS I mice present with a progressive reduction in collagen content (Figure 3e–g). At 12 months, the MPS I mice exhibited only 45% of the collagen levels observed in wt mice ($P < 0.01$).

Overall, the joint disease manifests as intracellular GAG accumulation and articular cartilage matrix abnormalities characterized by a significant increase in the volume of the extracellular matrix and limited inflammation. These changes cause further destruction of the joints in a process that, in some aspects, resembles osteoarthritis. Interestingly, articular lesions were asymmetric, given that the more severe joint was analysed. No inflammatory cells were observed in wt mice at any age.

Growth plate alterations

No differences in the lengths of the growth plates were found at any of the time points analysed. However, we observed an overall disorganization of the growth plate in the MPS I mouse tibiae (Figure 4), manifested as difficulty in identifying the axes of the chondrocytes.

MMP-2 and MMP-9 expression

MMP-2 expression was upregulated in MPS I mice (Figure 3h–j). At 6 months, it was already twofold the normal levels, although not significant ($P = 0.1$). At 8 and 12 months, MMP-2 was 1.6- and 2.3-fold the normal values ($P = 0.025$ and 0.013) respectively. MMP-9 expression was mildly elevated at 6 and 8 months, 1.4- and 1.2-fold the normal values respectively (changes were not significant). At 12 months, it was 1.9-fold the normal levels ($P = 0.019$, Figure 3m). The areas with increased MMP-2 and MMP-9 were those with reduced proteoglycan stain, specifically in the synovial membrane and cartilage.

Discussion

The pathogenesis of joint and bone disease in MPS is a critical process that requires studies focused on disease pathogenesis, given that the currently available treatments have shown only modest results in correcting these complications (Tylki-Szymanska *et al.* 2010).

Here, we have shown that MPS I mice present with a progressive disease that, in some of its histological aspects, resembles osteoarthritis. A previous study has reported that several genes differentially expressed in rheumatoid arthritis were also elevated on MPS VI synovial cells (Simonaro *et al.* 2008). These included genes related to inflammation as well as upregulation of proteases, which are also present in osteoarthritis. Our findings suggest that an inflammatory process is indeed occurring in MPS I mice, although of mild intensity. The degradation of proteoglycans is also present, yet histologically, the process in MPS I mice resembles that of osteoarthritis, which agrees with observations found in the mouse MPS IX model (Martin *et al.* 2008).

Previous studies (Hinek & Wilson 2000) have shown that proteins such as elastin may have an incorrect assembly in MPS I cells and that could affect bone and joints in these patients. However, the MPS I mice were normal at first and then developed joint alterations. This made us hypothesize that collagenases could have their expression altered and could be causing the destructive changes observed. Matrix metalloproteinases, including MMP-2 and MMP-9, have been identified in injured cartilage. MMP-2 has been shown to be upregulated in MPS VII mouse aortas (Baldo *et al.* 2011b) at the mRNA level, as well as in patients with osteoarthritis (Kevorkian *et al.* 2005). Importantly, MMP-2 is the most active MMP against collagen type II, which is the main collagen in the cartilage (Zhen *et al.* 2008). MMP-9 is known for its ability to degrade a series of substrates, which includes elastin, proteoglycans, laminin and fibronectin (Shapiro 1998). Those facts motivated us to investigate the expression of MMP-2 and MMP-9 in the joints, and they were upregulated in affected mice. Simonaro *et al.* (2005) have also demonstrated the upregulation of these two genes in the MPS VI synovium, which suggest that the pathogenic processes in MPS I and VI may share some common aspects (Simonaro *et al.* 2005). We conclude that the upregulation of MMP-2 and MMP-9 might contribute to joint disease in MPS I. Other extracellular matrix-degrading enzymes, including cathepsins, have been shown to be altered in the skeletal tissue of MPS I mice (Russell *et al.* 1998; Wilson *et al.* 2009) and may therefore contribute to the disease phenotype as well.

Growth plate width in MPS I mice did not show significant differences from age-matched controls. The previous papers analysing MPS I and VII growth plates have shown a reduction in the growth plate and an increase in the apopto-

sis of chondrocytes in the MPS VII mice, but not in MPS I mice (Metcalf *et al.* 2009). Our results strengthen those findings. Notably, MPS I patients often have a short stature of unknown origin, whereas the MPS I mice have very mild alterations in bone length (Metcalf *et al.* 2009) and stature (Russell *et al.* 1998), suggesting that not all aspects of the human disease can be found in the mouse model (Clarke *et al.* 1997). Interestingly, we have described in a previous publication that MPS I mice have abnormal gait at late stages in life (Baldo *et al.* 2012). Based on these current findings, we cannot exclude the possibility that the abnormalities observed might be due to joint or bone disease.

Conclusions

In conclusion, our results suggest that MPS I mice present with progressive symptoms of joint disease that is characterized by bone and cartilage resorption, mild inflammation, as well as the depletion of collagen and proteoglycans, possibly caused by an upregulation of destructive proteases, such as MMP-2 and MMP-9. These findings highlight the importance of studies on the pathogenesis of the joint disease in MPS I, given that patients may not obtain complete benefits from the current treatments.

Conflict of interest

The authors declare that they have no conflict of interest.

Funding source

CNPq, CAPES and FIPE funded and supported this research.

Authors' contributions

All authors were involved in drafting the article and/or critically revising it for important intellectual content, and all authors approved the final version to be published. Dr. Xavier had full access to all of the data in the study, and he assumes responsibility for the integrity of the data and the accuracy of the data analyses.

Acknowledgements

This work was supported by CNPq (Conselho Nacional de Desenvolvimento Científico e Tecnologico of Brazil), CAPES (Coordenação de Aperfeiçoamento de Pessoal de Nível Superior of Brazil) and FIPE (Fundação de Incentivo à Pesquisa do Hospital de Clínicas de Porto Alegre/RS-BR).

References

Baldo G., Wu S., Howe R.A. *et al.* (2011a) Pathogenesis of aortic dilatation in mucopolysaccharidosis VII mice may involve complement activation. *Mol. Genet. Metab.* **104**, 608–619.

Baldo G., Kretzmann N.A., Tieppo J. *et al.* (2011b) Bone marrow cells reduce collagen deposition in the rat model of common bile duct ligation. *Cell. Sci. Ther.* **2**, 1–6.

Baldo G., Mayer F.Q., Martinelli B. *et al.* (2012) Evidence of a progressive motor dysfunction in Mucopolysaccharidosis type I mice. *Behav. Brain Res.* **233**, 169–175.

Clarke L.A., Russell C.S., Pownall S. *et al.* (1997) Murine mucopolysaccharidosis type I: targeted disruption of the murine alpha-L-iduronidase gene. *Hum. Mol. Genet.* **6**, 503–511.

Giugliani R., Federhen A., Muñoz Rojas M.V. *et al.* (2010) Enzyme replacement therapy for mucopolysaccharidoses I, II and VI: recommendations from a group of Brazilian F experts. *Rev. Assoc. Med. Bras.* **56**, 271–277 [Article in Portuguese].

Hinek A. & Wilson S.E. (2000) Impaired elastogenesis in Hurler disease: dermatan sulfate accumulation linked to deficiency in elastin-binding protein and elastic fiber assembly. *Am. J. Pathol.* **156**, 925–938.

Kevorkian L., Young D.A., Darrah C. *et al.* (2005) Expression profiling of metalloproteinases and inhibitors in cartilage. *Int. J. Clin. Exp. Pathol.* **86**, 131–141.

Ma X., Tittiger M., Knutsen R.H. *et al.* (2008) Upregulation of elastase proteins results in aortic dilatation in mucopolysaccharidosis I mice. *Mol. Genet. Metab.* **94**, 298–304.

Martin D.C., Atmuri V., Hemming R.J. *et al.* (2008) A mouse model of human mucopolysaccharidosis IX exhibits osteoarthritis. *Hum. Mol. Genet.* **17**, 1904–1915.

Metcalf J.A., Zhang Y., Hilton M.J., Long F., Ponder K.F. (2009) Mechanism of shortened bones in mucopolysaccharidosis VII. *Mol. Genet. Metab.* **97**, 202–211.

Ohmi K., Greenberg D.S., Rajavel K.S., Ryazantsev S., Li H.H., Neufeld E.F. (2003) Activated microglia in cortex of mouse models of mucopolysaccharidoses I and IIIB. *Proc. Natl Acad. Sci. USA* **100**, 1902–1907.

Pastores G.M. & Meere P.A. (2005) Musculoskeletal complications associated with lysosomal storage disorders: Gaucher disease and Hurler-Scheie syndrome (mucopolysaccharidosis type I). *Curr. Opin. Rheumatol.* **17**, 70–78.

Russell C., Hendson G., Jevon G., *et al.* (1998) Murine MPS I: insights into the pathogenesis of Hurler syndrome. *Clin. Genet.* **53**, 349–361.

Schmitz N., Laverty S., Kraus V.B., Aigner T. (2010) Basic methods in histopathology of joint tissues. *Osteoarthr. Cartil.* **18**(Suppl. 3), s113–s116.

Shapiro S.D. (1998) Matrix metalloproteinase degradation of extracellular matrix: biological consequences. *Curr. Opin. Cell Biol.* **10**, 602–608.

Simonaro C.M., D'Angelo M., Haskins M.E., Schuchman E.H. (2005) Joint and bone disease in mucopolysaccharidoses VI and VII: identification of new therapeutic targets and biomarkers using animal models. *Pediatr. Res.* **57**(5 Pt 1), 701–707.

Simonaro C.M., D'Angelo M., He X. *et al.* (2008) Mechanism of glycosaminoglycan-mediated bone and joint disease - implications for the mucopolysaccharidoses and other connective tissue diseases. *Am. J. Pathol.* **172**, 112–122.

Tylki-Szymanska A., Marucha J., Jurecka A., Syczewska M., Czartoryska B. (2010) Efficacy of recombinant human alpha-L-iduronidase (laronidase) on restricted range of motion of upper extremities in mucopolysaccharidosis type I patients. *J. Inherit. Metab. Dis.* **33**, 151–157.

Visigalli I., Delai S., Politi L.S. *et al.* (2010) Gene therapy augments the efficacy of hematopoietic cell transplantation and fully cor-

rects mucopolysaccharidosis type I phenotype in the mouse model. *Blood* **116**, 5130–5139.

Wilson S., Hashamiyan S., Clarke L. *et al.* (2009) Glycosaminoglycan-mediated loss of cathepsin K collagenolytic activity in MPS I contributes to osteoclast and growth plate abnormalities. *Am. J. Pathol.* **175**, 2053–2062.

Zhen E.Y., Brittain I.J., Laska D.A. *et al.* (2008) Characterization of metalloprotease cleavage products of human articular cartilage. *Arthritis Rheum.* **58**, 2420–2431.

Supporting information

Additional Supporting Information may be found in the online version of this article:

Figure S1. Time-course for each abnormality observed in MPS I mice. (a) Fibrocartilaginous proliferation. (b) Cartilage resorption. (c) Bone resorption and (d) Inflammatory infiltrate. Each dot represents the score from a single mouse at each time point. In case of a, b and c, the score varies from 0 (normal) to 3 (severe alteration). In case of inflammatory infiltrate, it was considered only as 0-absent or 1-present, a sit was always considered discrete.